Finite element simulation of heat affected zone of welded joint in high strength steel.

Tensile specimen simulation

HÄMEEN AMMATTIKORKEAKOULU
HÄME UNIVERSITY OF APPLIED SCIENCES

Bachelor's thesis

Hämeenlinna University Centre, Construction Engineering

Spring 2021

Duc Le Anh Ngo

HAMK
HÄMEEN AMMATTIKORKEAKOULU
HÄME UNIVERSITY OF APPLIED SCIENCES

Degree program in Construction Engineering
Hämeenlinna University Centre

Author Duc Le Anh Ngo Year: 2021

Subject Finite Element Simulation of Heat Affected Zone of Welded Joint in High Strength Steel

Supervisors Zhongcheng Ma, Jarmo Havula and Dilip Neupane

ABSTRACT

This Bachelor's thesis is commissioned by HAMK Tech, a research unit in Häme University of Applied Sciences. The research topic of this thesis is a part of a bigger research project on high strength steel applications and welded connections. The main goal is to create finite element models of a S500 tensile specimen test. This thesis is the direct continuation work of a previous thesis research topic on finite element modelling of heat affected zone and another on the experimental tests of the effect of different heat inputs on welding of high strength steel.

This Bachelor's thesis aims to create different types of finite element models of the tensile specimen with LS-Dyna. The modelling can be categorized into the following main tasks: geometry creation, keywords definition, meshing technique, output data and especially the definition of material properties. The approach used in this thesis starts with the geometry building and the input process in LS-PrePost and continues with output data analysis and result examination in LS-Post Processing. References from previous Bachelor's theses are great assets to this thesis work, and so this thesis provides the continuation of the research and to provide a solid foundation for further inquiries.

This thesis achieved several substantial progresses in geometry creation, meshing technique, reduction of simulation time and, to a certain extent, the material properties of heat affected zone. The created models provide a realistic failure mechanism, similar to the actual tensile test. An advanced meshing technique used in the model allows the modeler to manipulate meshing shapes and sizes to reduce the simulation time. Two finite element models were constructed, one shell and one solid model, with an aim to simplify the material properties estimation work.

Keywords High strength steel, heat affected zone, FEM, LS-Dyna, LS-PrePost
Pages 83 pages and appendices 28 pages

Contents

1 Introduction....1
1.1 Introduction to high strength steel.... 1
1.2 Topic selection 1
1.3 Research objectives and research question 2
1.4 Future utilization.... 3
2 Background and Literature review....4
2.1 Literature review on high strength steel welding research.... 4
2.1.1 Weldability of high strength steel.... 4
2.1.2 Relationship between heat input and cooling time.... 5
2.1.3 Transformation of microstructure in the heat-affected zone 6
2.2 Literature review on Finite Element Analysis method 8
2.3 Weld run tests.... 9
2.4 Choice of S500 tensile specimen 11
3 LS-Dyna input model creation....11
3.1 Testing of S500 specimen 12
3.2 Geometry modelling 17
3.2.1 Geometry modelling of shell model.... 17
3.2.2 Geometry modelling of solid model 20
3.3 Section type.... 25
3.4 Material input data 28
3.4.1 Base material (S500) 29
3.4.2 Filler material (OK ARISTOROD 69) 32
3.4.3 Heat affected zone (HAZ).... 34
3.5 Loads & Boundary conditions 37
3.5.1 Load application 37
3.5.2 Boundary conditions 40
4 Results and Analysis 42
4.1 Output results of shell model 43
4.2 Output results of solid model 46
4.3 Discussion on failure strain 49
4.4 Discussion on Hourglass effect 49
5 Conclusion 52
6 Recommendations for future work....52

References 53
Appendix 1: Detailed design log for creating shell model.....56
Appendix 2: Detailed design log for creating solid model 67
Appendix 3: Methodology of converting Engineering to True values 82
Appendix 4: Approaches for material data input in MAT024 83

1 Introduction

1.1 Introduction to high strength steel

In the modern construction industry, structural steel has been commonly used in various projects, ranging from residential to industrial buildings. Numerous studies on the material properties of normal structural steel allow a better understanding of its strength and toughness. Many techniques have been invented to manipulate the material's properties through thermomechanical controlled processes and the optimization of chemical compounds. However, unlike normal steel, high strength steel is recently introduced to the industry and it comes with uncertainties about its material properties. Due to the insufficiency in research and understanding of this new material, there are great limitations in the applications of high strength steel according to the current standards and building codes. The biggest uncertainty, when it comes to high strength steel, is the welding process of this material. The higher steel grades mean higher melting points, which leads to intensively higher heat input and dissimilar cooling time of the welding process. This results in the change of the microstructure of the material. Therefore, previous thesis research by Nguyen (2018) aims to evaluate how much the intensive heat from the welding process affects the material properties of the high strength steel.

1.2 Topic selection

Among various options for choosing a thesis topic, why this topic? The finite element method is a challenging topic in the world of engineering. This method has been used as a platform to simulate many physical phenomena that happen in real life. However, the biggest challenge within finite element modelling is to find out how to set the right input parameters to correctly simulate the phenomenon. In order to do this, a deep understanding of the theoretical background is extremely essential. Different aspects contributing to a correct simulation can be material data, boundary condition, contact

condition, load, mathematical solver selection. The finite element model will not output a correct post-processing result unless all the input parameters are correct. It is an extremely difficult task to get all inputs to be correct at the first run, therefore, a technique called “trial and error” is very common in the world of finite element simulation. The model is run multiple times, and after each simulation, the output result is analyzed to modify the inputs for the next simulation. With this approach, the model will be running and modified until the output result is identical to the testing result. At this point, the input parameters have been correctly determined.

Despite the complexity of this topic, the finite element method is a fascinating topic and an extremely powerful tool for those who pursue a structural engineering career. Working with a finite element method topic does not only significantly improves your skill with any FEM software, but this also deepens your understanding of the physical and mathematical theories behind it.

1.3 Research objectives and research question

The research question of this thesis is to recreate and simulate a tensile testing specimen with finite element modelling, using LS-Dyna as the main FEM software. The objectives of this thesis are to create a finite element model that represents the geometry with the real test specimen and correctly define the material properties input for LS-Dyna. The material inputs must provide a correct output result, where the load-displacement curve must resemble the pattern of the curve from the tensile test performed by Nguyen (2018), to give a correct numerical estimation of the material properties of the HAZ. This thesis belongs to a larger research project on high strength steel, conducted at HAMK Tech which, in collaboration with SSAB, is performing multiple studies on high strength steel. The ongoing studies involve a large number of physical testings of connections and material properties of HSS. Previous Bachelor’s theses of Nguyen (2018), Giraldo (2016), Grecevci (2016), Abebe (2016) focused on the physical testing aspect of the research. However, usually, this type of testing is expensive, therefore this old testing approach should be seen in a new light, and

computational testing simulation can be a promising avenue. By constructing a correct finite element model with a realistic estimation of the material properties, the techniques and principles can be applied to construct new testing simulations of new materials. In this way, high expenses of physical testings can be reduced as the behaviour and mechanism of the test can be partially anticipated through finite element simulation.

1.4 Future utilization

Some research with physical testing on different aspects of HSS and HAZ were made before the beginning of this thesis. However, with regards to the finite element modelling of the heat-affected zone, this is the second research of this series. The first research focuses on constructing a shell model of a welded tee joint tubular sections made from SSAB StrenX S700. (Veresov, 2019) Although there is still room for improvement, Veresov (2019) opened a new and prospective approach to the problem. The shell model correctly predicted the failure mechanism of the real testing, whilst showed resemblance in the output data with the testing data through the load-displacement curves. Veresov (2019) has created a platform for the continuation of this topic by making the commencement with the geometry build of the shell model. The material data conversion from Veresov (2019) offers a great point of reference to the material data input of this thesis, alongside with the meshing technique, load and boundary condition data. This thesis is set to follow the same purpose to obtain similar output data with the testing result and to create a platform for the commencement of the next thesis research. This thesis provides information on the geometry build of both shell and solid model of the tensile specimen. The bias meshing technique used in this thesis will give instructions on how to reduce the number of elements, thus shortening the simulation time of the finite element model. The failure strain analysis of the heat-affected zone of this thesis can be utilized for estimating the failure strain, as well as the material input data in MAT024. The documentation of this thesis work presents an overall view of the principles and approaches to construct a finite element model of any tensile specimen, both shell and solid.

2 Background and Literature review

2.1 Literature review on high strength steel welding research

Article: Peltonen, M. (2014). Weldability of high-strength steels using conventional welding methods. Master's thesis. Degree Program in Design and Production Engineering. Aalto University

2.1.1 Weldability of high strength steel

Peltonen (2014, p.20-22) gives a clear overview of high strength steels and what are the major differences in the welding procedure of high strength steels compared to normal steels. This chapter explains why the chemical composition and the microstructure lead to the existing difficulty in welding of high strength steels.

Inside the composition of high strength steel contains two contradicting properties that bring a challenge to the welding process, which are the hardenability and the weldability. HSS have higher tensile strength than normal steels due to their hardenability. With higher hardenability, the tensile strength of steel increases, but simultaneously the formability and weldability of steel decreases. To solve this issue, improved weldability can be achieved by lowering the carbon content of HSS. This approach helps to reduce the hardenability of steel; however, it also reduces the carbon content inside HSS, which downgrades the tensile strength of HSS back to normal steel. Another existing issue with the weldability of high strength steel is that, when the hardness and strength of steel increase, the requirements of the welding process of HSS become more demanding. This is a problem, not only to steel manufacturers but also to welders and manufacturers of the welding machines and consumables. Higher steel grades require higher heat inputs, which set a limitation for welding because only a restrained number of welding machines and consumable selection are applicable to this advance process. Costs for welding of HSS are also considerably higher than normal steel due to its complexity, which makes it more

difficult for manufacturers to make an appealing offer to their customers. This partially explains why HSS is not yet popular and widely used in the field of construction.

This section provides well-rounded background information of the current situation as well as different challenges that the research on HSS weldability is facing.

2.1.2 Relationship between heat input and cooling time

Peltonen (2014, p22) explains the main principles and defines the relationships between heat affected zone, heat input and cooling time. These chapters also present how the heat input, cooling time, along with other factors such as thermal conductivity, preheat temperature, plate thickness and joint configuration can affect the microscopic structure of the heat affected zone after welding.

The heat-affected zone and its mechanical properties such as tensile strength or impact toughness are highly dependent on input energy and the cooling time. Heat input is the key parameter to assess the weldability and how much thermal energy can be applied to a material. In conventional welding method, the process is more difficult to control, which can result in excessive heat input. This leads to some conditions that do not meet the requirements and each zone of the HAZ gets wider and loses its initial strength. Apart from the heat input, the cooling time has a significant impact on determining the resulting microstructure of the heat-affected zone. Cooling time represents the time that is needed for a welded joint to cool down from 800 to 500 ºC ($\Delta t_{8/5}$). As the $\Delta t_{8/5}$ decreases the cooling rate increases and the hardness in HAZ increases, therefore the microstructure in the HAZ has many different phases which highly depend on the $\Delta t_{8/5}$ and the composition. The cooling time is also directly related to and influenced by the amount of heat input. Higher heat input can expand the area of the weld and the heat-affected zone, thereby increasing the time to cool down the welded area. It is highly recommended in HSS welding to use a minimal heat input to achieve the shortest cooling time possible and to establish the similar mechanical properties of HAZ with those of the base material.

These chapters give a detailed definition of how each factor can affect the properties of the heat-affected zone. They also present a clear definition of other contributing factors and how they are directly related. With the provided information, the 1 weld run tensile specimen series in Nguyen (2018) can easily be predicted to be the most critical series. The content of these chapters also supports role and consolidates the approach used in Nguyen (2018).

2.1.3 Transformation of microstructure in the heat-affected zone

Peltonen (2014, p26) presents a detailed description of the heterogeneous microstructures at the welded joint created due to different thermal influences from the heat input and cooling time.

There are three main zones that can be categorized at a welded joint (Kou, 2002):

- Fusion zone (FZ)
- Partially melted zone (PMZ)
- Heat affected zone (HAZ)

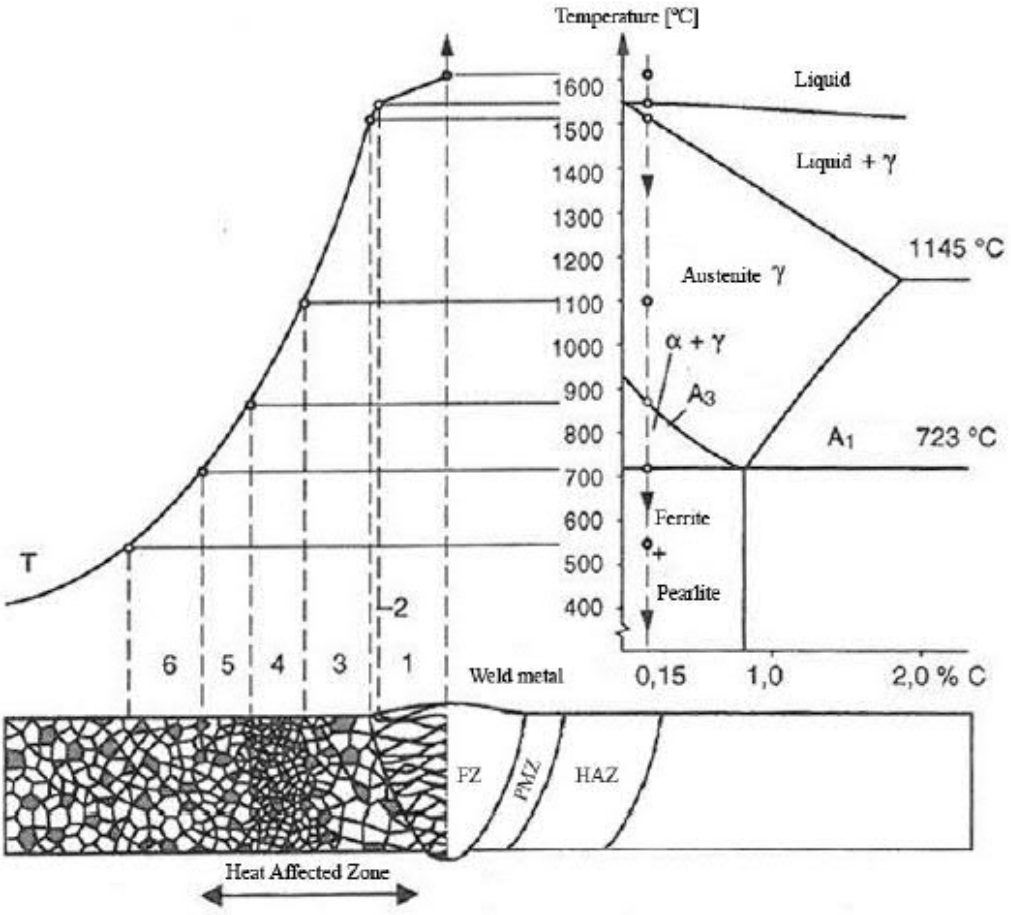

Figure 1. A schematic presentation of different regions at the welded joint.

The HAZ is sub-divided into three main regions:

- Coarse-grained heat-affected zone (CGHAZ)
- Fine-grained heat-affected zone (FGHAZ)
- Inter critical heat-affected zone (ICHAZ)

CGHAZ is the most critical zone inside HAZ, which makes HAZ the weakest link within the welded joint. CGHAZ is located next to the FZ and is exposed to high temperatures around 1200 - 1500 ºC. The grain size of austenite grows at high temperature and the coarsening depends on many factors. They can be the peak temperature, the time above zone A3 temperature in Figure1 when the coarsening happens and the chemical composition of the HSS. The carbon content in HSS now results in the mechanical

properties change of the zone. During the cooling stage, the coarse-grained austenite transforms to non-equilibrium products which significantly depend on the cooling rate. With rapid cooling rate, hard phases can form during cooling. Hard phases like upper bainite or even martensite appear and reduce the toughness and hardness of HAZ. (Peltonen,2014)

In the finite element model of this thesis, the heat-affected zones are modelled as 1 region with uniform material properties, which mainly resembles the properties of CGHAZ. However, for the continuation after this thesis, a more detailed model can be constructed with more regions inside heat affected zone to give a more precise estimation to each region.

2.2 Literature review on Finite Element Analysis method

Article: Erhart, T. (2011). Review of Solid Element Formulations in LS-Dyna. Stuttgart. LS-Dyna Forum 2011. Retrieved on the 06th of January 2021 from:

https://www.dynamore.de/en

The article gives a clear overview of the ELFORM (Element Formulations) parameter that is used by LS-DYNA for implicit calculations of shell and solid model. With a clear understanding of the ELFORM options, a suitable formulation is determined for the shell and solid model of this thesis. The article approaches the ELFORM categorization by sorting suitable formulations for the element's shape and geometry.

With hexahedra elements, ELFORM 1, ELFORM 2 (-1/-2) and ELFORM 3 are applicable, while with tetrahedron elements, ELFORM 4, ELFORM 13, ELFORM 16 and ELFORM 17 are more suitable. In this review, formulations for hexahedra elements are analyzed more thoroughly, since they have the direct application to solid element shape of this thesis model.

ELFORM 1 solves the physical state of an element with a single integration point. This method is much faster than the full integration and it proves to be more stable with large states of deformation simulation. However, when severe deformation appears, solid models with ELFORM 1 tend to encounter the Hourglass effect, due to the under integrated elements. This can be managed by introducing an Hourglass control formulation to stabilize the non-physical deformation that results in the Hourglass phenomenon.

ELFORM 2 uses a fully integrated element formulation, therefore the Hourglass effect does not appear, and an Hourglass stabilization control is not required. However, in this formulation, eight points of the hexahedra are all integrated and that leads to an over stiffness problem of the model. ELFORM 2 is also more unstable with large deformation and when shear locking effect occurs, enhanced strain formulations must be used. ELFORM -1 and –2 formulations are introduced to fix the issue of shear locking by reducing the spurious stiffness without affecting the true physical behavior of the element.

ELFORM 3 also uses the fully integrated element, combines with nodal rotations, which allows up to 6 degrees of freedom per nodes. Considering the extranodal rotations, this formulation is suitable for locations where solid elements are connected to shell elements.

Under comparison for total CPU time, EFORM 1 is the most economical and efficient with the lowest simulation time.

2.3 Weld run tests

Cooling time can be managed by using different welding methods, which results in a different number of weld runs needed to be performed, in order to reduce the cooling time of each run and subsequently decrease the cooling time of the entire weld.

Previous Bachelor's theses in this topic were set to study this problem (Nguyen, 2018, Grecevci, 2016). Similar test programs were performed to find the influence of a different number of welds runs on the ultimate tensile strength of steel grades from S420 to S960. Both studies measured the cooling time and heat input and use them as quality control parameters, which later become the definition of welding procedures. However, a practical parameter to the efficiency of different number of weld runs is based on tensile tests, where the results from two studies are very different.

Despite the efforts to explain the causes of the differences between Nguyen (2018) and Grecevci (2016), the exact reasons for the variety in the tensile test results of similar steel grades were not conclusive. This variation can be caused by unevenness of the welding process itself, poor surface preparation before welding, unsuitable filler material and a few other issues. For the purpose of this thesis, it is important to state that this thesis will not pursue to give an explanation to the differences between the two studies. Testing data used in this thesis is extracted solely from Nguyen (2018).

The problem with cooling time and heat input is that ultimately the basic unit of energy input into welding is the same, therefore the joint will be weaker as a result. The process of conventional electric arc welding requires a default unit of energy input to reach the melting point from any number of welds, leaving cooling time as the primary quality control parameter of welding quality of HSS.

This creates a challenge in implementing the cooling time results in the design of welded joints since the welds must be the strongest part of the connection to ensure the safety of the structure. However, due to the weakening nature of the cooling process of the welds, it leaves the most critical uncertainties to the mechanical properties of HAZ to be determined.

2.4 Choice of S500 tensile specimen

S500 tensile specimen is chosen for modelling the simulation of this thesis, and the reason for this selection will be clarified in this paragraph. The tensile testing was performed with high strength steel specimen ranging from S420 to S960, however, specimens with steel grades S700 and S960 have unpredictable tensile results due to the cracks appeared in at the joints. The filler material used for these steel grades also has weaker tensile strength than the base material, which can lead to failure at filler material zone instead of heat-affected zone. From Nguyen (2018), it was concluded that S420 and S500 specimens provide more reliable results. Both S420 and S500 specimens follow the anticipated trend of the lower the cooling time, the higher the tensile strength. Alongside with the tensile test, hardness tests for these specimens were also performed. The hardness values were converted to tensile strength using conversion formula extracted from Zhang et al (2011). The comparison between tensile test values and the converted harness test values also gives a consolidating result to the S420 and S500 specimens.

3 LS-Dyna input model creation

The content of this section aims to present the transformation of the testing data from Nguyen (2018) into input data in LS-Dyna finite element model.

Geometry creation, mesh generation, keyword management as well as output control are done through LS-PrePost, which is an LS-Dyna platform for creating and preparing the model before simulation. The model is then processed, and simulation is performed by LS-Dyna manager. The final step belongs to the Post-Processing platform, through binary plot file, to extract and analyze results of the finite element model.

The main approaches and concepts of constructing the shell and solid model of the tensile specimen are presented to give an overall description of the modelling process,

but the actual process can be more arbitrary and more sophisticated when the requirements for the model are more specific. The justification for choosing an S500 specimen is given in section 2.2, while the results to achieve from the testing data is stated in section 4.1. The creation procedure of the geometry, boundary regions and materials of the model are described, followed by the determination of material model and its material properties. This section also presents the definition of load application and support conditions of the model. A more detailed procedure of a step-by-step construction of the finite element model can be found in Appendix 1 and Appendix 2.

3.1 Testing of S500 specimen

From the commencement of the thesis process, a testing specimen needed to be chosen from 48 specimens with presented results in Nguyen (2018). The 48 specimens were categorized into 4 steel grades and 3 types of weld run (1 weld run, 2 weld runs, and 3 weld runs). The steel grades used for testing were S420, S500, S700 and S960, chosen from SSAB catalogue, manufactured from thermomechanical hot-rolled steel. For each number of weld run, 2 steel plates with the dimensions of 200x200x8mm are welded together. The end of each plate is cut at an angle of 60˚ where they were welded together. Plates' dimensions and geometry can be found in Figure 3 from Nguyen (2018). While the base material (or parent material) are different steel grades mentioned above, all specimens used the same filler material (or weld material) 1.2mm OK ARISTOROD 69 (or ESAB x69). The welding process was performed in Tavastia Vocational School, Hämeenlinna by a professional welder Mr. Harri Nieminen to ensure the uniform quality of the welds. The selection criteria are:

- A clear failure mechanism
- Equivalent stress-strain results
- Clear geometry for modelling

As presented in more detail in chapter 2.2, S700 and S960 have unpredictable tensile results because of the early cracks in the connection area and their filler material has a lower tensile strength than its base material. S420 and S500 provide more

predictable and reliable results as they follow the trend of the lower the cooling time, the higher the tensile strength.

The S500 series was tested with 6 specimens, divided into 3 groups of 1 weld run, 2 weld runs, and 3 weld runs. During the welding process, the heat input must rise above the melting point of the material. This leads to different cooling times and cooling times resulted after different weld runs were applied. With 1 weld run, the weld requires higher heat input and longer cool time per run, while more weld runs require lower heat input and less cooling time per run, which significantly changes the material properties of base material around the weld, turning them in the heat-affected zones. As concluded in Nguyen (2018), 1 weld run exerted the most detrimental effect on the heat-affected zone due to the high heat input, S500 specimen with 1 run was chosen for finite element model of this thesis, particularly specimen S500-1R-2.

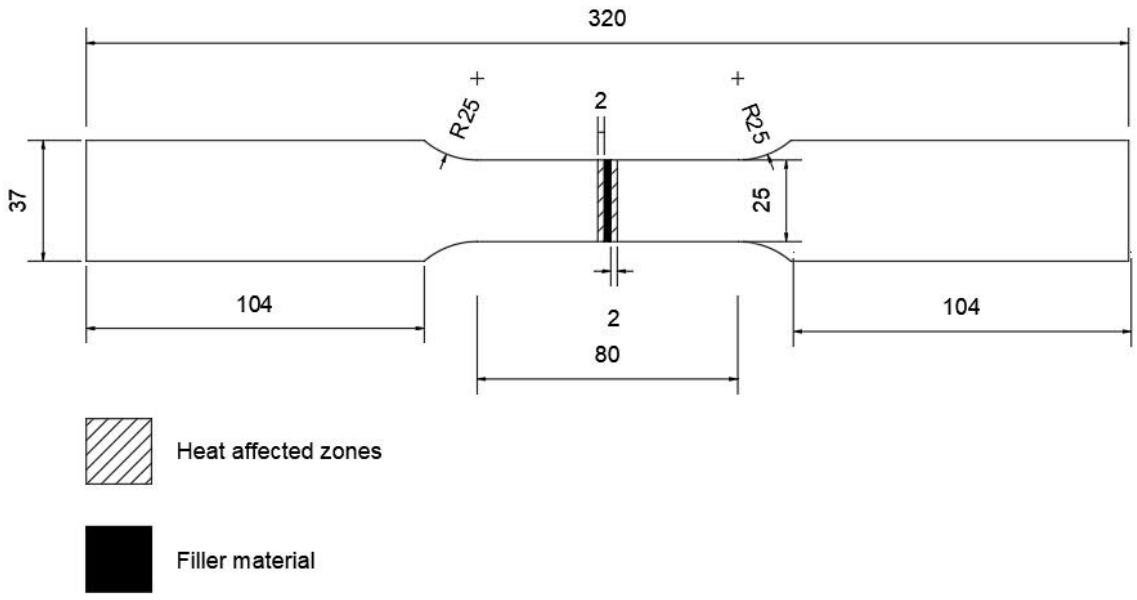

Figure 2. S500-1R-2 bottom view dimensions

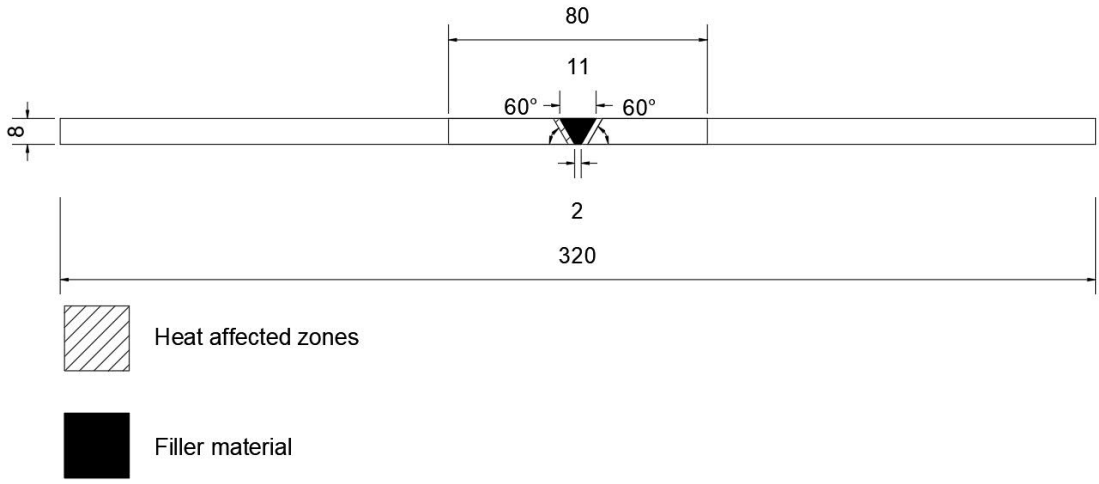

Figure 3. S500-1R-2 side view dimensions

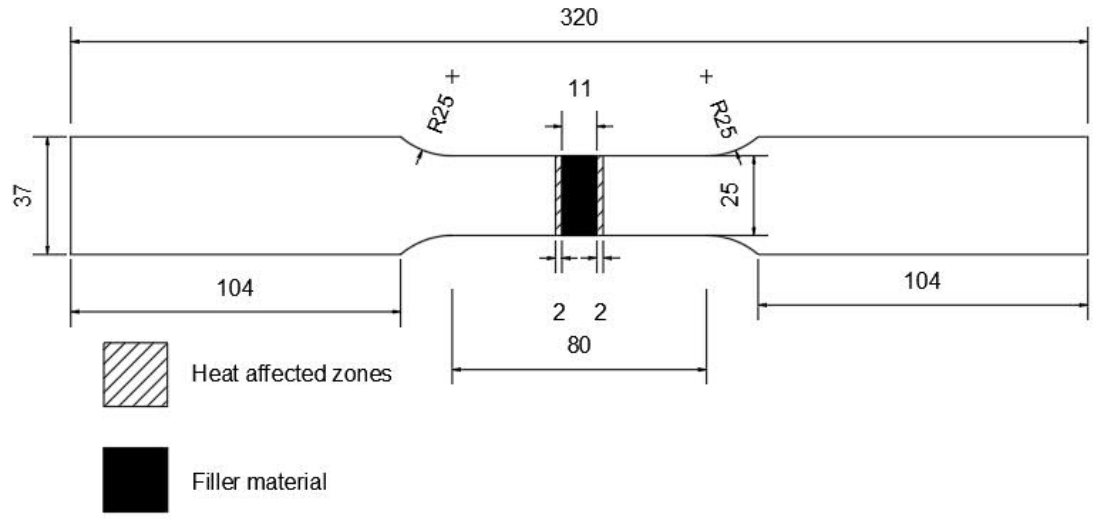

Figure 4. S500-1R-2 top view dimensions

The correct dimensions were retrieved from the testing preparation documents from Nguyen (2018). More detailed dimensioning is provided in the drawings in Figure 1, Figure 2 and Figure 3 to serve the later purpose of 3D modelling the finite element solid model.

Apart from the detailed geometry of the tensile specimen, a clear failure pattern and testing result curves are extremely crucial to the transformation of the material parameters.

Figure 5. Failure pattern of specimen S500-1R-1 from (Nguyen, 2018, p77)

Figure 6. Failure pattern of specimen S500-1R-2 from (Nguyen, 2018, p77)

From Nguyen (2018), stress-strain curves of the tensile test are used for data conversion inputs to LS-Dyna. To compare results between the model specimen and testing specimen, the load-displacement curve of the testing specimen can be retrieved by extracting points from the stress-strain curves and using these conversion formulas:

- Displacement (d) = Engineering strain (ε_e) x Gauge length (L_0)
- Load (F) = Engineering stress (σ_e) x Cross sectional area (A)

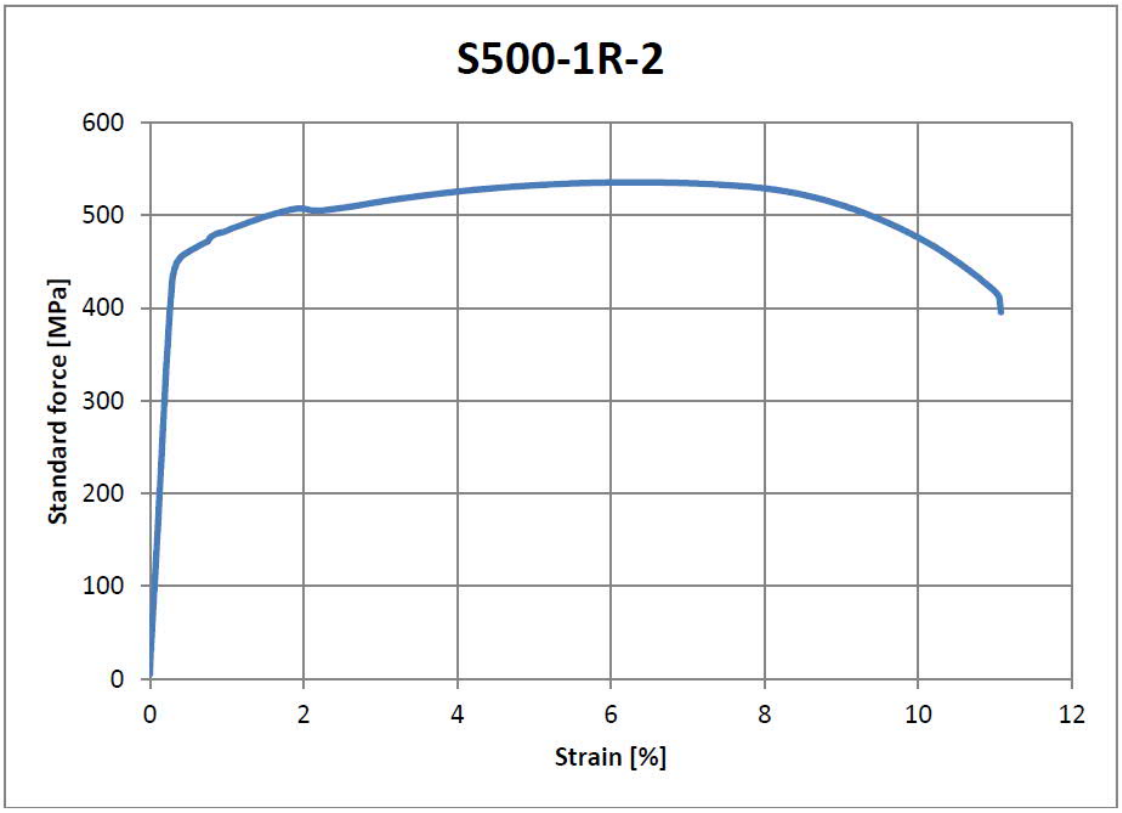

Figure 7. Stress-strain curve of specimen S500-1R-2 (Nguyen, 2018, p67)

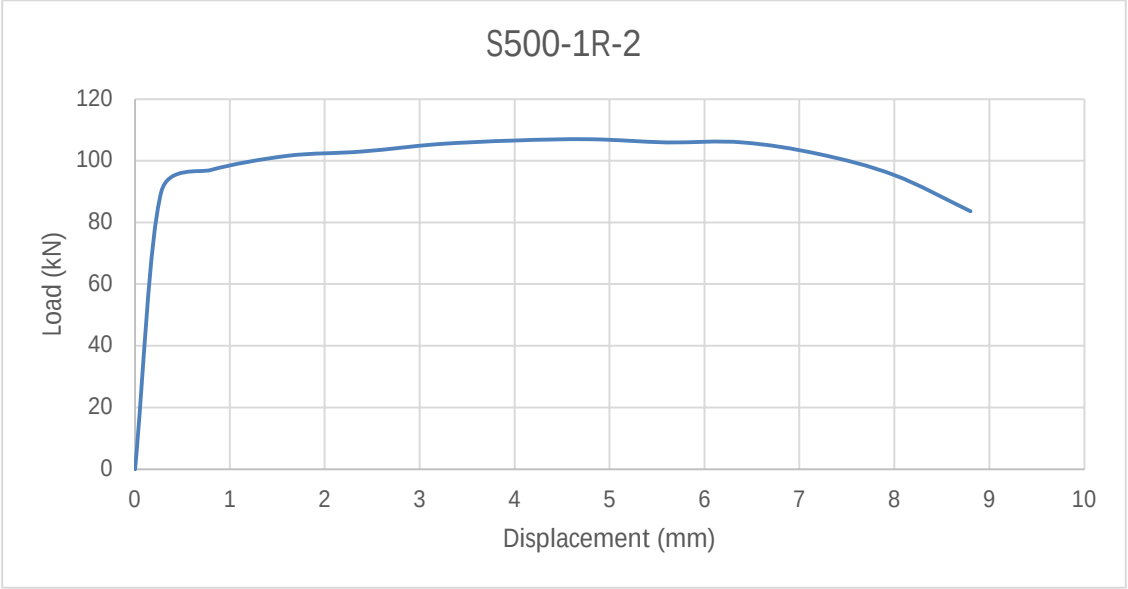

Figure 8. Converted load-displacement curve of specimen S500-1R-2

3.2 Geometry modelling

3.2.1 Geometry modelling of shell model

Different views of the tensile specimen are given in Figure 2, Figure 3 and Figure 4. These figures provide the required dimensions for the purpose of constructing the geometry of the shell model. From an observation of the failure pattern of the real testing specimen, as well as the failure mechanism of the solid model simulation, the failure always starts from the bottom face of the specimen at the heat-affected zones. This has proven that the HAZ area of the bottom is the most critical region of the specimen and thus the bottom view scheme, shown in Figure 2, is used as for the geometry creation of the shell model.

The main principle of creating a shell model is to build the tensile specimen with a 2D geometry. This 2D geometry contains the width and the length dimensions of the specimen, while the third dimension (thickness) is defined through the model shell section keyword, specified in chapter 3.3.

The idea of creating a 2D geometry can be given away as an easy task, however, there many different approaches to solving this question, and the key task is to identify the most optimal and economical approach. The procedure of creating the geometry of the shell model can be separated into three main steps:

- Initial geometry creation
- Mesh creation
- Creating material regions

For the sake of simplicity, the process starts with creating the initial geometry by using the 2D Mesh Generation tool in LS-PrePost platform.

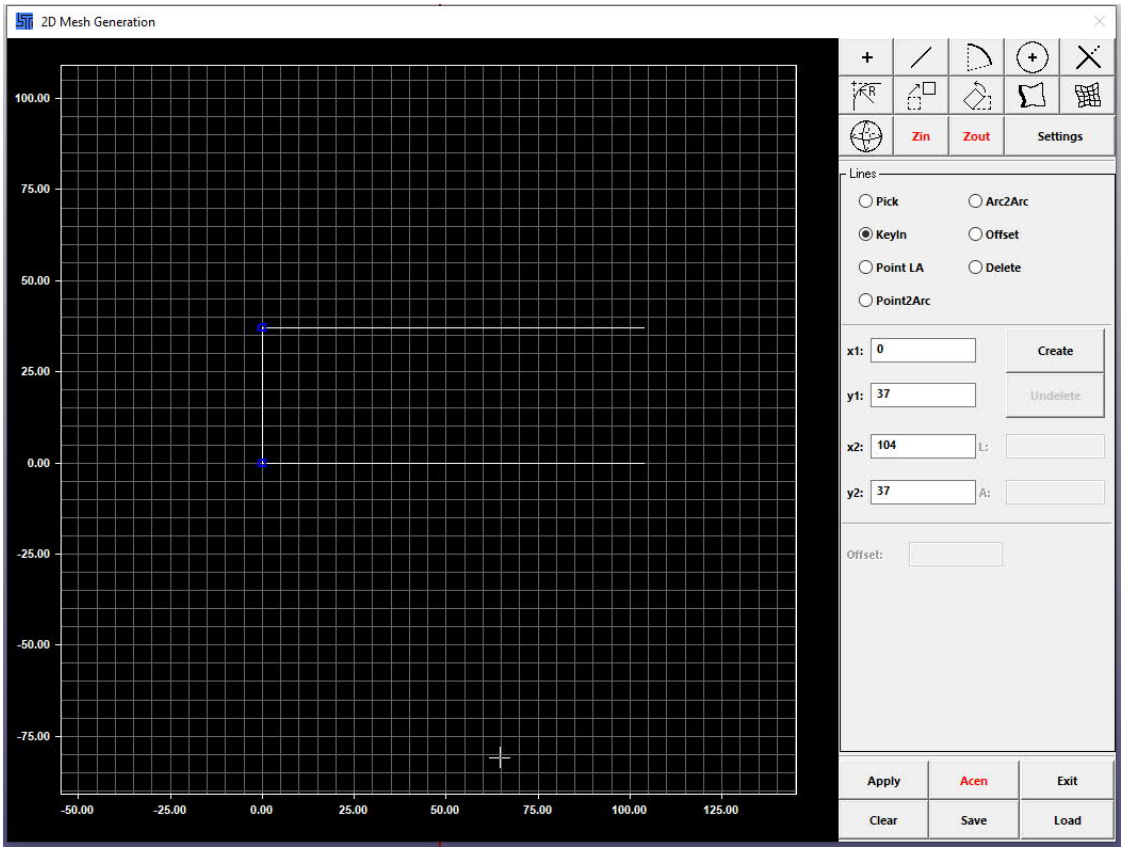

Figure 9. 2D Mesh Generation tool from LS PrePost

Figure 9 illustrates the principles of creating the initial geometry of the shell model. Lines and curves of the shell model were created separately by inserting the start and end coordinates.

After the initial geometry has been created, edges of the specimen are defined to assign the number of elements per edge. This is the beginning of the meshing stage when the meshing density and the element sizes are determined. When the number of edges is defined and the elements per edge are defined, the meshed shell structure is created from the initial geometry.

Since the specimen comprises of 3 different materials, the regions of these materials must be redefined from the newly meshed shell model. This can be done through the Move or Copy tool from the Element tool. This tool helps to transfer the properties of a created part to a new part. By selecting the area and assign them with new PID (part

ID), the material regions will be created and assigned with a new part ID and color. When the meshed regions are created separately, a connecting step must be performed to merge the separated nodes, otherwise, the material regions will act as individual parts, not as a whole specimen. To fix this, the Duplicate Nodes tool helps to merge the separated nodes together, thereby creating 1 whole shell model with different material regions. The detailed guideline for creating the shell model is documented in Appendix 1.

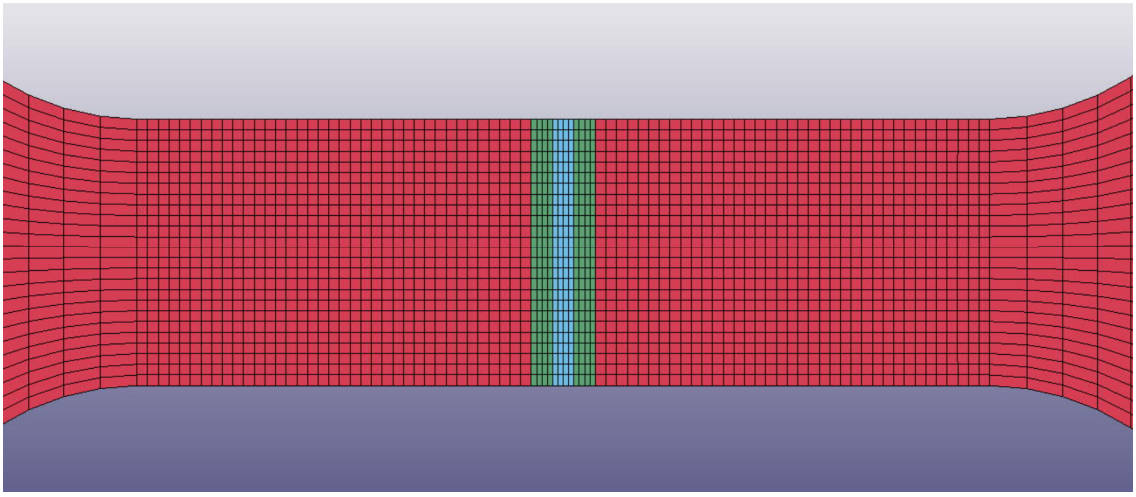

Figure 10. Bottom view of the material regions in shell model

Figure 10 shows the general division of the mesh regions used on the shell specimen. Red mesh indicates parent material, green for heat-affected zone (HAZ) and light blue for filler material. 2 mm width influence zone of HAZ was chosen based on a scientific approximation of the weld fusion concept and thus interprets the properties of the coarse-grained heat-affected zone, discussed in chapter 2.1.3. Figure 11 also presents the regions of each material in the real testing specimen, which the width of HAZ was measured to be roughly 2mm. This leaves a critical 2mm wide region of the heat-affected zone (also called baking zone) with reduced properties.

With regards to element size, Filler material & HAZ have element size of 0.5 mm x 1mm x 1mm (width x length x height), while base material has 1 mm x 1mm x 1mm elements within gauge length region, and 1 mm x 5mm x 1mm elements outside gauge length

region. This size system provides a gradually increased mesh structure, in order to reduce the simulation processing time, while the element sizes are still well kept within a good aspect ratio of 1:5 for both ratios of dimension-to-dimension in one element, as well as element-to-element dimensions.

3.2.2 Geometry modelling of solid model

The transition from modelling geometry of a shell model to a solid model undergoes a different process and approach in initial geometry generation and mesh creation. In the shell model, the main principle of geometry modelling is to create a 2D mesh, then the third dimension of the specimen is defined through the shell section keyword. This approach is not applicable to the solid model, due to the considerations of element quantity, element size, element shape, aspect ratio and nodal interfaces. The most challenging task for transforming the shell model to the solid model is modelling of the heat-affected zones. The tensile specimen has a butt weld connection between the 2 base material plates at an angle of 60°. This increases the complexity of the modelling procedure of the HAZ and filler material since the contact surfaces between different regions are required to be smooth, while still maintaining a correct nodal interface between materials. During the process of creating a correct geometry, many experimental solid models were made and analyzed with different HAZ geometries. Figures below show the original image of HAZ from the testing specimen, and some experimental HAZ models that were constructed before the final model is obtained:

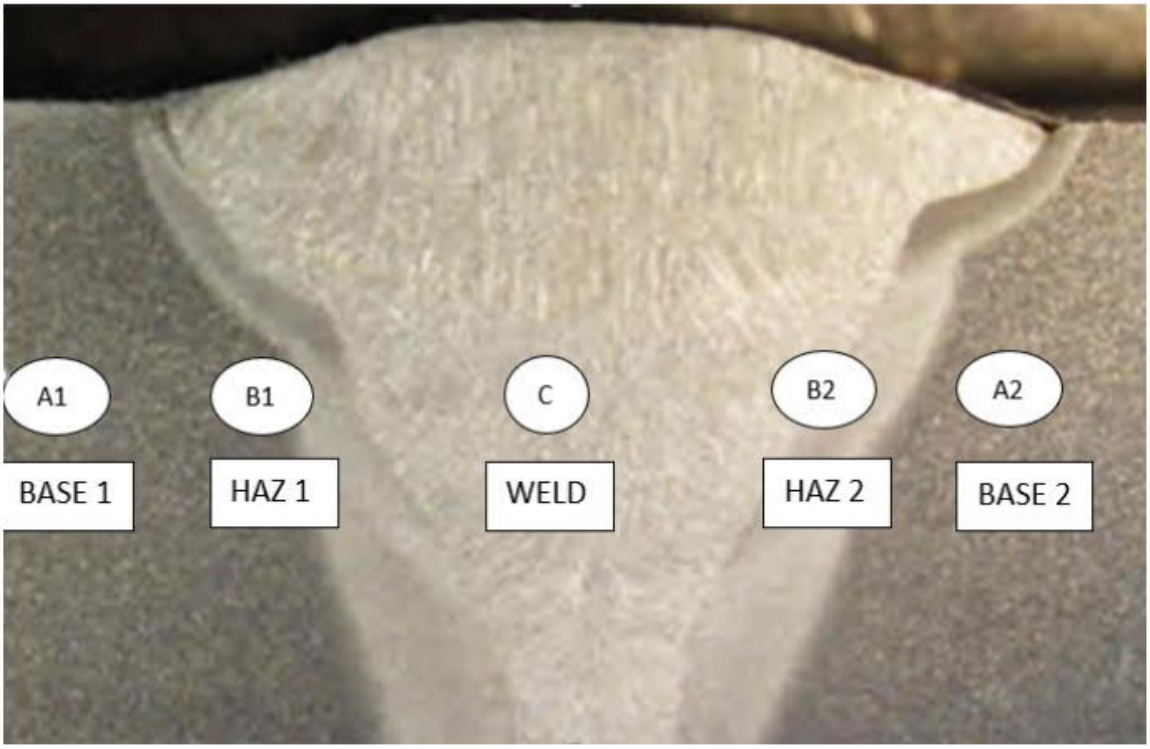

Figure 11. Original HAZ image from the testing specimen (Nguyen, 2018, p22)

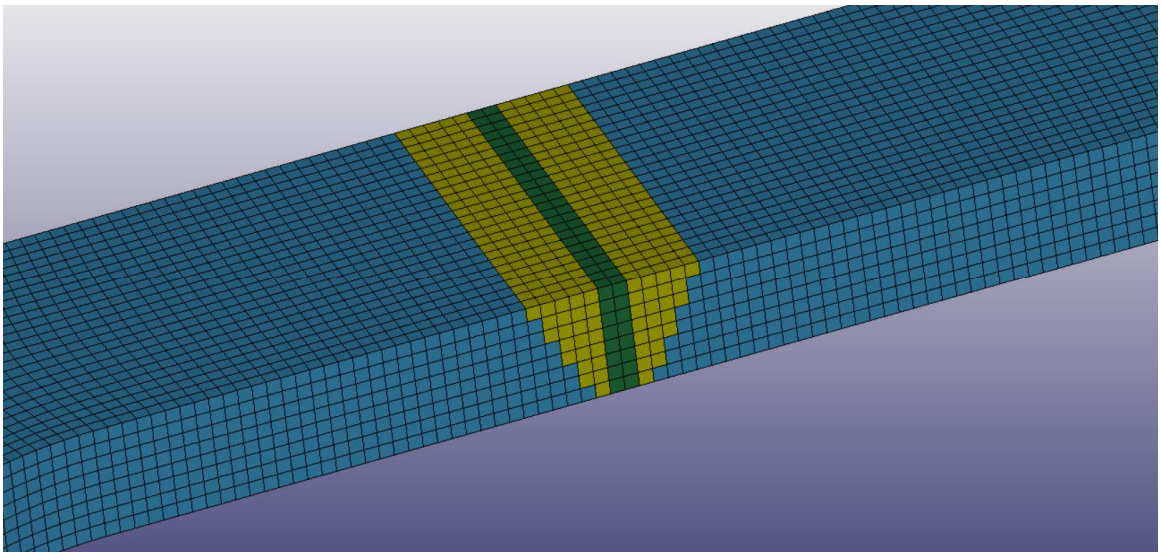

Figure 12. Experimental solid model 1 with triangular HAZ zone

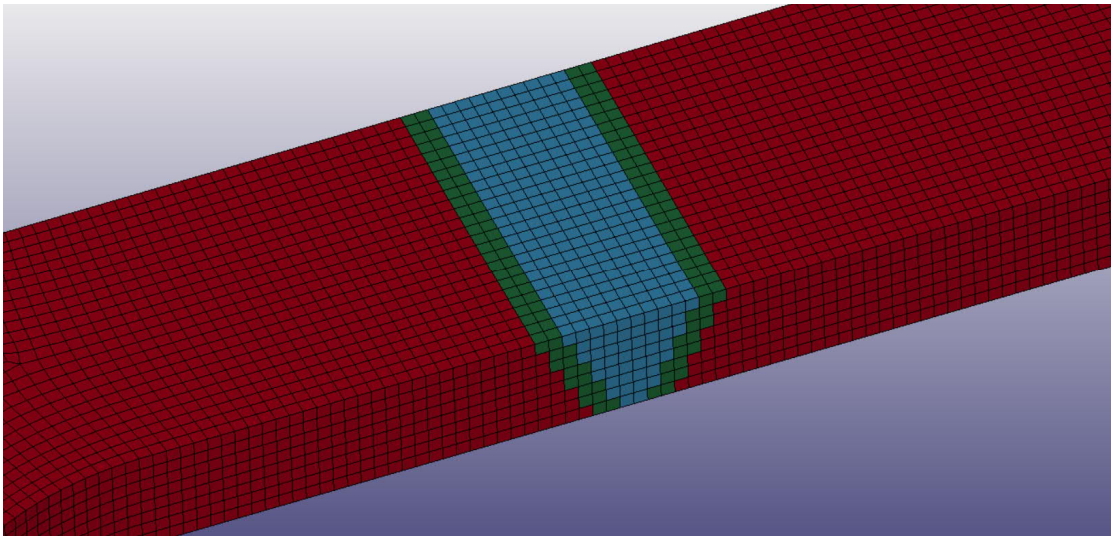

Figure 13. Experimental solid model 2 with 2mm unsmoothed HAZ zone

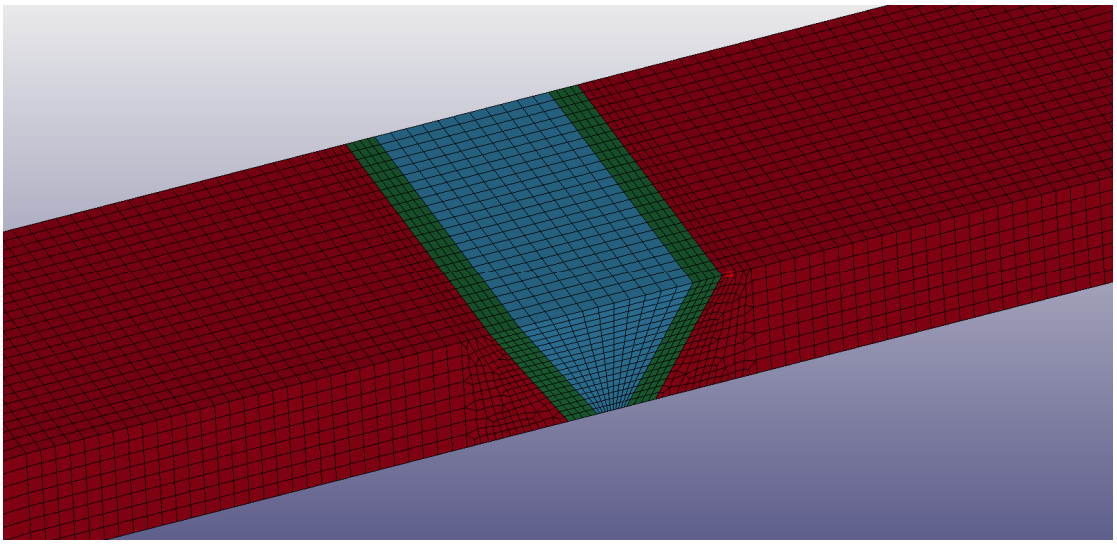

Figure 14. Final solid model with 2mm smoothened HAZ zone

In Figure 12, the unsmoothed HAZ zone shares similar geometry principle to the final model shown in Figure 13, with 2mm width and 60° angle of HAZ to the horizontal plane, while the difference is where the elements of HAZ were created perpendicularly to the direction of the applied force. The modelling work of experimental model 2 is much more simple than the final model, however, this model is not precise, since the direction of the elements should be parallel to the real HAZ angle, otherwise the

simulation will predict a deviated physical state of these elements from the real testing HAZ due to the incorrect orientation.

The biggest challenge for creating the solid model originates from many specific requirements that must be fulfilled to keep it in check with the real testing specimen. The HAZ elements must be modelled at 60° angle orientation, while still maintaining a correct nodal interface with other material elements next to them. This is a very intricate task since the HAZ elements are skewed, while base elements are straight, not mentioning the element size must always be kept within a correct aspect ratio and shape. Simultaneously, the element size should not be kept identical throughout the whole specimen, otherwise, the simulation time will be enormous. From this standpoint, a new approach in creating the solid model must be taken to fulfil the mentioned requirements. The new procedure can be divided into the following steps:

- Initial geometry creation
- Mesh shell creation
- Extrusion of 2D mesh
- Nodal interface connection

Different from the approach used in chapter 3.2.1, the process of initial geometry creation uses Line Segment and Curve Arc tools to generate line by line and curve by curve of the 3D geometry of the tensile specimen. Different regions of the specimen must be separated correctly by the single lines with closed edges, as this will be vital in the step when establishing the mesh shells.

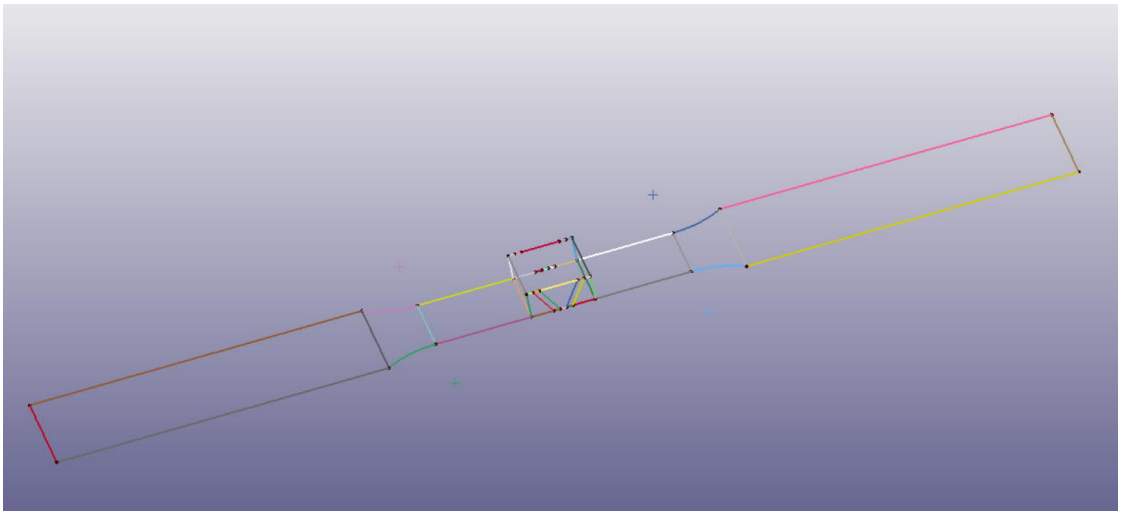

Figure 15. Single line geometry of the 3D model

After the line skeleton of the specimen is created, a new technique will be used to generate the mesh shells, since the old technique used in chapter 3.2.1 can only be applied to 2D geometry. N-Mesher tool with 4 lines Shell option is used for this purpose.

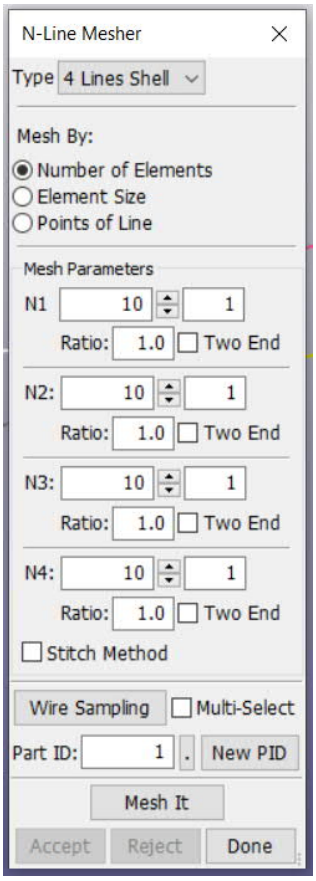

Figure 16. N-line Mesher tool with 4 Lines Shell type

4 Lines Shell type allows the most authority to manipulate the number of elements assigned per edge, since 4 edges of a quadrangle are defined with a biased number of elements assigned to each edge, in this way the size of an element is defined through edge's length divided by the number of elements per edge.

In the extrusion of 2D mesh step, to achieve 60° skewed elements in HAZ regions, shell meshes of filler material, HAZ and parts of base material must be created in XZ plane and extruded in the Y direction. While for the rest of the base material, shell meshes must be created in XY plane and extruded in the Z direction, due to the change of geometry at specimen curves. Element size at contact surface is kept uniform at 1mm x 1mm to ensure a linear correspondence of the nodal interfaces between 2 adjacent material's surfaces. If the interfaces are well modelled, the nodal connecting step between 2 surfaces becomes a simple task of merging the duplicate nodes, like the procedure done for the shell model, mentioned in chapter 3.2.1.

3.3 Section type

Section type is an extremely crucial keyword that determines what formulation will be used in the simulation process to solve for the physical state of the elements. The technical work of this thesis is divided into 2 separate processes of constructing the shell and solid model. The shell model has a clear advantage in the simulation time and the simplicity of the model. However, the shell model can only capture partially the failure pattern at the bottom side of the tensile specimen, leaving the most critical failure along the 60° angle line of HAZ unobtained. Therefore, the thesis work continues with the solid model to obtain a more detailed look into the failure mechanism of HAZ. However, the solid model needs a massive simulation time, which lasts for 15 hours. This makes the shell model becomes an extremely useful tool in experimenting with different material properties, before using the inputs on the solid model. The shell model helps with predicting the output load and displacement of the model specimen corresponds to the testing specimen or not. This serves as an evaluation parameter for the material properties inputs, helping to decide if they are

precise and realistic enough for the solid model experiment. The approach of using the shell model as a material property experiment for the solid model raises a question in what element formulation should be used to make the 2 models reciprocally correspond.

With the shell section, choices for element formulations are more available since its simulation time is not as significantly large as the solid model. There are 3 possible formulations that are applicable to the shell section: ELFORM 2, ELFORM 12 and ELFORM 13.

ELFORM 2 is not suitable for the tensile test simulation, due to the substantially longer simulation time, which was caused by its additional stiffness that leads to the excessive perpendicular forces, making up for the lack of a third dimension. This is not an economical and proper formulation for this simulation.

ELFORM 12 and ELFORM 13 are similar for the purpose of this simulation, with the difference in the consideration of uniform stress throughout the thickness or uniform strain throughout thickness respectively.

ELFORM 12 for plane stress is chosen to be the main formulation of the shell model, with single integration point element, since the main principle of the shell model fits a plane stress framework, where the stress is equally distributed in a thickness direction. The thickness of 8mm of the specimen is also inserted to this keyword.

The shell section formulation is shown in Figure 17.

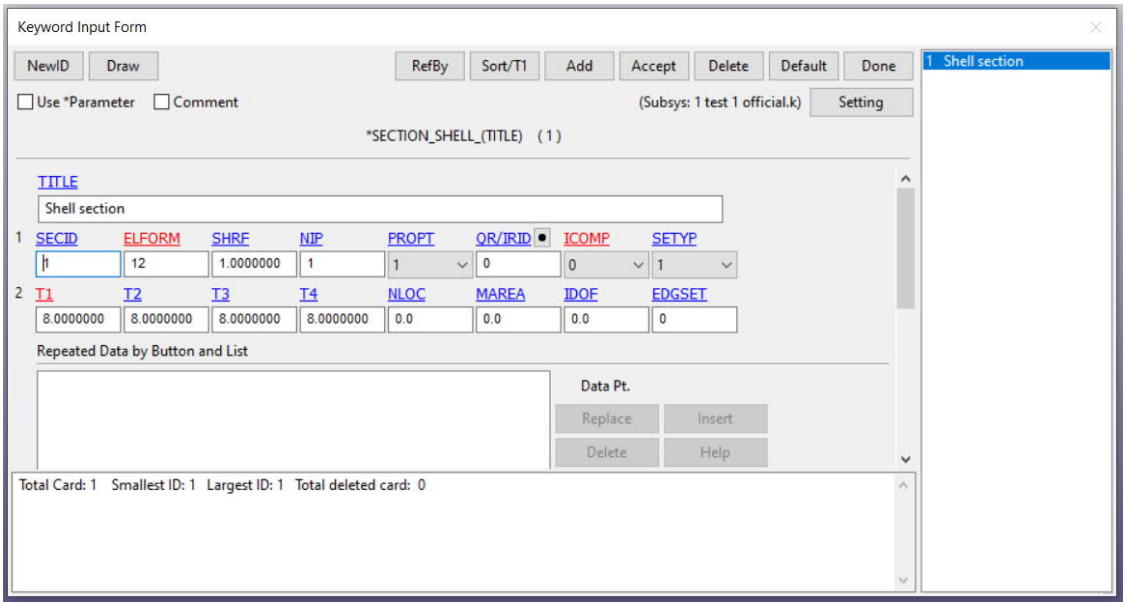

Figure 17. Shell section with ELFORM 12 for plane stress

With a solid section, suitable formulations are discussed in chapter 2.2.
For the solid model of this thesis, the 3 most suitable formulations are: ELFORM 1, ELFORM 2 and ELFORM 3.

ELFORM 1 is the most suitable for the solid model since this formulation is much faster than the full integration and it proves to be more stable with large states of deformation simulation. However, when using ELFORM 1 for the model, Hourglass effect must be controlled, due to the under integrated elements. This can be managed by introducing an Hourglass control formulation to stabilize the non-physical deformation that results in the Hourglass phenomenon.

ELFORM 2 uses a fully integrated element formulation, therefore the Hourglass effect does not appear, and Hourglass control is not required. However, the full integration in this formulation leads to a massive amount of simulation time and over stiffness problem of the model. ELFORM 2 is also more unstable with large deformation.

ELFORM 3 also uses the fully integrated element combines with nodal rotations. However, this formulation also requires large simulation, and since there is no

connection between solid and shell elements in this model, this formulation is not relevant.

ELFORM 1 for constant stress solid is chosen to be the main formulation of the solid model due to the most efficient simulation time. The formulation also works well in model with large deformation. Hourglass control of this model is discussed more specifically in chapter 4.3.

The solid section formulation is shown in Figure 18.

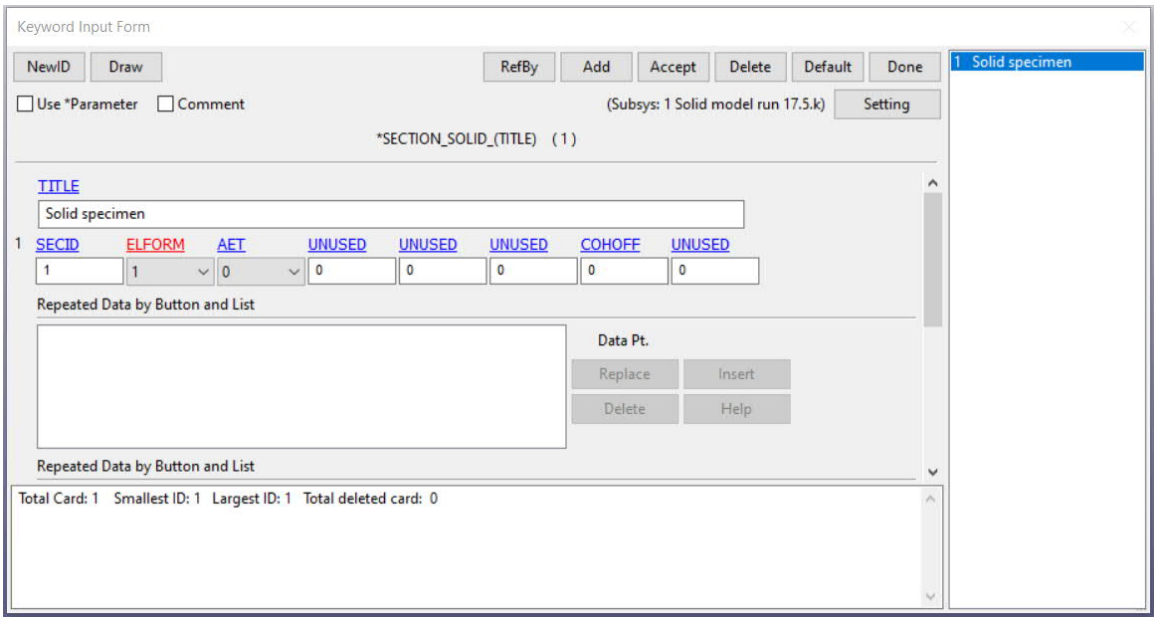

Figure 18. Solid section with ELFORM 1 for constant solid stress

3.4 Material input data

This chapter presents the procedure to obtain the material properties of the model. This process involves a transformation of engineering stress and strain values of the material into true stress and strain for LS-Dyna input data. S500 as parent material and OK ARISTOROD 69 as filler material have well researched homogeneous properties, therefore the transformation procedure is not as challenging as HAZ. For the heat-

affected zone, due to the inconsistency in the cooling time and the baking effect, strength reduction, as well as the plastic behavior of this material, must be carefully investigated.

At the start of the process, a correct material keyword type must be defined. LS-Dyna has a wide range of available options for roughly 300 material models (LS-Dyna user's manual volume 2). However, MAT024 was designated as a material model in Veresov (2019), where the material properties are identical to this thesis. The Piecewise Linear Plasticity (MAT024) is the most used material model in LS Dyna to simulate a plastic and isotropic material behavior with a clear definition of failure parameters, which serves the exact purpose of this thesis to simulate a tensile test until failure.

All LS-Dyna input values presented in this chapter follow the unit system: kg, mm, ms, kN, GPa, kN*mm

MASS	LENGTH	TIME	FORCE	STRESS	ENERGY	DENSITY	YOUNG's	35MPH 56.33KMPH	GRAVITY
kg	m	s	N	Pa	J	7.83e+03	2.07e+11	15.65	9.806
kg	cm	s	1.0e-02 N			7.83e-03	2.07e+09	1.56e+03	9.806e+02
kg	cm	ms	1.0e+04 N			7.83e-03	2.07e+03	1.56	9.806e-04
kg	cm	us	1.0e+10 N			7.83e-03	2.07e-03	1.56e-03	9.806e-10
kg	mm	ms	kN	GPa	kN-mm	7.83e-06	2.07e+02	15.65	9.806e-03
g	cm	s	dyne	dyne/cm²	erg	7.83e+00	2.07e+12	1.56e+03	9.806e+02
g	cm	us	1.0e+07 N	Mbar	1.0e+07 Ncm	7.83e+00	2.07e+00	1.56e-03	9.806e-10
g	mm	s	1.0e-06 N	Pa		7.83e-03	2.07e+11	1.56e+04	9.806e+03
g	mm	ms	N	MPa	N-mm	7.83e-03	2.07e+05	15.65	9.806e-03
ton	mm	s	N	MPa	N-mm	7.83e-09	2.07e+05	1.56e+04	9.806e+03
lbf-s²/in	in	s	lbf	psi	lbf-in	7.33e-04	3.00e+07	6.16e+02	386
slug	ft	s	lbf	psf	lbf-ft	1.52e+01	4.32e+09	51.33	32.17
kgf-s²/mm	mm	s	kgf	kgf/mm²	kgf-mm	7.98e-10	2.11e+04	1.56e+04	9.806e+03
kg	mm	s	mN	1.0e+03 Pa		7.83e-06	2.07e+08		9.806e+03
g	cm	ms	1.0e+1 N	1.0e+05 Pa		7.83e+00	2.07e+06		9.806e-04

Figure 19. Unit table extracted from LS Dyna Support website, Consistent units

3.4.1 Base material (S500)

The material properties of structural steel are usually based on research studies or the manufacturer's catalogue. For testing of specific batches of steel, the tensile test

should be performed beforehand and delivered by the manufacturers in order to certify the conformity of the material to the relevant standards. However, the manufacturer's data for S500 specimen used in Nguyen (2018) are not available, therefore the material properties used for the base material is derived from a research publication on high strength steel. (Rules of high strength steel, 2016, Figure 2-22)

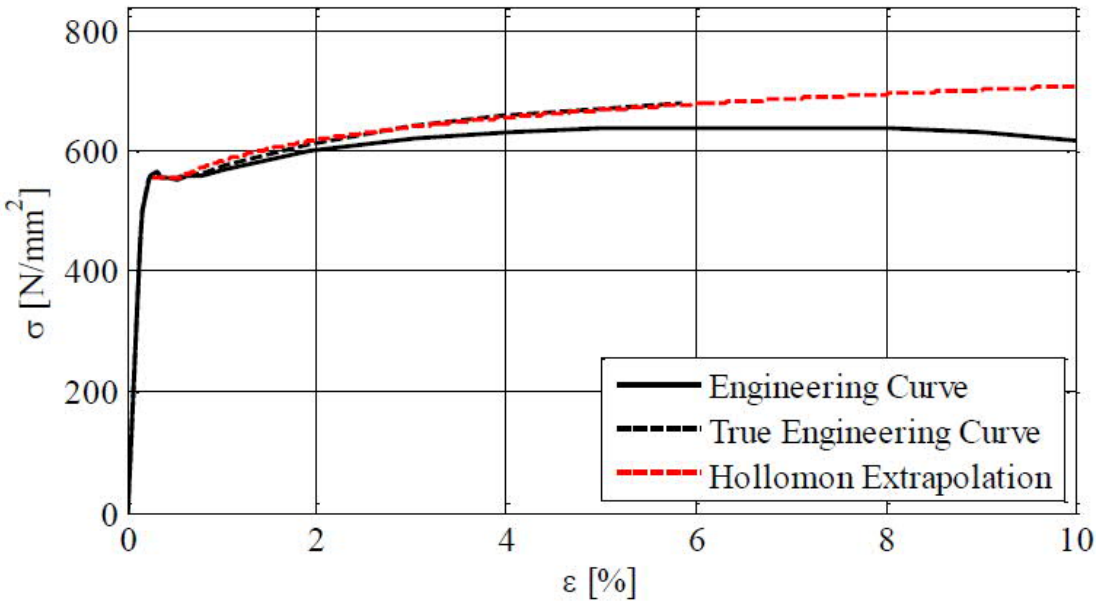

Figure 20. S500 Engineering and True stress-strain curves

Extracted points on the engineering curve are shown in Table 1

Engineering Strain (%)	Engineering Stress (MPa)
0,25	500
0,75	558
1,01	572
2,00	610
3,00	639
4,00	657
5,00	667
5,82	676

Table 1. Engineering input values of base material

Engineering values from Table 1 are converted to True values following the methodology stated in Appendix 3. True stress and strain values are shown in Table 2

True strain	True stress (GPa)
0,003	0,500
0,008	0,558
0,010	0,572
0,020	0,610
0,030	0,639
0,040	0,657
0,050	0,667
0,058	0,676

Table 2. True input values of base material

From True stress and strain values, the effective plastic strain and corresponding stress are calculated, using the conversion formulas in Appendix 3.

Effective plastic strain	Corresponding stress (GPa)
0,0000	0,500
0,0047	0,558
0,0072	0,572
0,0169	0,610
0,0268	0,639
0,0367	0,657
0,0467	0,667
0,0548	0,676

Table 3. Official MAT024 input data for base material

After producing the material input data shown in table 3, they can be input into the model in LS-PrePost in the following form for "MAT024 Piecewise Linear Plasticity". A more detailed discussion of the failure strain parameter can be found in chapter 4.2

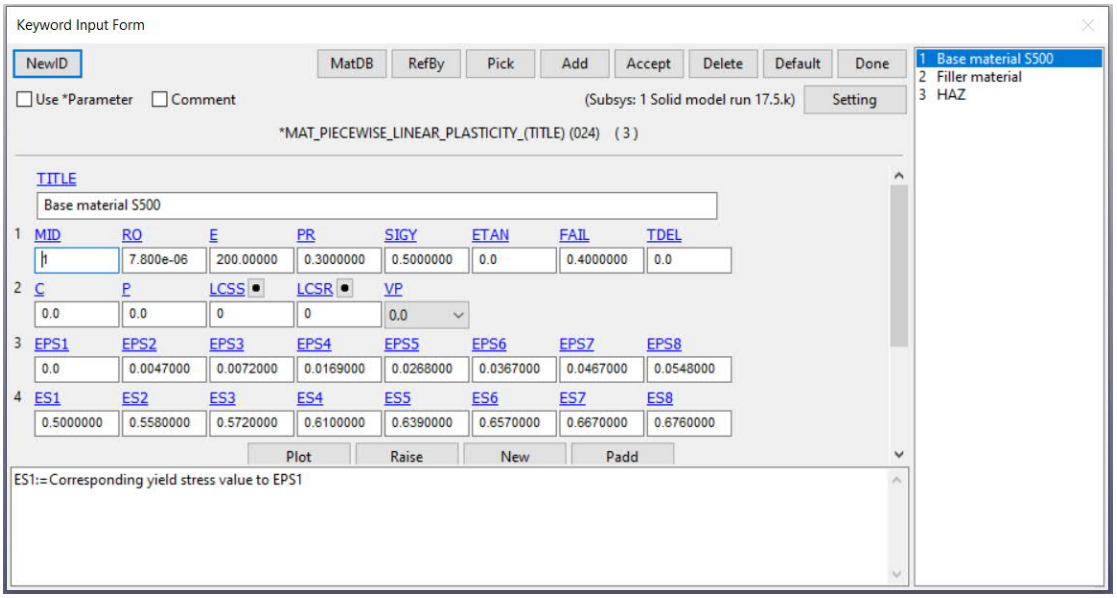

Figure 21. S500 base material input parameters

3.4.2 Filler material (OK ARISTOROD 69)

The filler material is a crucial part of the weld. To ensure that the connection is structurally safe, the filler material must have an appropriate strength, either equal or higher than the base material. The filler material used in Nguyen (2018) is "OK ARISTOROD 69", with its properties shown in Figure 22 below from the manufacturer:

Typical strength values

Tila	In welded mode	Heat treated	In welded mode
Shielding gas	AWS 80Ar / 20CO2 (M21)	EN 80Ar / 20CO2 (M21)	EN 80Ar / 20CO2 (M21)
Tensile strength	805 MPa	750 MPa	800 MPa
Yield strength	715 MPa	690 MPa	730 MPa
Stretch	17 %	20 %	19 %
Testing time		15 hr	
Test temperature		620 degC	

Figure 22. Engineering properties of the filler material from ESAB website

In this thesis, the properties of the welded mode material will be used, as referenced from Veresov (2019). Table 4 shows the engineering values of filler material OK ARISTOROD 69:

Engineering strain (%)	Engineering stress (MPa)
0	714
13	800
17	805
46	817

Table 4. Engineering input values of filler material

From engineering stress-strain values, true values are calculated according to methodology given in Appendix 3.

True strain	True stress (GPa)
0,004	0,717
0,122	0,904
0,157	0,942
0,4	1,2

Table 5. True input values of filler material

From true stress-strain values, defined in Table 5, effective plastic strain and corresponding stress are calculated, by subtracting elastic deformation from plastic deformation as shown in Table 6 below:

Effective plastic strain	Corresponding stress (GPa)
0,000	0,717
0,118	0,904
0,152	0,942
0,394	1,2

Table 6. Official MAT024 input data for filler material

Filler material input in MAT024 form is shown in Figure 23. A more detailed discussion of the failure strain parameter can be found in chapter 4.2:

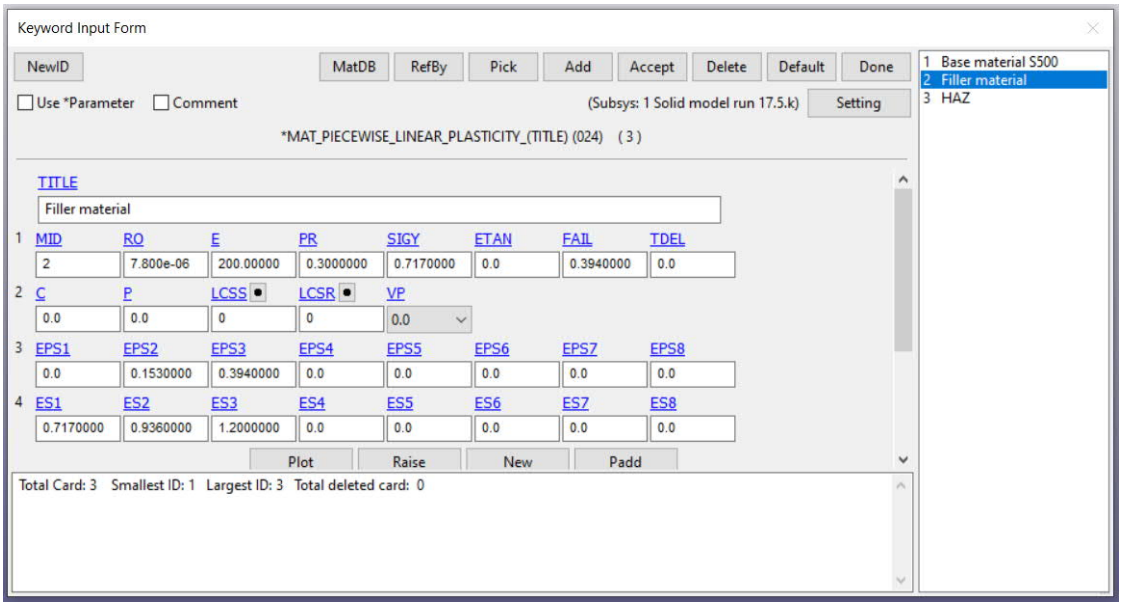

Figure 23. OK ARISTOROD 69 filler material input parameters

3.4.3 Heat affected zone (HAZ)

Determination of the heat-affected zone properties is a difficult process. A few assumptions must be made along with the procedure (Veresov, 2019, p.25):

- Homogeneity of properties in all directions
- Uniformity of stress and strain throughout the thickness of HAZ

There are several uncertainties that must be addressed, before the properties of HAZ can be estimated. From the discussion in chapter 2.1.3, due to the coarsening effect during the formation of HAZ, the ultimate tensile strength of HAZ is lower than this property of the base material. The second challenge in defining the tensile strength of HAZ is due to its evenness. Schematically, the HAZ is usually illustrated to have an even surface. However, the direction of the heat input and local reaction of tempered steel is not always evenly distributed. The phenomenon also appears in the cooling process. This makes the 2 specimens of the same batch, treated under the same procedure, rarely have the same yielding and failure behavior. (Veresov, 2019)

Since the uniformity in the failure stress has yet been concluded from previous theses, and the properties have not been generalized, an assumption must be made to define the HAZ properties that would correspond to the behavior of specimen S500-1R-2. From the failure pattern shown in Figure 6, the specimen failed at the HAZ area, correctly follow the 60° angle of the HAZ orientation. This allows a logical assumption to be made, which connects the testing stress-strain curve of specimen S500-1R-2 to the properties of HAZ. Since the testing specimen failed at the HAZ area, this part can be taken as the weakest part of the weld. During the test, result data of the testing specimen stopped recording right now when HAZ failed. Therefore, it can be logically assumed that the recorded test curve has a direct correlation with the properties of HAZ. When comparing the test curve of specimen S500-1R-2 (Figure 7) to a standardized S500 curve (Figure 20), the tensile strength behavior of the test curve is roughly 10% lower than the standardized curve. The same assumption was made for the HAZ properties, where the ultimate tensile strength of HAZ was taken as 90% of the base material in Veresov (2019). For the material inputs to LS-Dyna, engineering values of HAZ are extracted points from Figure 7 and shown in Table 7 below:

Engineering strain (%)	Engineering stress (MPa)
0,20	400,00
1,00	484,17
2,00	507,34
3,08	515,83
4,00	525,87
5,00	532,82
6,00	535,91
7,00	535,14

Table 7. Engineering input values of HAZ

From engineering stress-strain values, true values are calculated according to the methodology given in Appendix 3.

True strain	True stress (GPa)
0,002	0,401
0,010	0,489
0,020	0,517
0,030	0,532
0,039	0,547
0,049	0,559
0,058	0,568
0,068	0,573

Table 8. True input values of HAZ

From true stress-strain values, defined in Table 8, effective plastic strain and corresponding stress are calculated, by subtracting elastic deformation from plastic deformation as shown in Table 9 below:

Effective plastic strain	Corresponding stress (GPa)
0,000	0,401
0,008	0,489
0,017	0,517
0,028	0,532
0,036	0,547
0,046	0,559
0,055	0,568
0,065	0,573

Table 9. Official MAT024 input data for HAZ

After producing the material input data shown in Table 9, they can be inserted into the model in LS-PrePost in the following form for "MAT024 Piecewise Linear Plasticity". A more detailed discussion of the failure strain parameter can be found in chapter 4.2

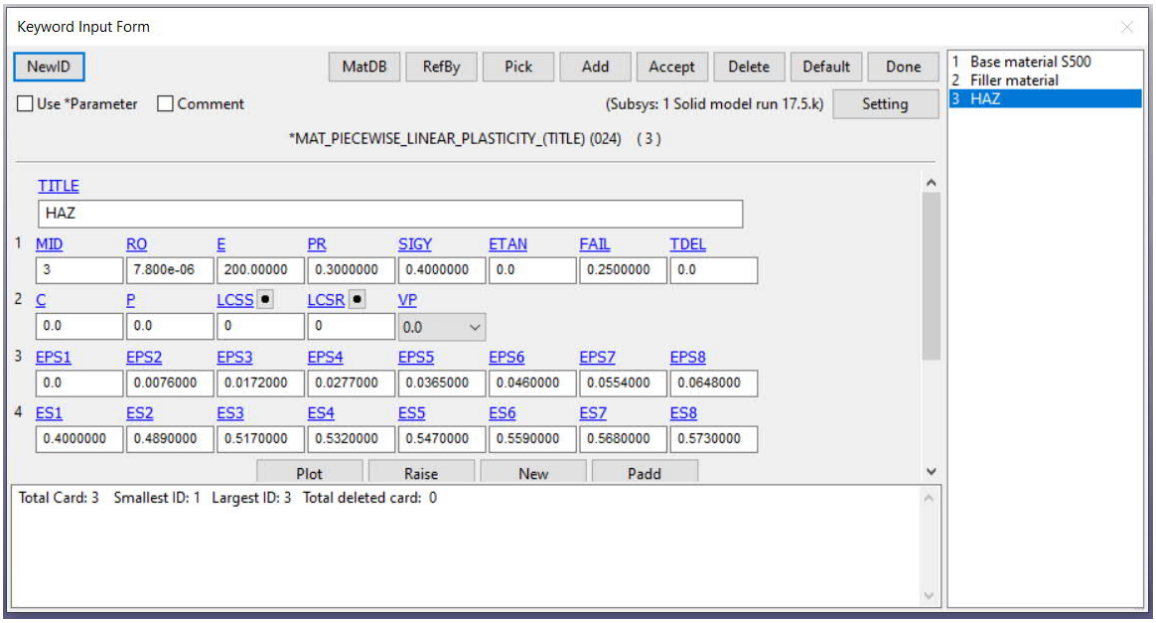

Figure 1. HAZ input parameters

3.5 Loads & Boundary conditions

This chapter presents a description of load definition, load curve as well as the definition of boundary conditions.

3.5.1 Load application

The load application is described in LS-Dyna by Boundary_Prescribed Motion Set keyword, which assigns movement to a set of nodes in any direction. In the testing arrangement presented in Nguyen (2018), the load is applied through the top side of the specimen, by two claws gripping it from both sides.

Figure 25. Testing arrange of Nguyen (2018)

For modelling purpose in LS-Dyna, since the specimen model is created at 90° rotation from the real testing arrangement, a simplification is used, as the load is applied through the set of nodes at the right side of the specimen. In this way nodes under pulling force are moved uniformly in one direction. Figure 26 illustrates this explanation.

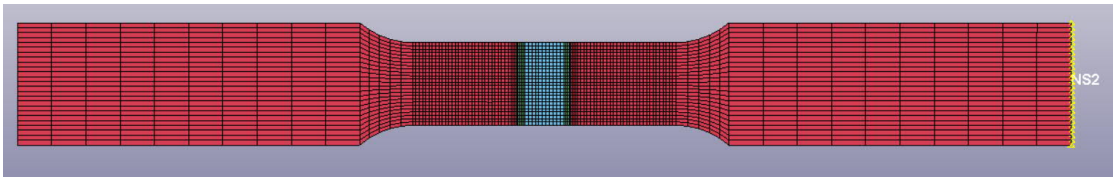

Figure 26. Highlighted moving node set

For Prescribed Motion Set keyword, a load curve must be defined. There are 3 ways in LS-Dyna to define the loading condition of the testing arrangement through displacement, velocity or acceleration. In the real test, Zwick Roell Z250 tensile tester was used. This is the same tensile testing machine used in Veresov (2019), therefore the load curve is defined identically to predefined curve used in the previous thesis. Similar to Veresov (2019), the load is applied using displacement curve.

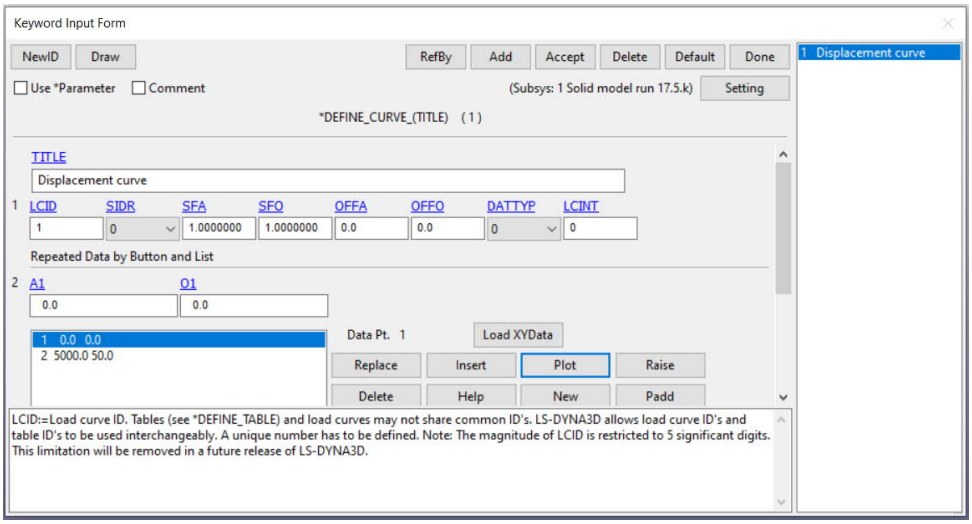

Figure 2. Load curve definition

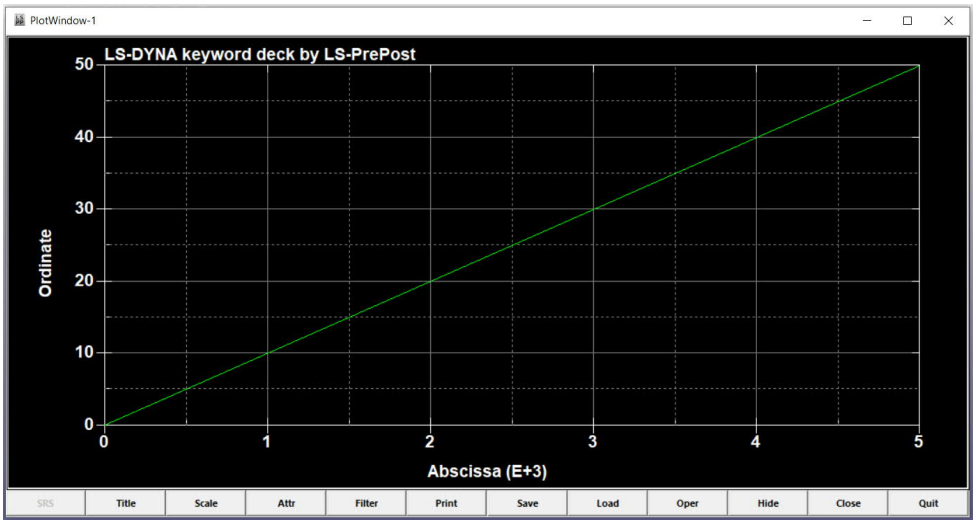

Figure 28. Displacement vs time plotted graph

The ordinate of the graph shows millimeters while abscissa shows milliseconds. A slow increase rate of 0.01 mm/ms is used to assure that the model is not subjected to any abrupt effects. This small rate simultaneously keeps the model under static behavior and thus true to structural applications. If the dynamic effect appears, the output load-displacement graph can be examined with the presence of high-frequency nonlinearities. The displacement and time are measured in millimeters and milliseconds respectively to follow a uniform unit system, defined in Figure 19. Due to the universal system used in LS-Dyna, which does provide an automatic definition of units, the units of input values must be controlled and double-checked by its users.

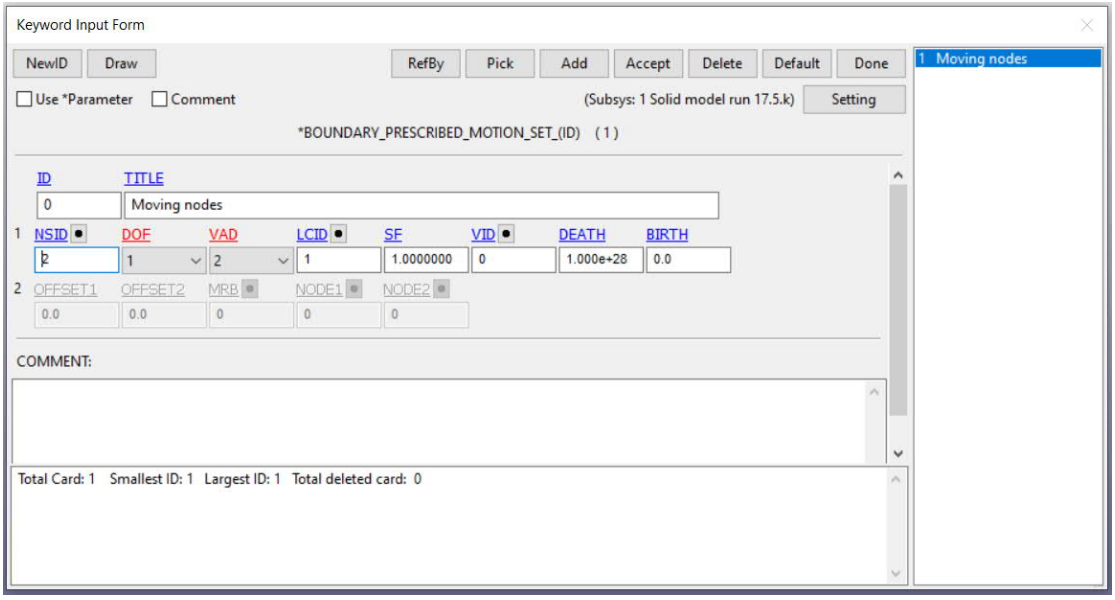

Figure 29. Boundary - Prescribed Motion Set keyword input

3.5.2 Boundary conditions

In the real testing arrangement of Zwick Roell Z250 tensile tester machine (shown in Figure 25), the top part is subjected to a pulling force, while the bottom part of the specimen is fixed. To resemble correctly this arrangement, while still follow the geometry of the specimen, a node-set at the right end side of the specimen model is displaced in X direction. Since the specimen only pulled in 1 direction, the X direction is the only interested direction for the moving node-set. Therefore, the boundary

conditions of the set allow the nodes to move in the X direction, while fixing all the rest directions. The boundary conditions can be expressed through Boundary – SPC Set keyword:

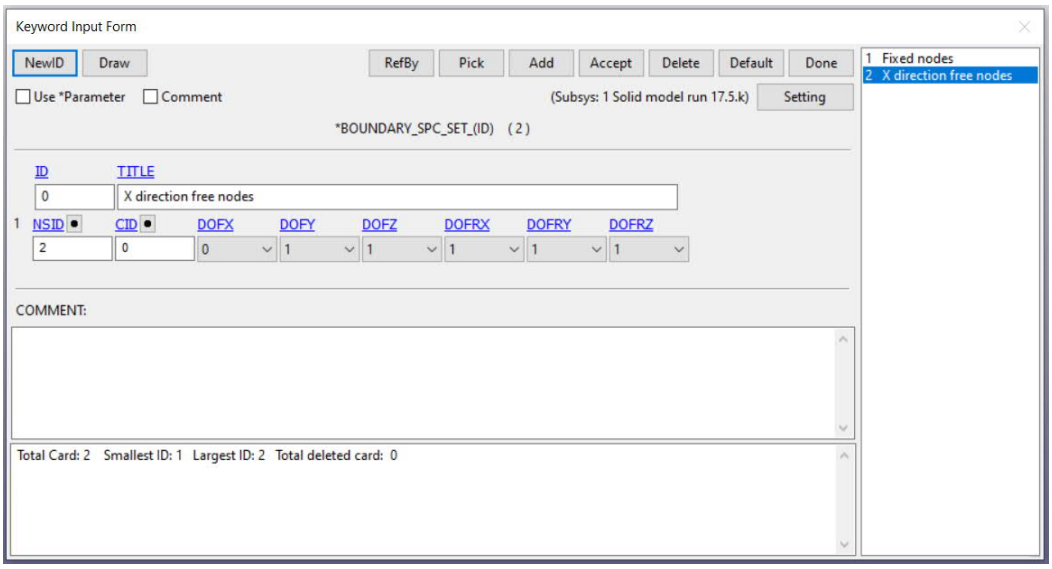

Figure 30. Boundary conditions for moving nodes set

In Figure 30, 0 represents the direction that the nodes are free to move, 1 indicates the directions that the nodes are constrained from moving while DOF defines the degree of freedom in which direction. On the left side of the specimen model, the end nodes set is defined to be fixed in all directions:

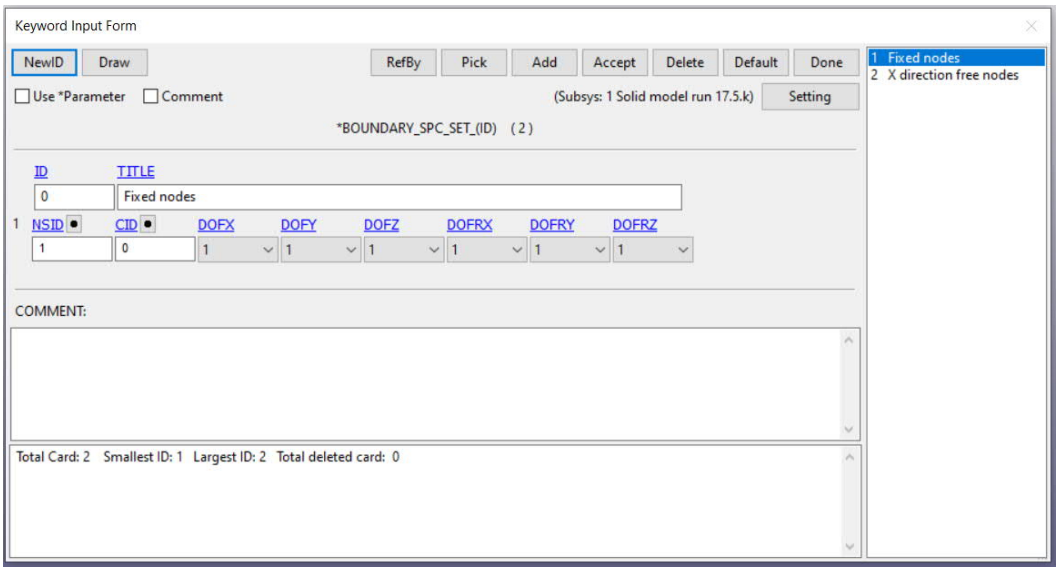

Figure 31. Boundary conditions for fixed nodes set

4 Results and Analysis

This chapter presents the analysis and comparison of the modelling result, following these principle parameters:

- Comparison of the failure pattern between specimen and model
- Comparison of the load-displacement curves of specimen and model

The comparisons will also be done respectively between the shell model results and the solid model results.

As shown in Figure 6, the failure pattern of the real testing specimen happened exactly in the HAZ area. The failure formation follows the 60° angle where the filler material connects to the base material.

Figure 32. A closer view at the failure area of specimen S500-1R-2

4.1 Output results of shell model

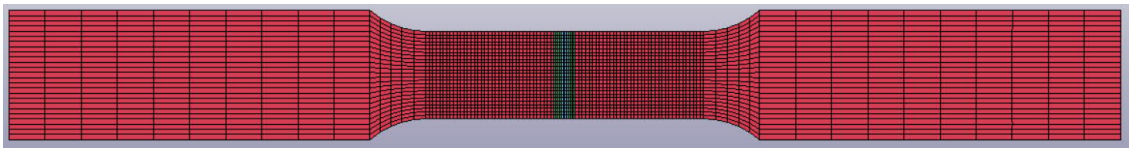

Figure 33. Geometry of the shell model

The shell model correctly predicts the necking effect before rupture, as seen in the pattern shown in Figure 32:

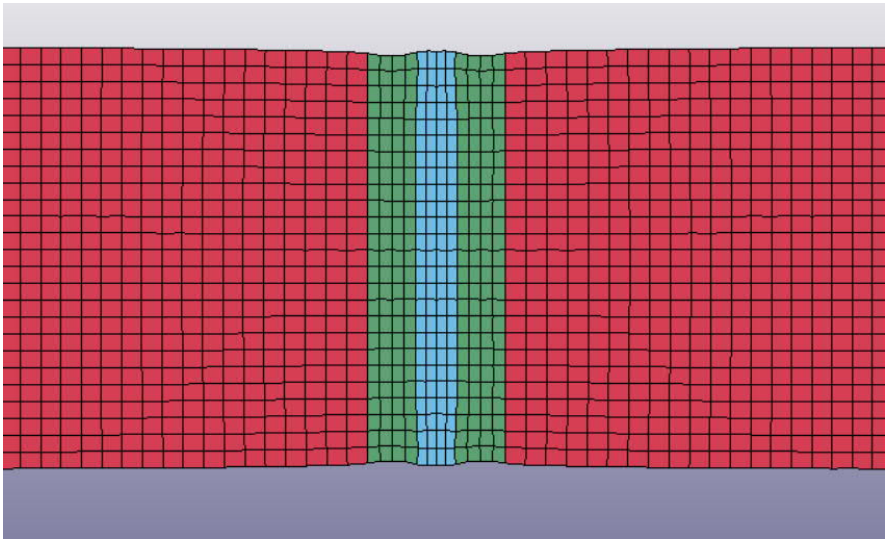

Figure 34. Necking effect of shell model before rupture

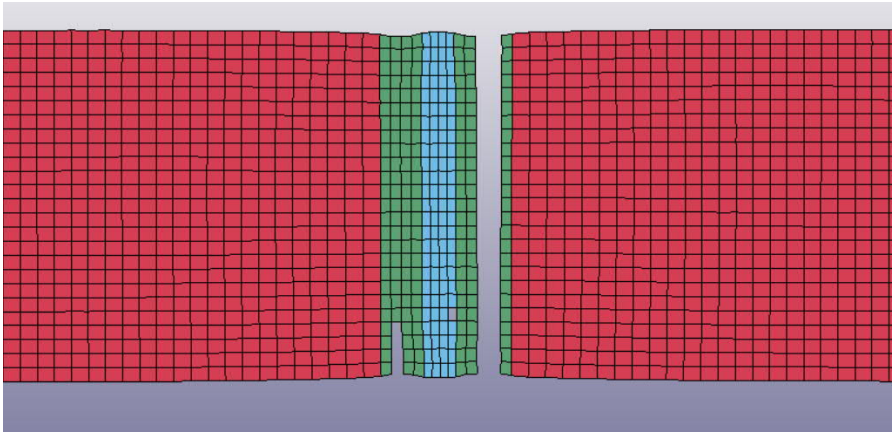

Figure 35. Failure pattern of shell model

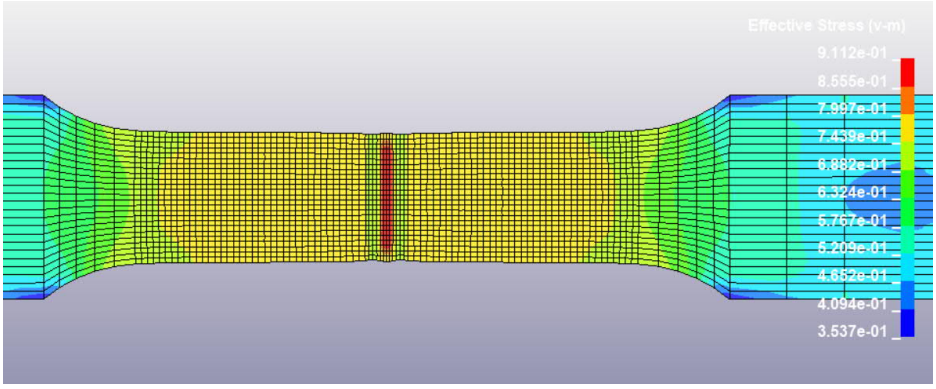

Figure 36. Shell model Von Mises stress

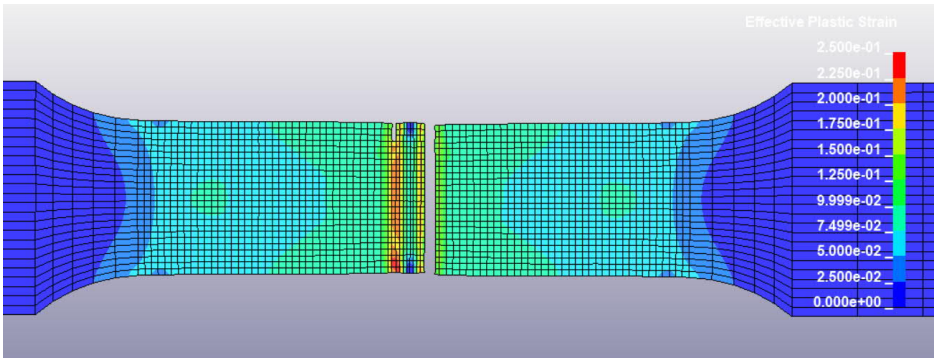

Figure 37. Shell model effective plastic strain

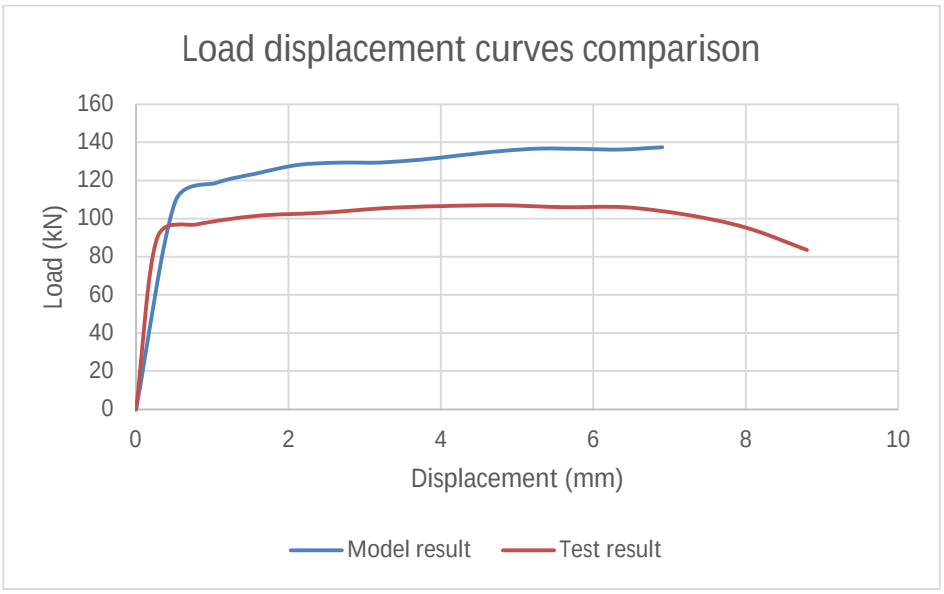

Figure 38. Load displacement curves comparison

In Figure 38, the red curve represents the load-displacement curve of the test specimen. This curve is identical to the curve shown in Figure 8, where the data of the stress-strain graph is a converted load-displacement. Since the graph has engineering values, the converted load-displacement curve also presents the necking phenomenon in the downfall trend at the end of the curve. The values at the necking phase are not relevant for comparison with the model result, and the point for comparison considers the displacement value where the ultimate strength is reached. As for the model specimen, since the input values are true values, the result data does not include the necking phase. Therefore, the displacement at the failure of the model result is compared with the displacement at the ultimate strength of the testing result, which in this case is similar, around 6.5mm.

The force result between test and model specimen is approximately 20kN different. This may be due to the unevenness in the testing specimen caused after the welding process when the tensile specimens were ground at the welded area to remove excess material. This leads to a smaller actual cross-sectional area of the specimen than the standard area used in modelling. (Nguyen, 2018)

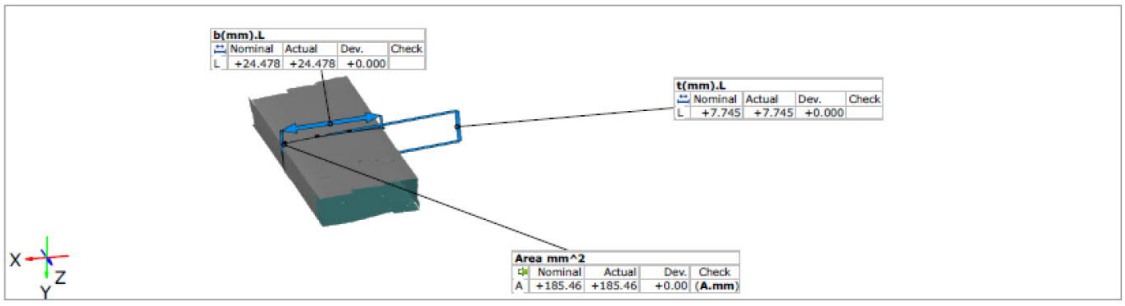

Element	Datum	Property	Nominal	Actual	Tol -	Tol +	Dev	Check	Out
Area mm^2		A	+185.46	+185.46			+0.00		
b(mm)		L	+24.478	+24.478			+0.000		
t(mm)		L	+7.745	+7.745			+0.000		

Figure 39. Actual cross-sectional area from Nguyen (2018)

4.2 Output results of solid model

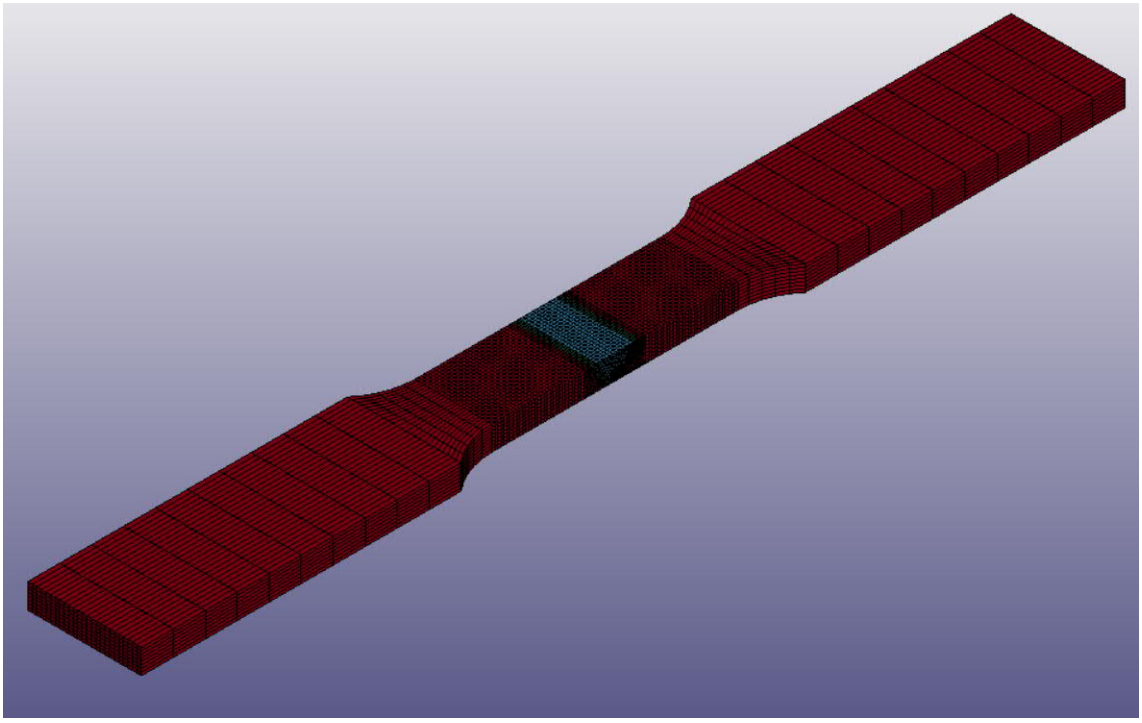

Figure 40. Geometry of the solid model

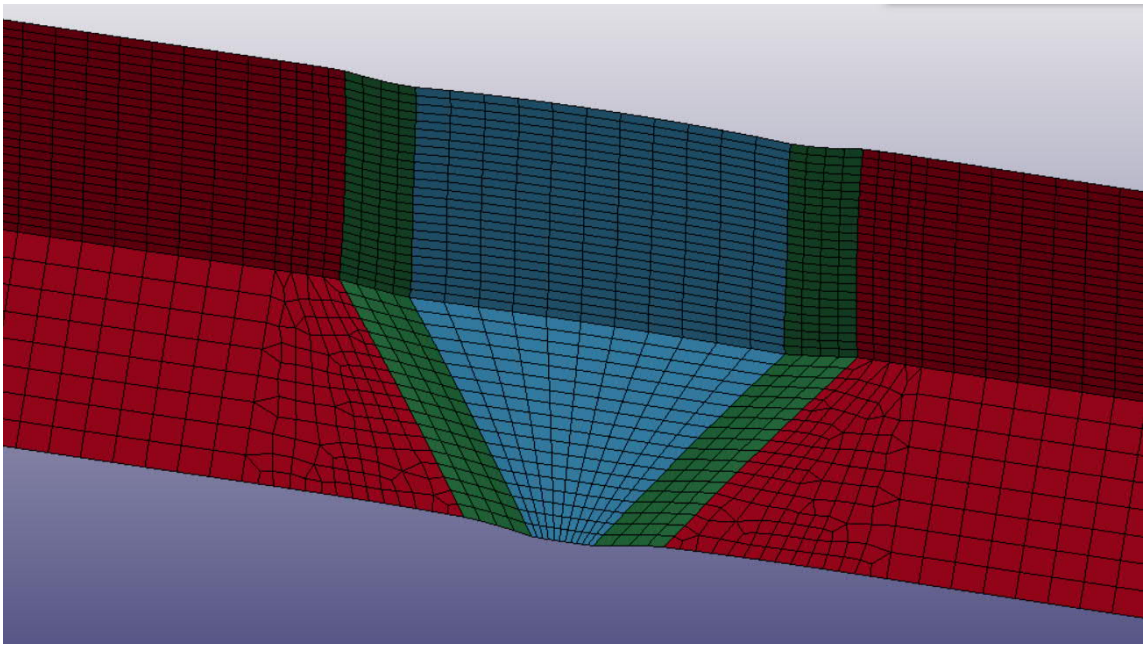

Figure 41. Necking effect of solid model before rupture

As the shell model, the solid model correctly predicts the necking effect of the specimen before rupture.

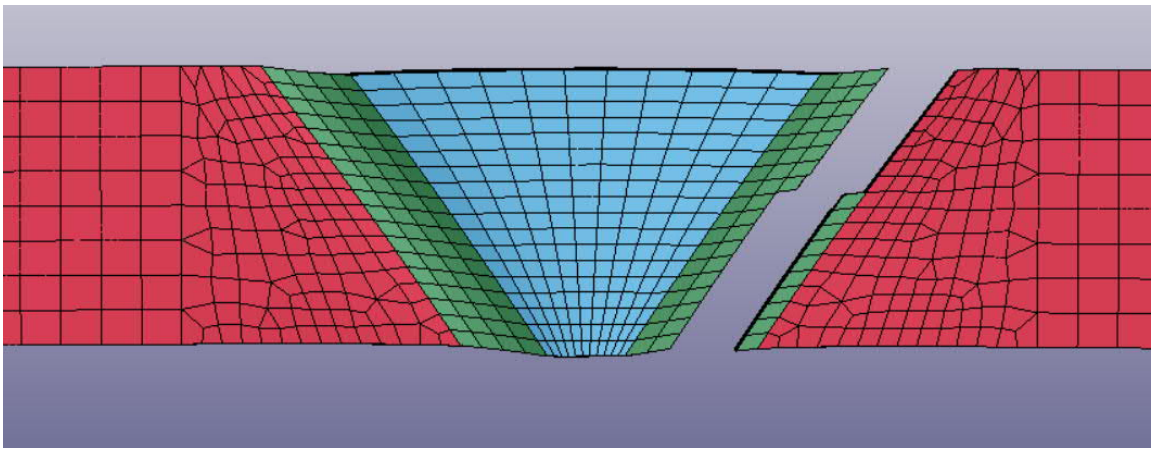

Figure 42. Failure pattern of Solid model

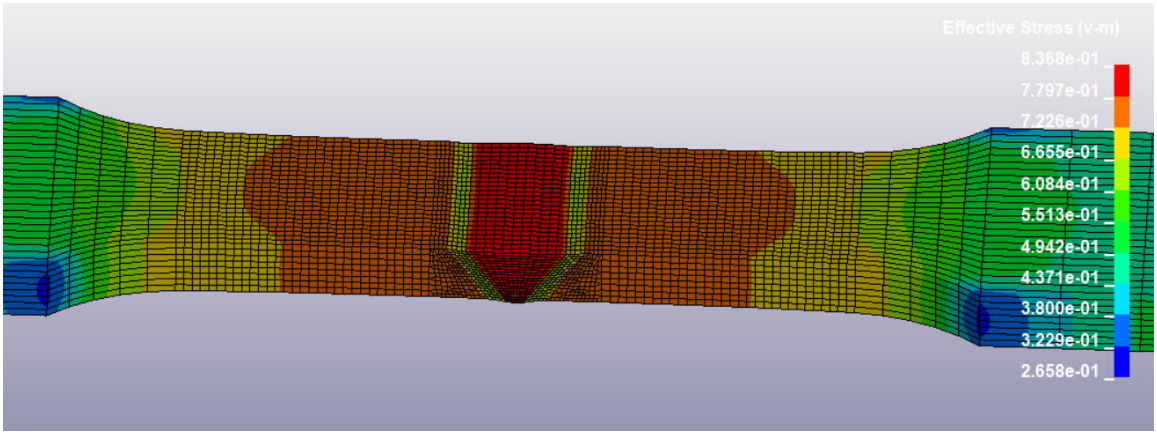

Figure 43. Solid model Von Mises stress

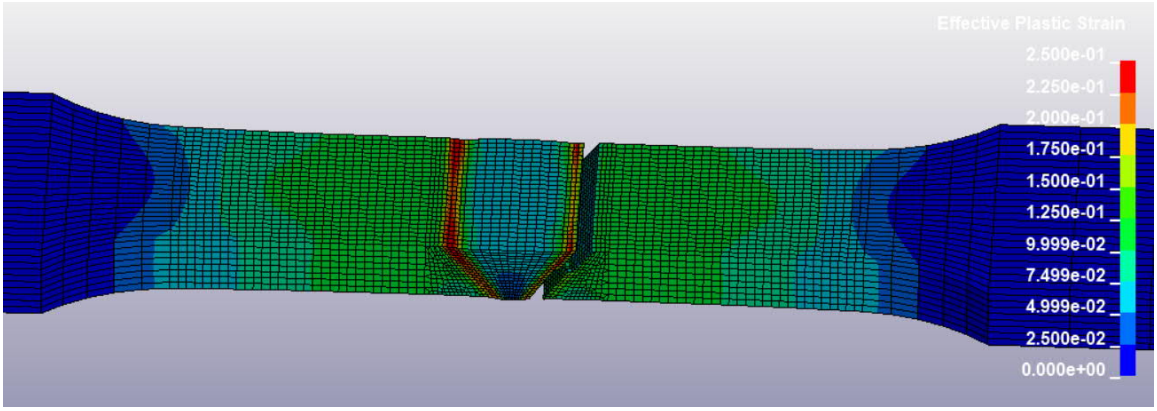

Figure 44. Solid model effective plastic strain

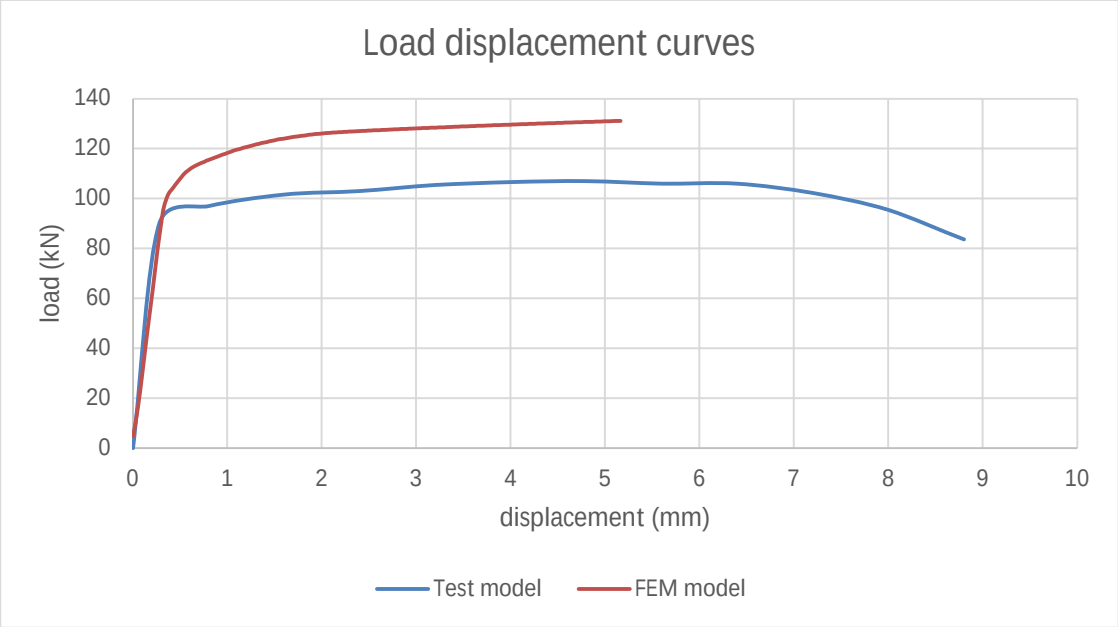

Figure 45. Load displacement curves comparison

In Figure 45, the red curve represents the load-displacement curve of the test specimen. As in the case of the shell model's result comparison, the displacement at the failure of the model result is compared with the displacement at ultimate strength of the testing result, which in this case is similar, around 5.5mm. The final displacement of the model result is heavily dependent on failure strain input. To achieve a more matching displacement result, the true failure strain input for HAZ can be increased from 0.25 as used in this model to 0.3 (up to 0.4). A more detailed discussion on this topic can be found in chapter 4.3

There is approximately 20 kN difference in the force result between the test and model specimen for the same reason stated in chapter 4.1 for the results of the shell model.

4.3 Discussion on failure strain

MAT024 is the most used keyword in LS-Dyna for defining materials with plastic behavior. The main principle of this keyword is to use a defined material stress-strain curve as a parameter for that material's properties. The keyword also allows user to predefine the failure strain of the material, which determines at what strain value the material will fail. This is an extremely important input since it also influences directly the stress-strain behavior of the material.

This value is commonly mistaken to be the final and biggest strain value of a stress-strain curve, which is not precise. The input value for LS-Dyna must be a true failure strain value of the material, while the value provided from the stress-strain curve is usually an engineering value. Based on a discussion with Professor Ma from HAMK Tech Research Unit, for standard normal structural steel, the true failure strain value of the material is approximately 0.4. For the case of high strength steels, the true failure strain values can still vary between 0.25 to 0.4 and have not been generalized. For this thesis work, true failure strain value of the base material and filler material is set to be around 0.4, while 0.25 is used for the input of the heat-affected zone.

4.4 Discussion on Hourglass effect

Hourglass effect is nonphysical mode of deformation that occur in under integrated elements and produce no stress. As mentioned earlier in chapter 2.2 and chapter 3.3, the Hourglass phenomenon appears in a finite element model when the model is under a large deformation stage, while using an under integrated element formulation. To stabilize this effect, an Hourglass control keyword must be used. A correct Hourglass control formulation type as well as an Hourglass coefficient must be defined. The control formulation helps the software to correctly understand what type of simulation the Hourglass control is applying. Simultaneously, the Hourglass coefficient must be estimated in addition to the control formulation, to generate an additional nonphysical stiffness to compensate for the under integrated elements.

There are 3 approaches from LS-Dyna to address the Hourglass effect: Viscous, Stiffness or Co-rotational Stiffness formulation. (LSTC document on Hourglass Modes).

In Viscous Hourglass control formulation for solids, the formulation generates hourglass forces proportional to components of nodal velocity that contributes to hourglass modes. Therefore, Viscous forms of hourglass control are more suitable for high velocity/high strain rate problems. The Hourglass coefficient for this formulation is recommended to be kept less than 0.15

In Stiffness Hourglass control formulation for solids, the formulation generates hourglass forces proportional to components of nodal displacement contributing to hourglass modes. This formulation is more suitable for low strain rate solid simulation as shown in this thesis. However, using the stiffness control may lead to artificial over stiffness due to overestimated Hourglass coefficient. The recommended Hourglass coefficient is between 0.03 to 0.1

In Co-rotational Stiffness Hourglass control formulation for solids, an assumed strain field and the material's elastic properties are used to calculate an assumed stress field. That stress field is integrated over the element to develop an hourglass force which allows the element to behave as a fully integrated element. This type of formulation is more suitable for soft material with plastic behavior. The coefficient for this formulation should be kept at 0.1
After the simulation, to assure that the defined Hourglass coefficient is correct for the control formulation, the Hourglass energy should be < 10% of the internal energy.

After the simulation, the shell model of this thesis did not show any Hourglass effect. For the solid model, the Hourglass effect appeared when large deformations took place before rupture. To stabilize the model, an Hourglass control keyword was introduced using Stiffness formulation 5, with an Hourglass coefficient of 0.05:

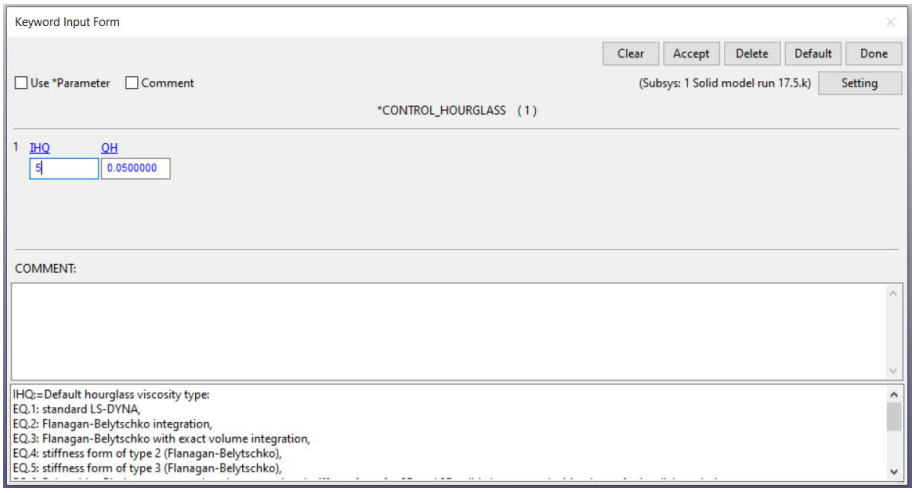

Figure 46. Control Hourglass keyword

After the Hourglass control keyword was introduced, the Hourglass phenomenon was eliminated. To assure that the stiffness coefficient of the formulation is correct, the Hourglass energy is plotted and checked with the Internal energy:

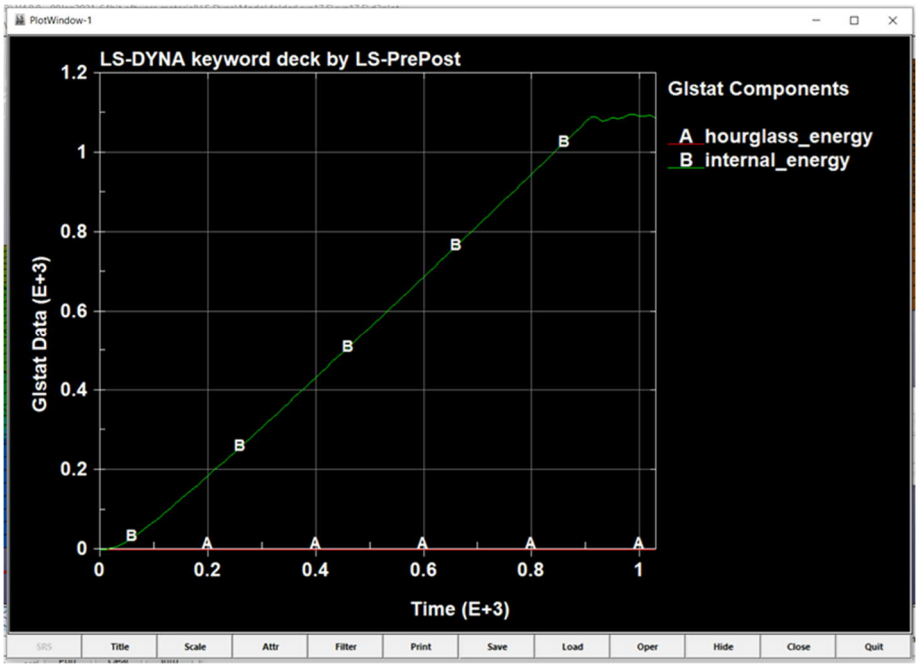

Figure 47. Hourglass energy and Internal energy curves

In Figure 47 the Hourglass energy is less than 10% of the peak internal energy, confirming that the used hourglass control formulation and coefficient are correct.

5 Conclusion

Both shell and solid models have correctly simulated the failure pattern of the test specimen. While there is still room for improvement, the load-displacement curves of the FEM models show similar results and good corresponding load results.

A new method of bias meshing has been successfully applied during the modelling process to manipulate the mesh structure and optimize the model. This technique results in a significant decrease in the simulation processing time, which provides a much more efficient and economical solution to solid simulation in the future.
During the data processing stage, problems regarding material inputs, failure strain, Hourglass effect have been successfully addressed, leaving a solid reference to future thesis work on FEM-related topic.

6 Recommendations for future work

For the future continuation of this thesis topic, several points are recommended for the improvement of this model:

- A quarter model of the tensile specimen: this thesis is dedicated to creating a whole model of the tensile specimen. However, despite the full optimization of the mesh size and number of elements, the model still needs 15 hours of simulation of a 32 CPU workstation. This is a significantly large amount of processing time, which can be improved by a quarter model using SPC_SYMMETRY_PLANE keyword

- The model creation method can be applied to a new testing series: Although Nguyen (2018) has been a great reference to this thesis, some crucial information about the process of obtaining the result is still missing, such as the gauge length, pre-processed data recorded from tensile tester machine, other types of tests for the material parameters of each material separately.

References

Abebe, E. (2016). Effect of heat input on the mechanical properties of strength steel half V-welded joints. Bachelor's thesis. Degree Program in Construction Engineering. Häme University of Applied Sciences. Retrieved on the 06th of January 2021 from: Theseus.fi

Erhart, T. (2011). Review of Solid Element Formulations in LS-Dyna. Stuttgart. LS-Dyna Forum 2011. Retrieved on the 06th of January 2021 from: https://www.dynamore.de/de/download/papers/forum11/entwicklerforum-2011/erhart.pdf

ESAB. OK ARISTOD 69 Product Information. Retrieved on 06th of January 2021 from: https://www.esab.co.uk/gb/en/products/welding-consumables/mig-mag-wires-gmaw/low-alloy-wires/ok-aristorod-69.cfm

Giraldo, J. (2018). Effect of heat input on the mechanical properties of high strength steel T-joints. Bachelor's thesis. Degree Program in Construction Engineering. Häme University of Applied Sciences. Retrieved on the 06th of January 2021 from: Theseus.fi

Grecevci, B. (2016). Effect of heat input on the mechanical properties of high strength steel butt-weld joints. Bachelor's thesis. Degree Program in Construction Engineering. Häme University of Applied Sciences. Retrieved on the 06th of January 2021 from: Theseus.fi

Kou S. (2002). Welding Metallurgy. 2nd edition. New Jersey: John Wiley & Sons, Inc

LSTC (2017). Basic tutorials for tensile tests. 1st edition. Livermore Software Technology Corporation (LSTC). Retrieved on the 06th of January 2021 from: www.dynamore.de

LSTC (2012a). LS-Dyna Introduction on Hourglass modes. Livermore Software Technology Corporation (LSTC). Retrieved on 13th of January 2021 from: https://ftp.lstc.com/anonymous/outgoing/support/FAQ_docs/hourglass.pdf

LSTC (2012b). LS Dyna support from engineering to true strain true stress. Livermore Software Technology Corporation (LSTC). Retrieved on 15th of January 2021 from: https://ftp.lstc.com/anonymous/outgoing/support/FAQ_docs/hourglass.pdf

LSTC (2012c). LS-Dyna User's Manual Volume 1 (for version 971 R6.1.0). Livermore Software Technology Corporation (LSTC).

LSTC (2012d). LS-Dyna User's Manual Volume 2 (for version 971 R6.1.0). Livermore Software Technology Corporation (LSTC).

Nguyen, V. (2018). Effect of heat input on the mechanical properties of butt-welded steel joints. Bachelor's thesis. Degree Program in Construction Engineering. Häme University of Applied Sciences. Retrieved on the 06th of January 2021 from: Theseus.fi

Peltonen, M. (2014). Weldability of high-strength steels using conventional welding methods. Master's thesis. Degree Program in Design and Production Engineering. Aalto University. Retrieved on the 06th of January 2021 from: https://aaltodoc.aalto.fi/handle/123456789/14537

Publications Office of the European Union. (2016). Rules of high strength steel (RUOSTE). 1st edition. Luxembourg: RFCS Publications

Veresov, P. (2019). Finite Element Modelling of a High Strength Steel Tee Joint. Bachelor's thesis. Degree Program in Construction Engineering. Häme University of Applied Sciences. Retrieved on the 06th of January 2021 from: Theseus.fi

Zhang, P., Li, S. and Zhang, Z. (2011). General relationship between strength and hardness. Materials Science and Engineering. Chinese Academy of Sciences

Appendix 1: Detailed design log for creating shell model.

This appendix records the step-by-step procedure of creating the shell model:

Step 1: Create the initial geometry with single line and curves using key-in tool in 2D Mesh Generation

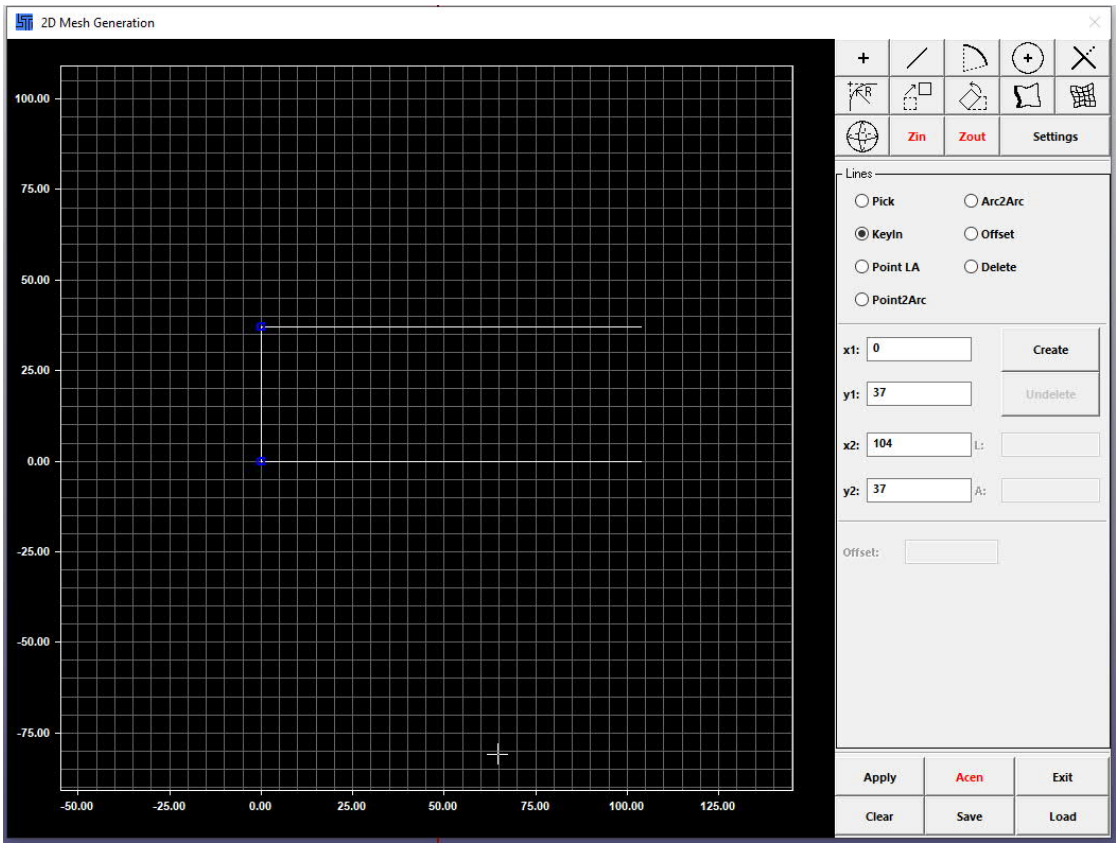

Step 2: Define an edge with “Create”

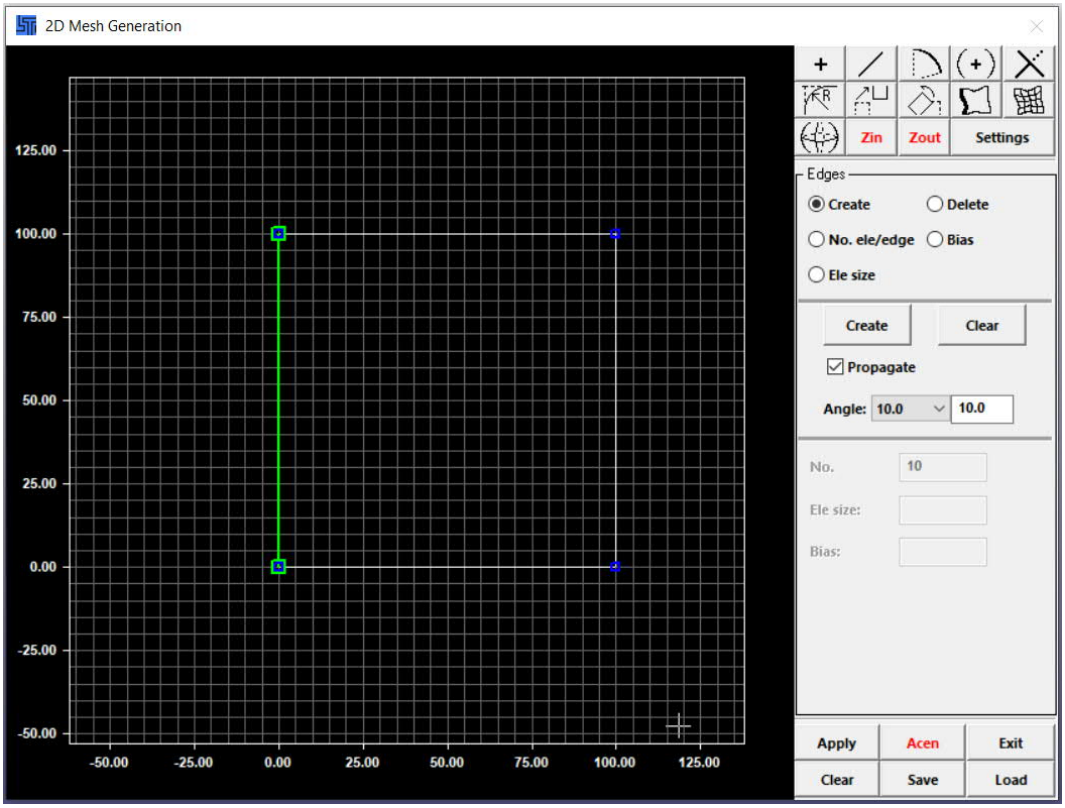

Step 3: Define the number of element of that edge and assign, finish with “Apply”

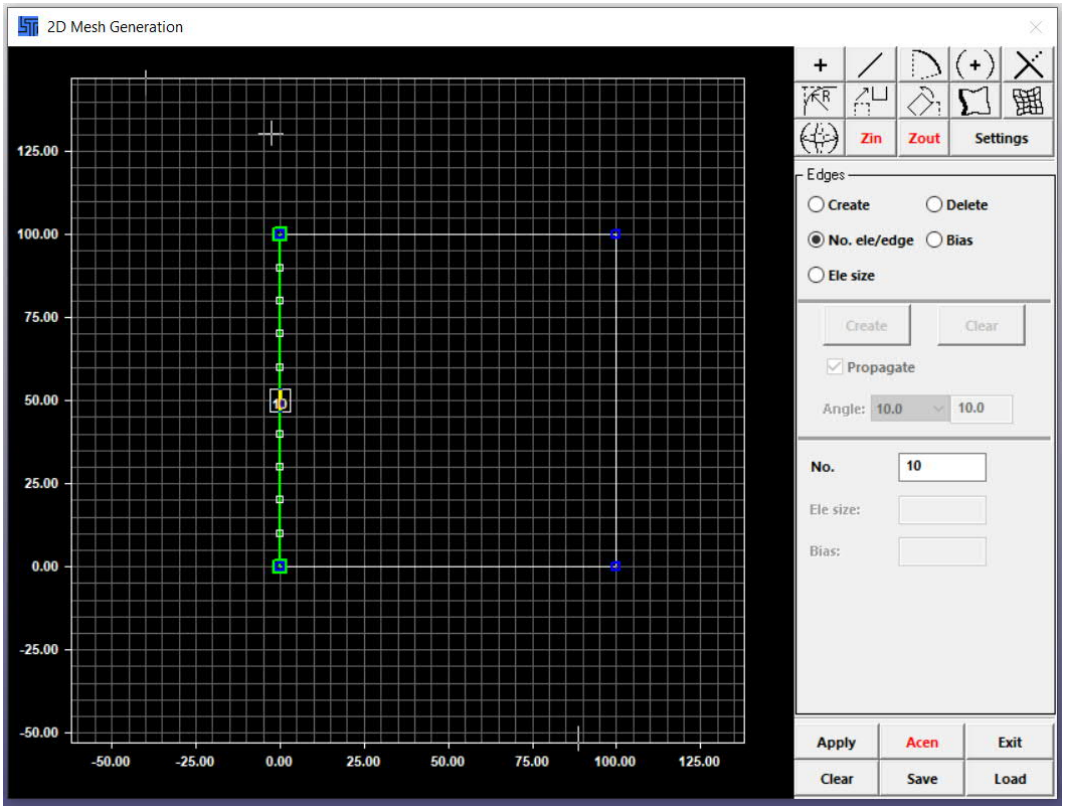

Step 4: Do the rest of the geometry with this technique, defining elements per edge

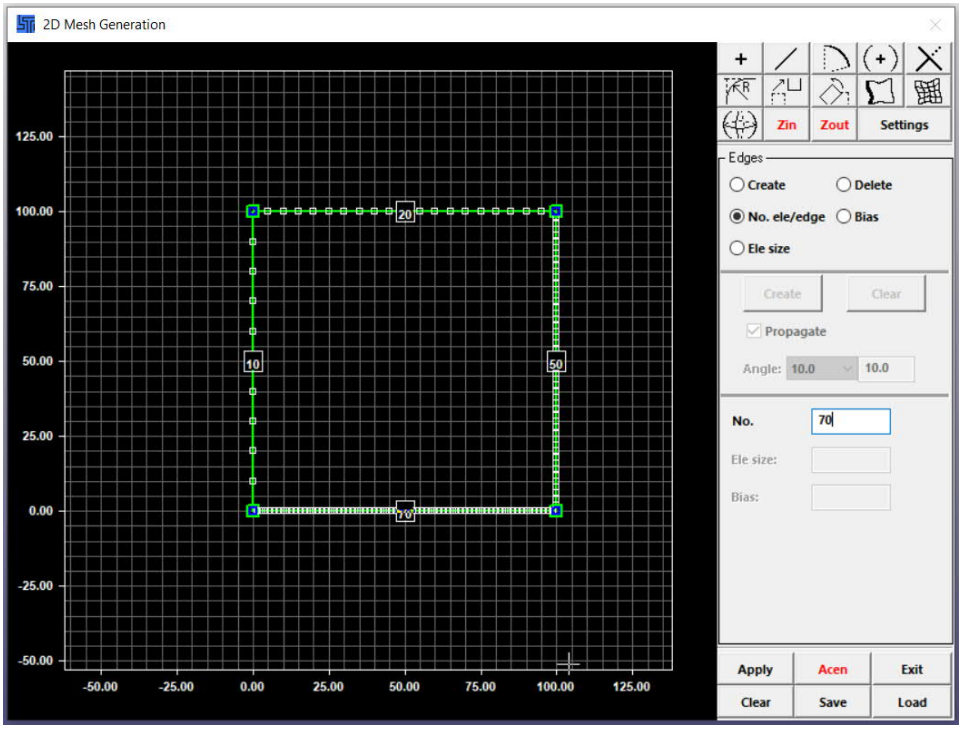

Step 5: Create mesh shell using free squad mesh and “Accept”

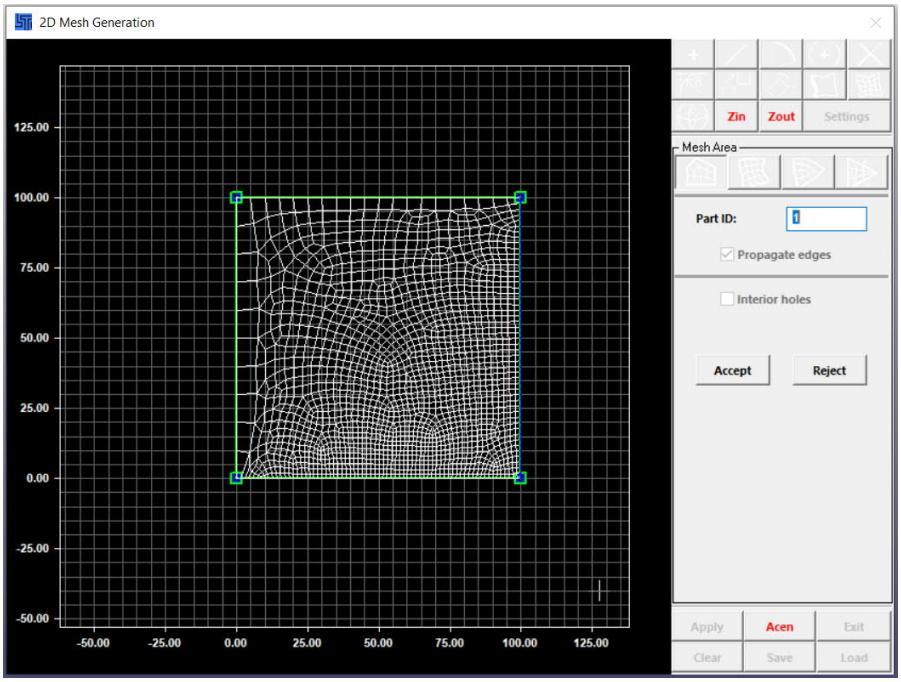

Step 6: After the shell mesh has been created, the duplicate nodes must be merged between 2 different materials Show Dup Nodes -> Merge Dup Nodes:

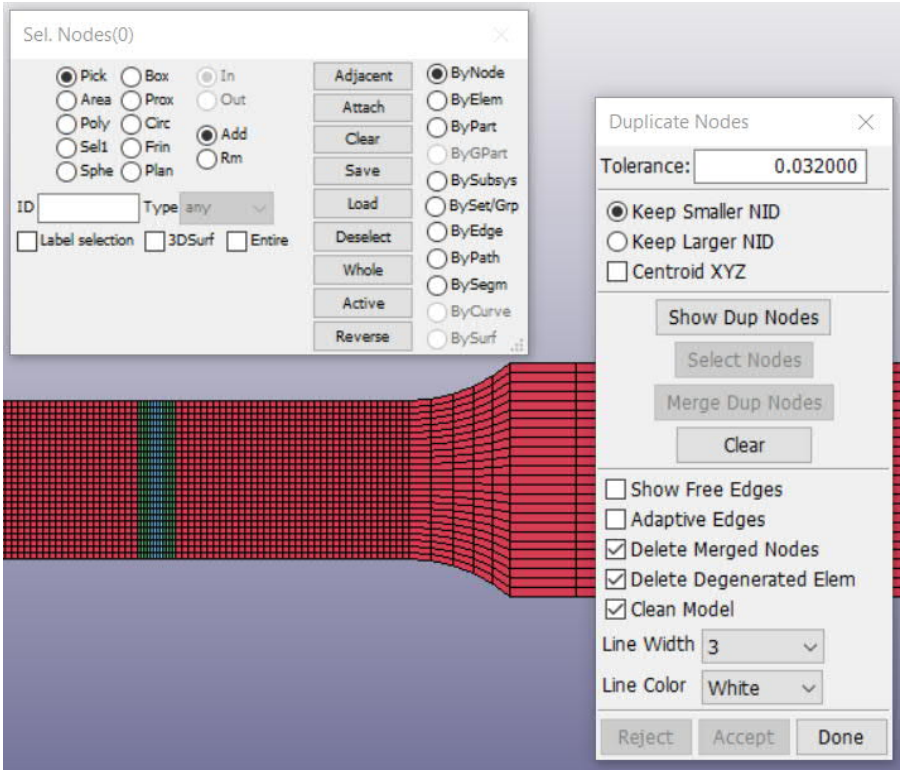

Step 7: Define SECTION_SHELL keyword

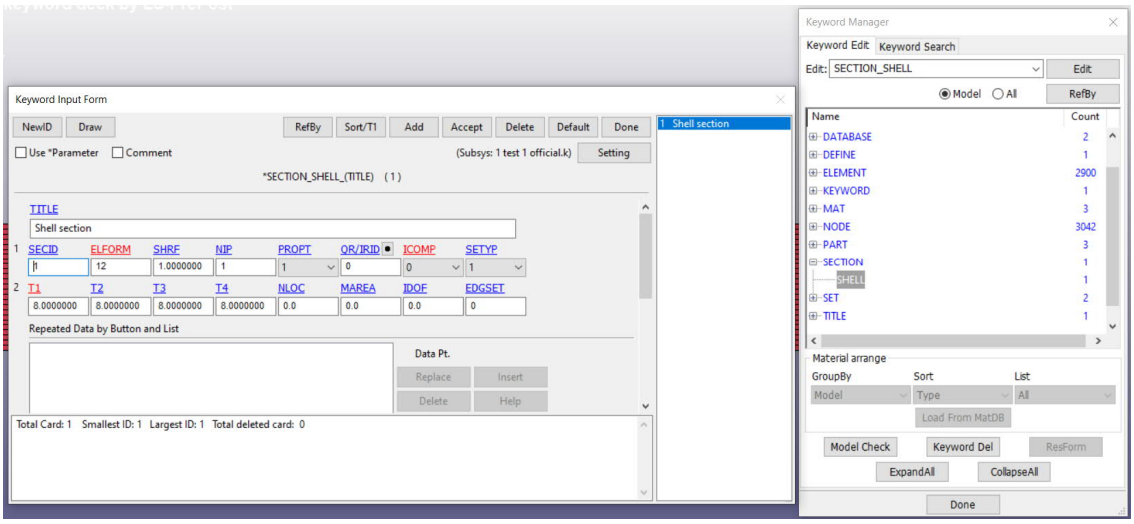

- ELFORM 12: Explained in chapter 3.3
- NIP: Number of integration point per element, 1 is the most economical solution that requires the least simulation time
- T1 to T4: Thickness of the geometry (mentioned in chapter 3.2.1)

Step 8: Material properties must be defined in MAT024 keyword, specified in chapter 3.4

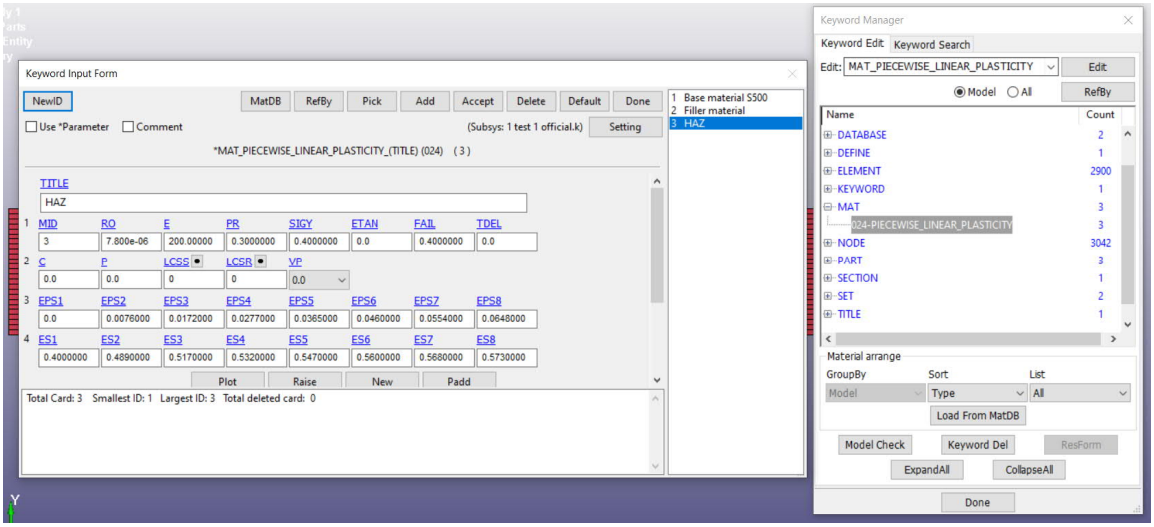

Step 9: Define PART keyword to assign the shell section and material to each part

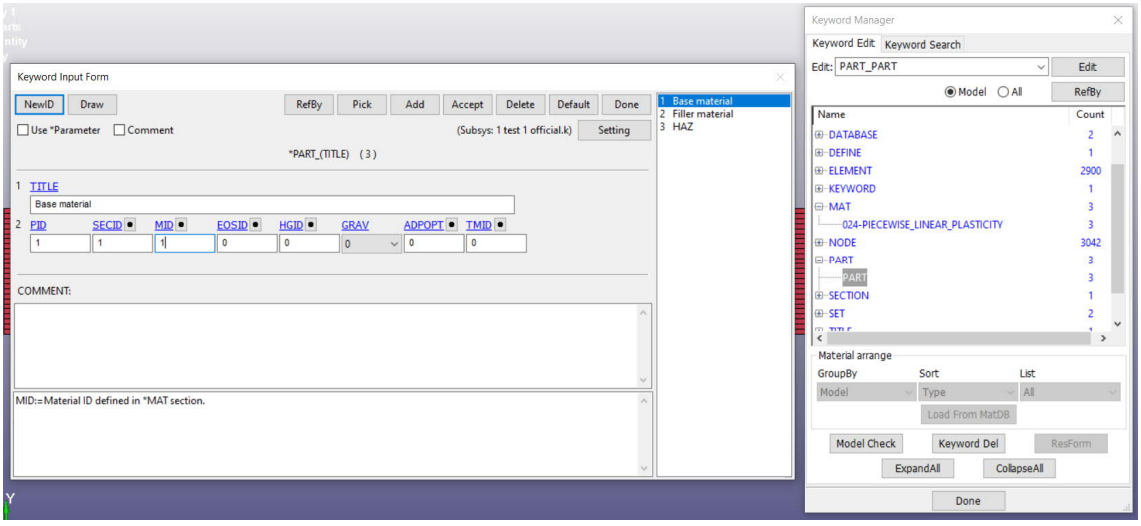

Step 10: Create node sets using Create Entity tool

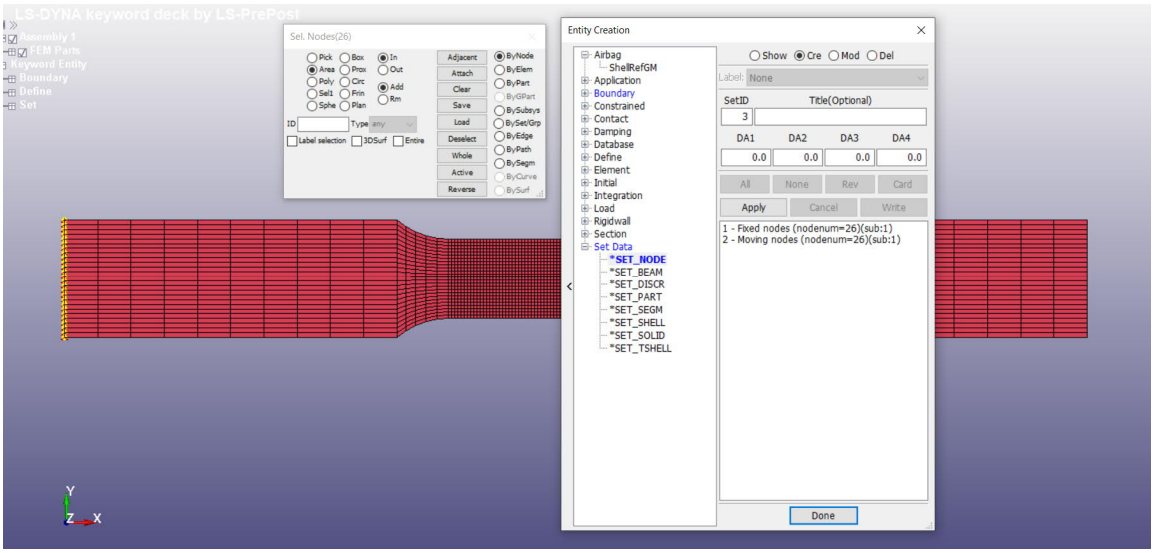

Choose ByNode or ByElement, Area and choose the end nodes. After the end nodes have been highlighted, press Apply. 2 sets of nodes must be defined at 2 ends, 1 for fixed condition and 1 for pulling force.

Step 11: Define Load curve, details are mentioned in chapter 3.5.1

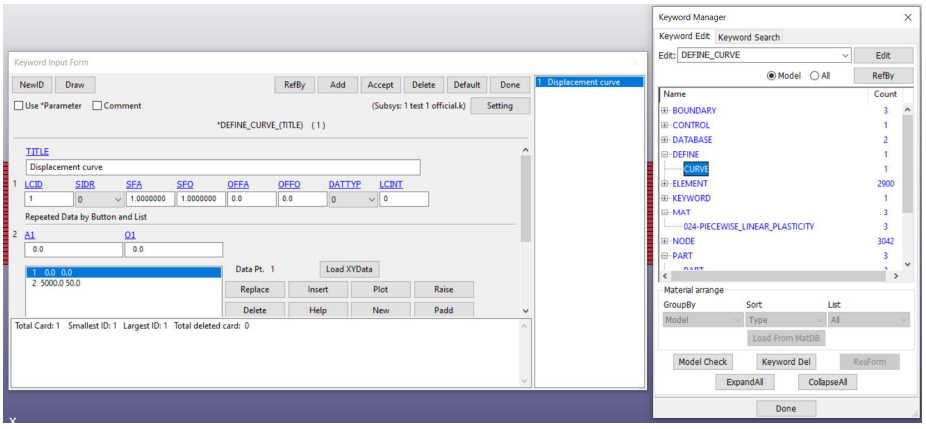

Step 12: Define Fixed condition at left side and X direction free at right side using BOUNDARY_SPC SET

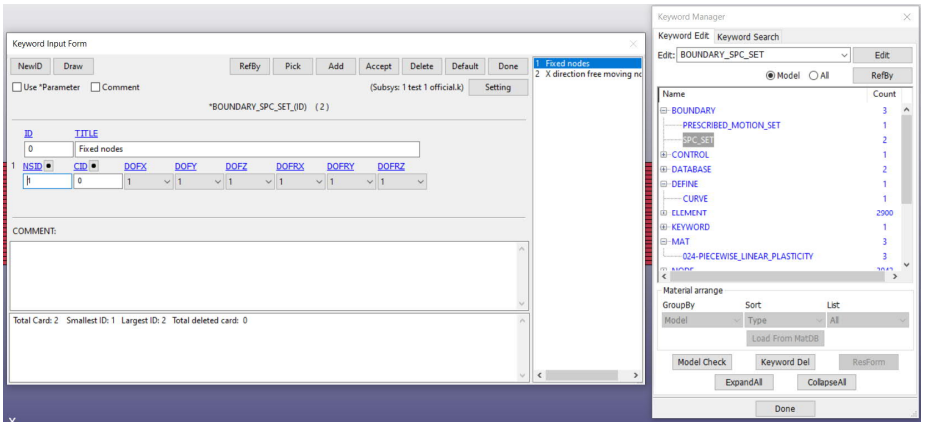

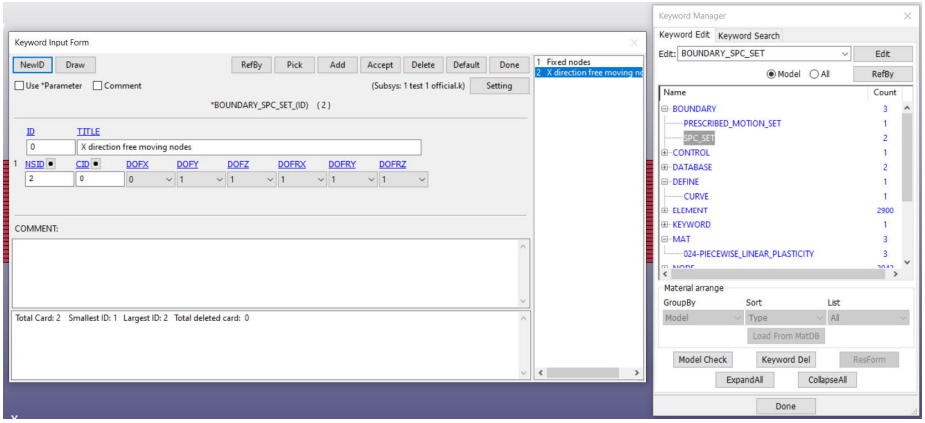

Step 13: Define Pulling force at right side by assigning load curve to the moving using BOUNDARY_PRESCRIBED MOTION SET

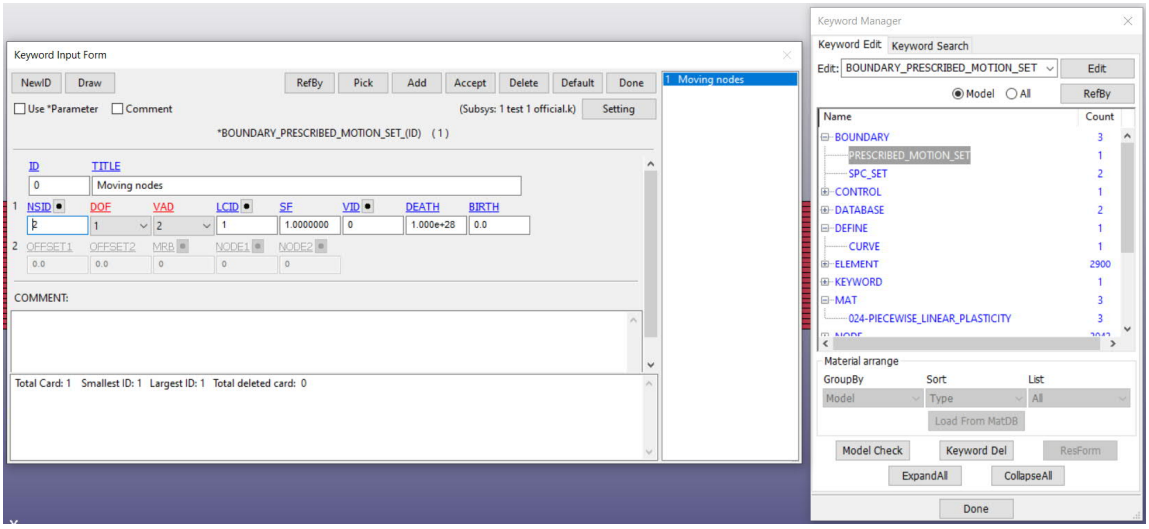

NSID: Node set ID, assign the moving node set

DOF: 1 for X translation movement

VAD: 2 for displacement equation

LCID: Load curve ID, assign displacement curve

Step 14: Define the simulation time for the model (the simulation time should be long enough for the specimen to fail). Keyword: CONTROL_TERMINATION

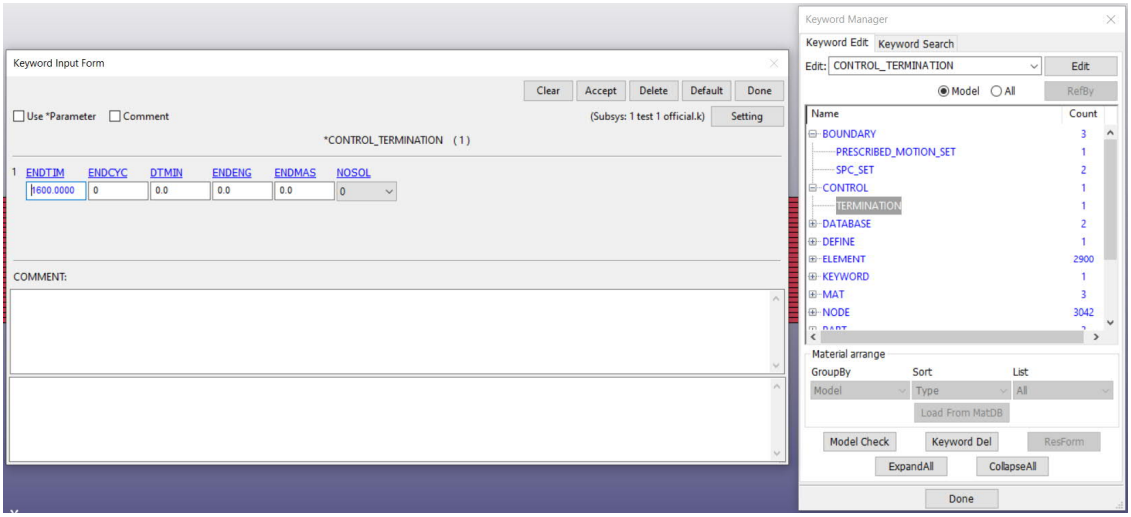

Step 15: Define output result which will be printed out through ASCII_option

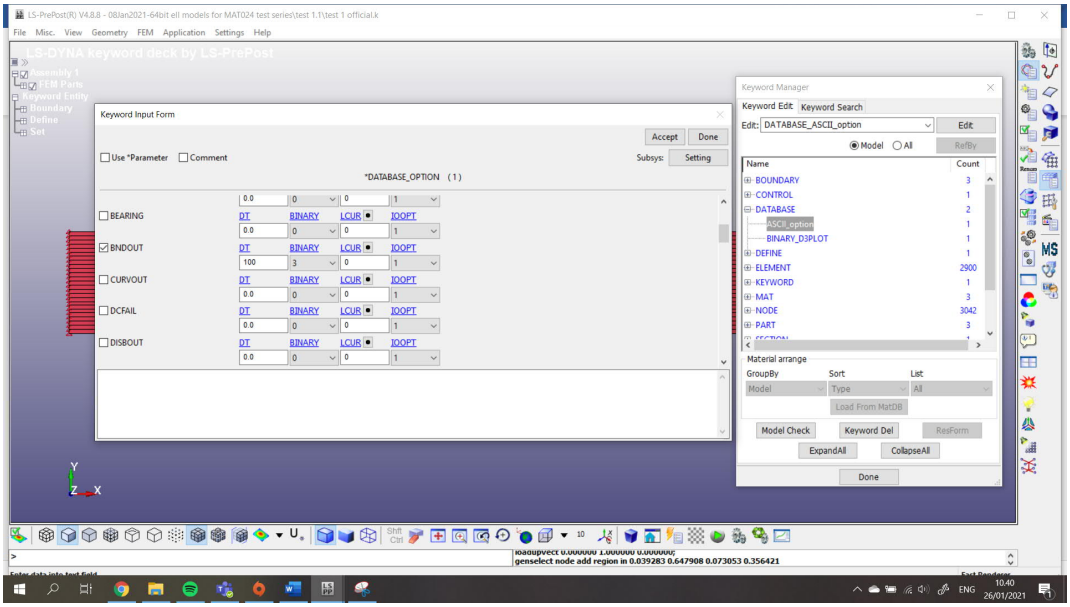

BNOUT: to output the load result of the simulation

DT: the time intervals between each time your result is written out

BINARY: 3 so that your result is printed out to a BINOUT file, this is extremely important so that when the model is processed by an MPP solver, this is the only option to record your result data

Step 16: Define the time intervals between each time your result is written out for HISTORY output file (for displacement output)

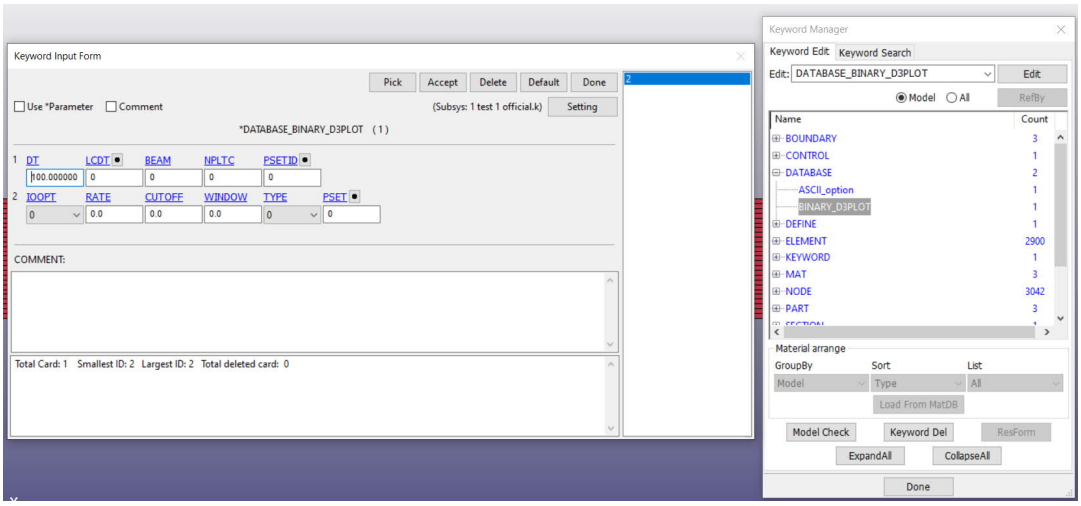

Step 17: For post simulation process, to obtain load result:

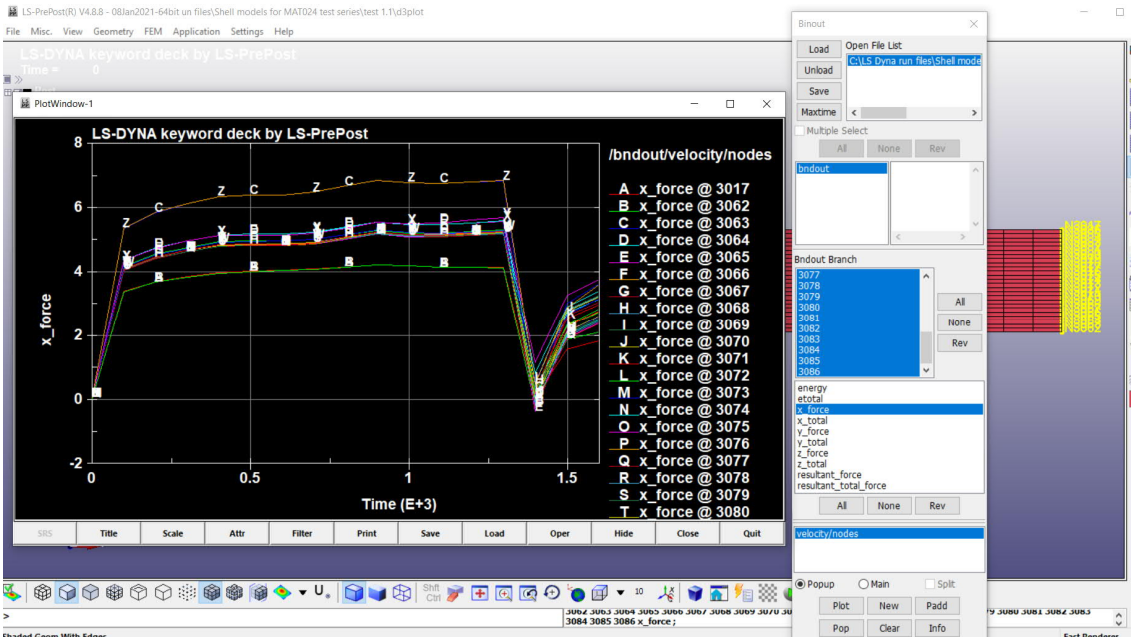

Open D3_Plot file, Binout -> Load printed binout file from the processed folder -> choose the file -> choose bnout -> choose All -> choose X force -> Plot

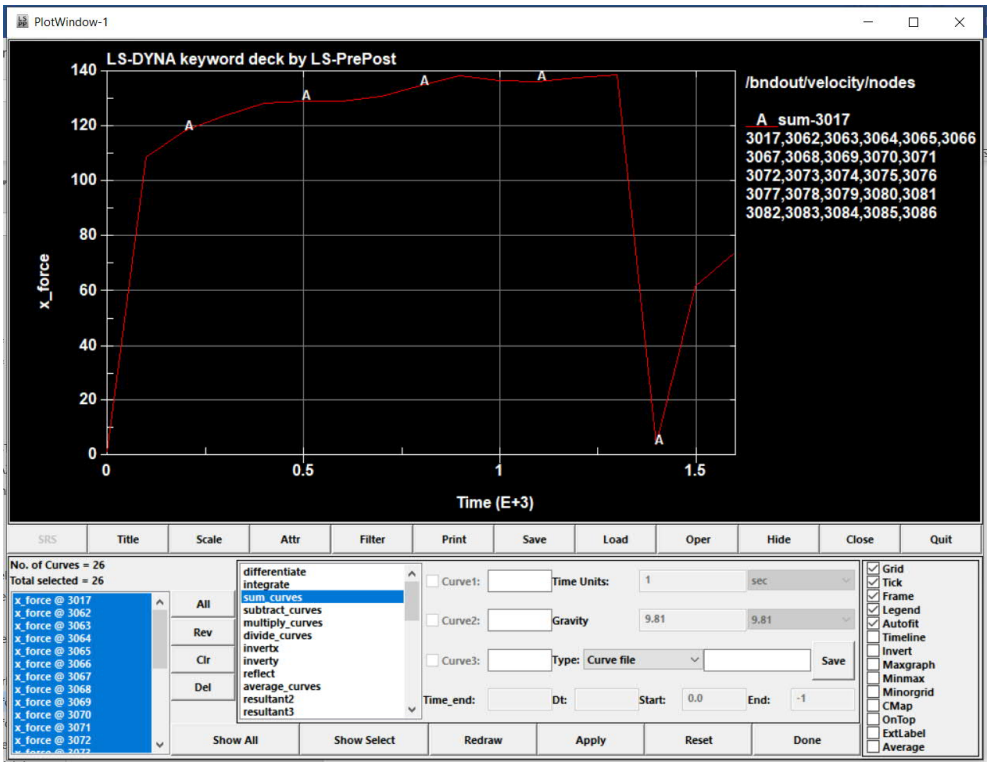

In plot window, Oper -> sum_curves -> choose All -> Apply -> Save -> Save csv file

Step 18: For post simulation process, to obtain displacement result:

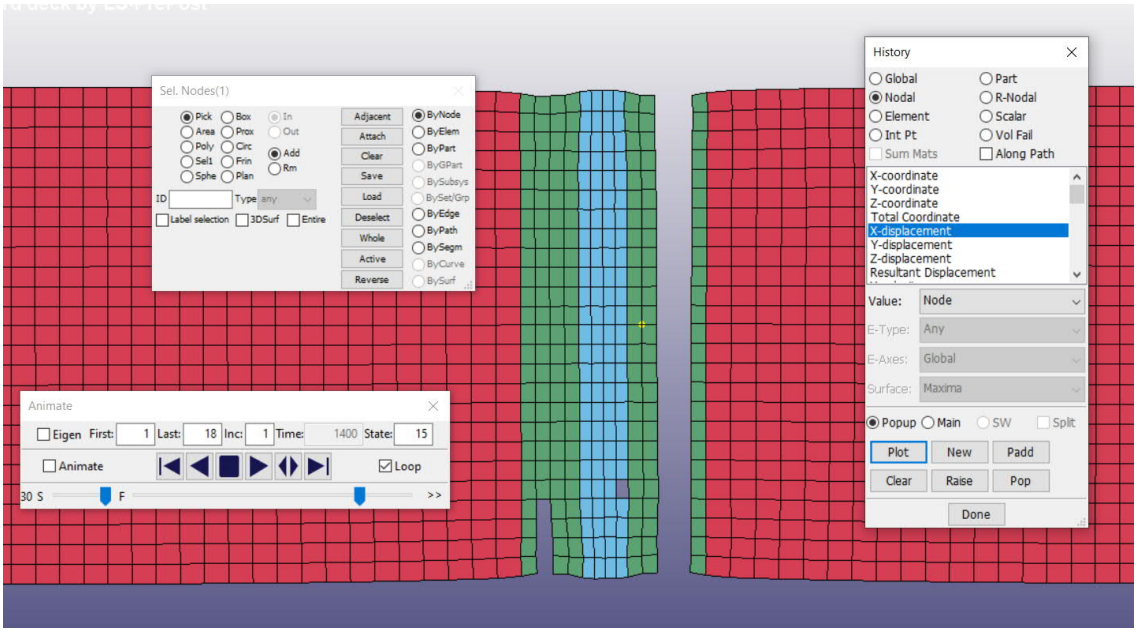

Open D3_Plot file, History -> Nodal -> choose the file -> X displacement -> choose a node at HAZ area -> choose X displacement -> Plot -> Save csv file

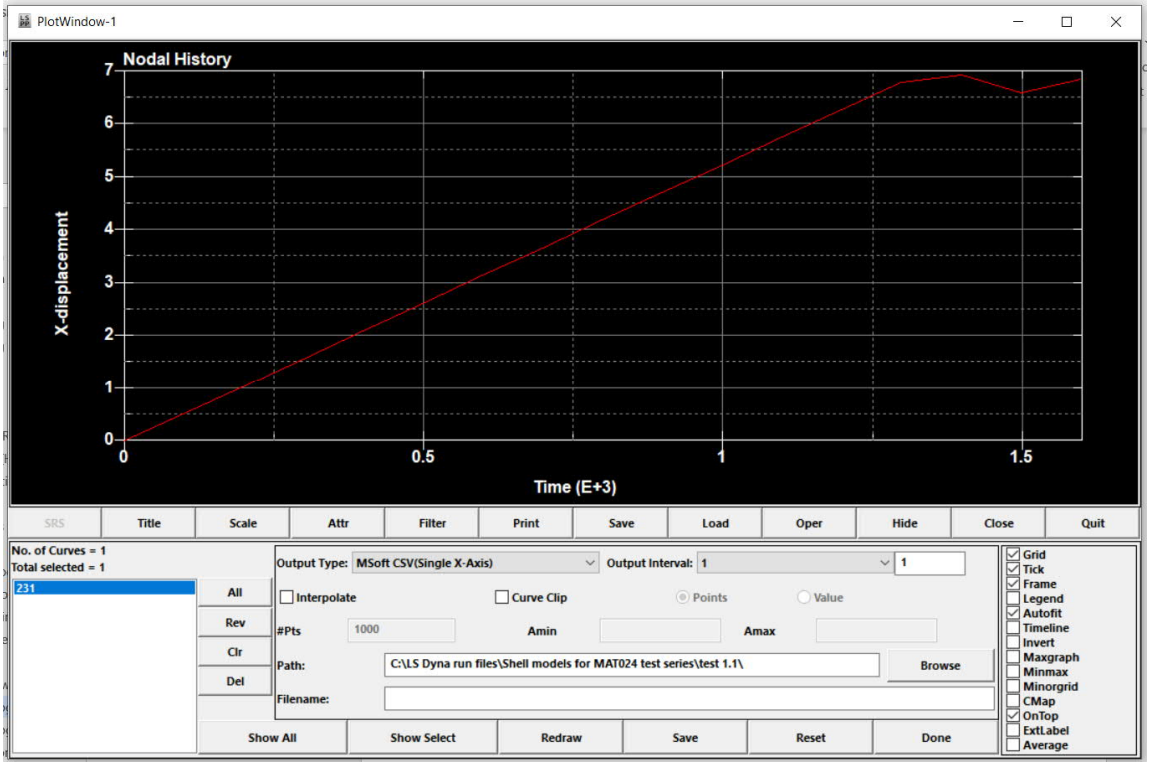

Appendix 2: Detailed design log for creating solid model

Step 1: Create the initial geometry with single line and curves. Tips: each region or area of different materials must be created with separate lines with closed borders.

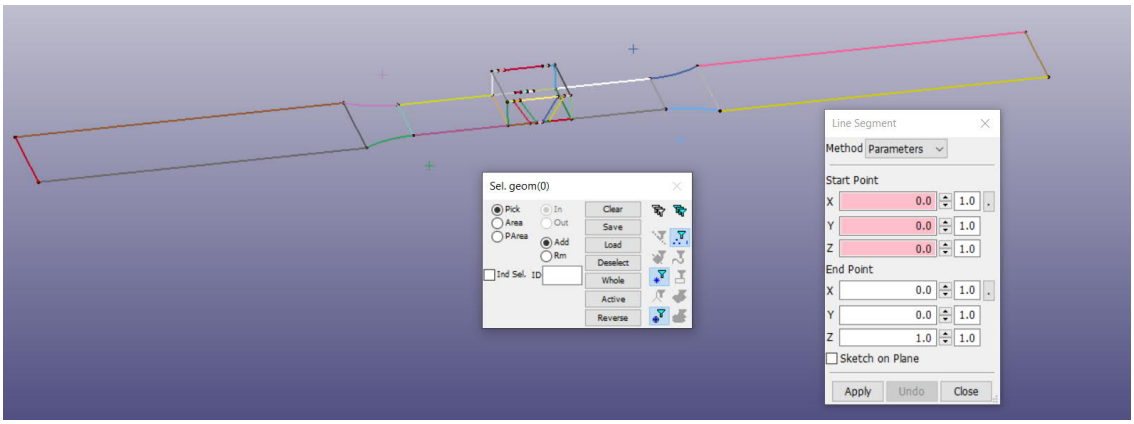

Step 2: Assign number of elements per edge using N-Line Mesher

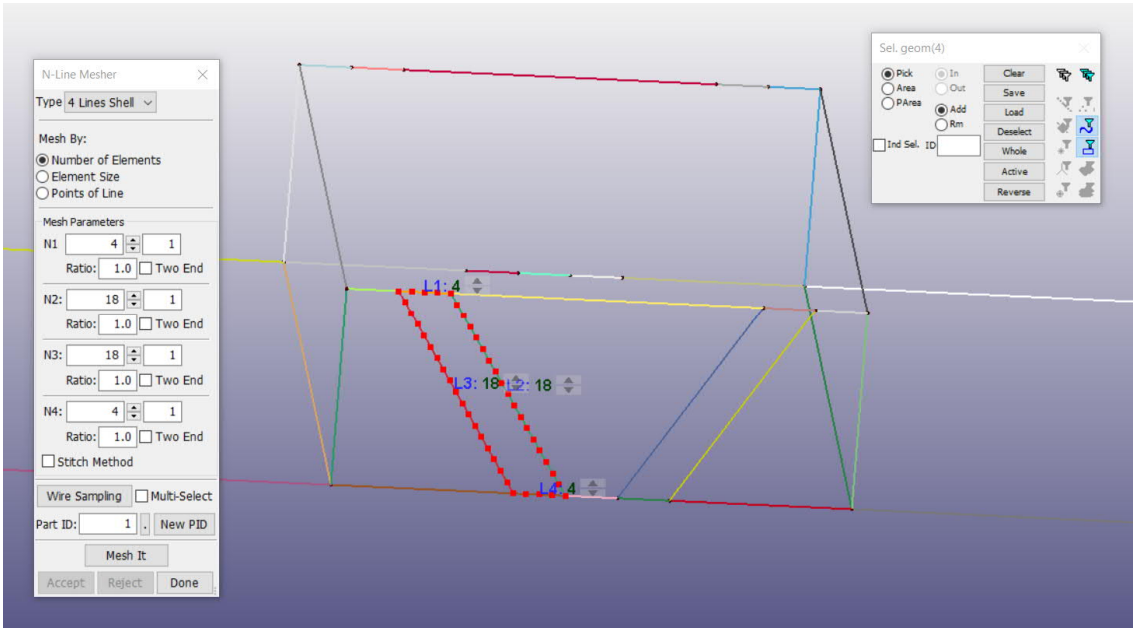

After assigning the number of elements, click Mesh it and Accept to create the mesh shells

Note: The number of elements per shared line must be identical

Step 3: Create the Mesh shells of the HAZ area in XZ plane

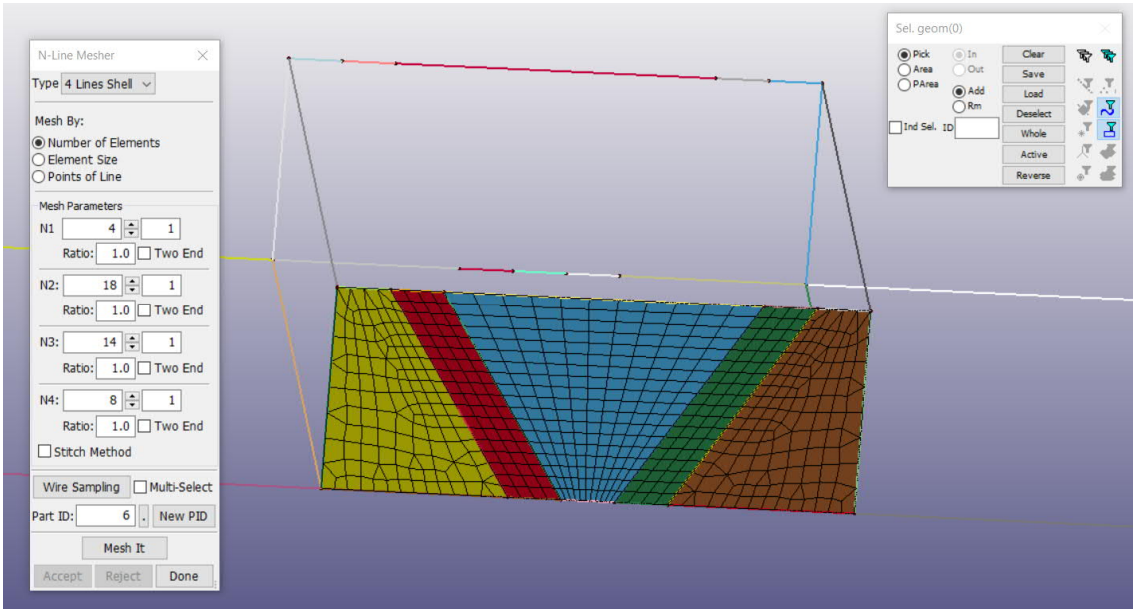

Step 4: Change the part ID of the shell mesh to the correct part ID for each material using Move or Copy tool:

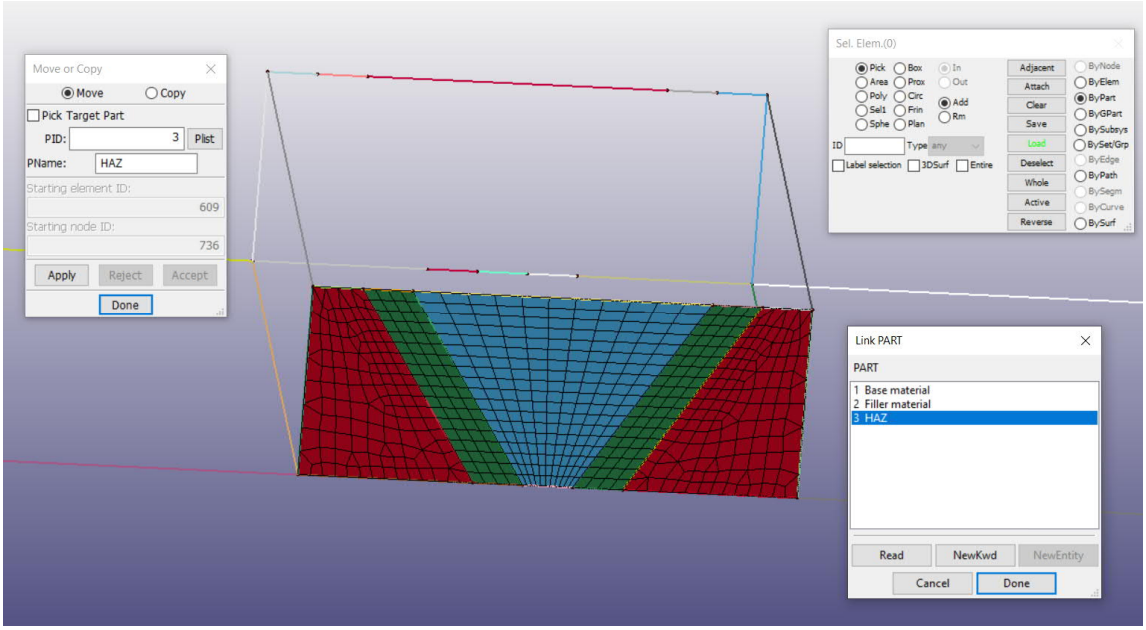

Choose ByPart -> assign the part ID number -> Apply -> Accept

Step 5: Extrude part-by-part the shell mesh to Y direction to create the solid parts using Element Generation_ Solid

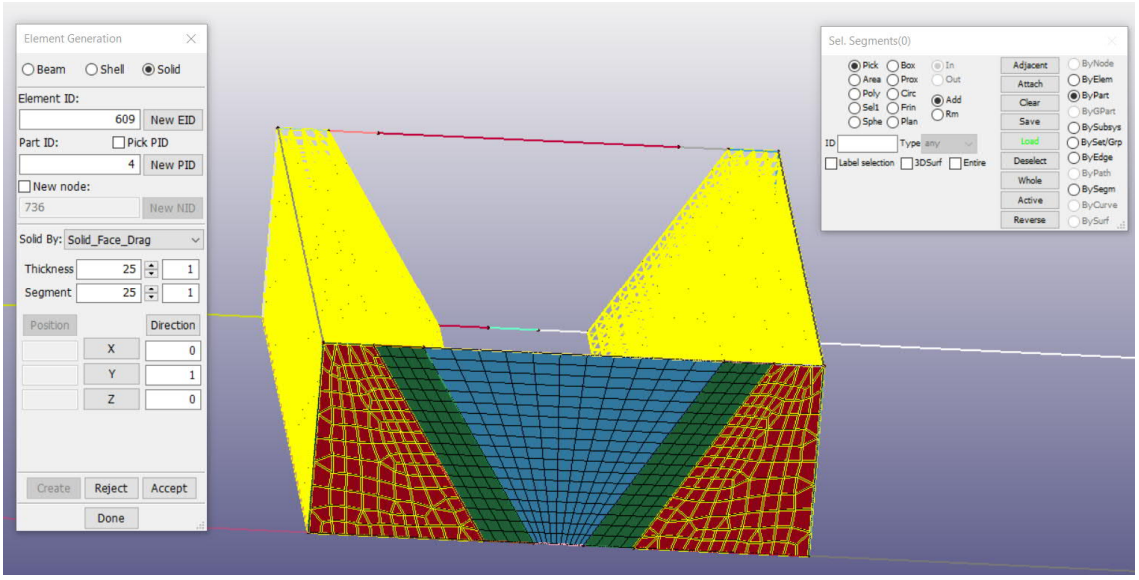

Define thickness in Y direction and number of segments to define the element size.

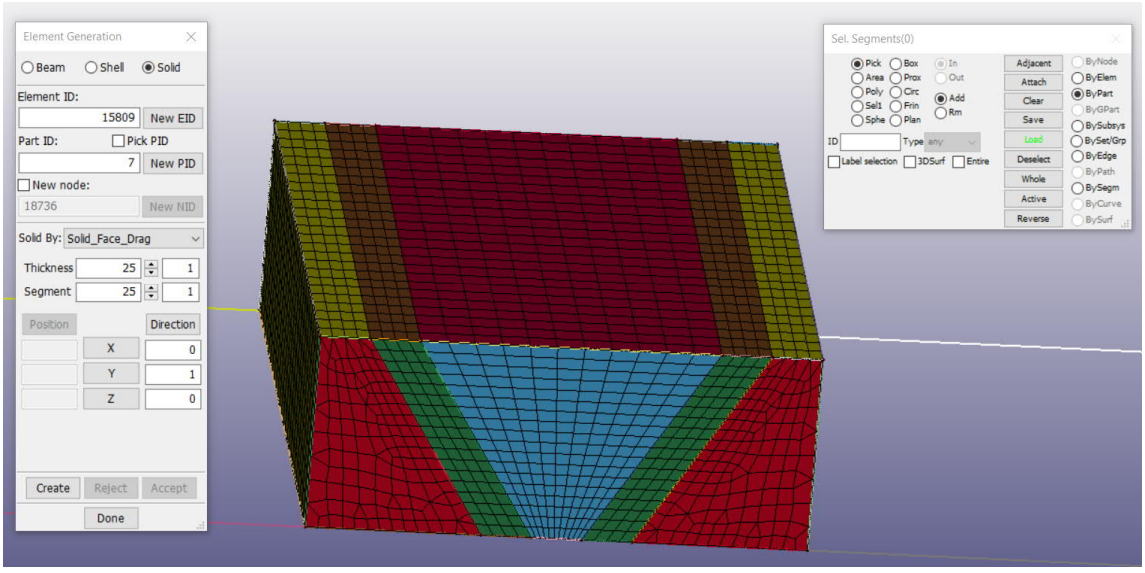

Do the extrusion for each part individually. After the solid meshes have been created, delete the shell meshes.

Step 6: Create the shell meshes for the rest of the specimen in XY plane using N Line Mesher with the aspect ratio mentioned in chapter 3.2.2

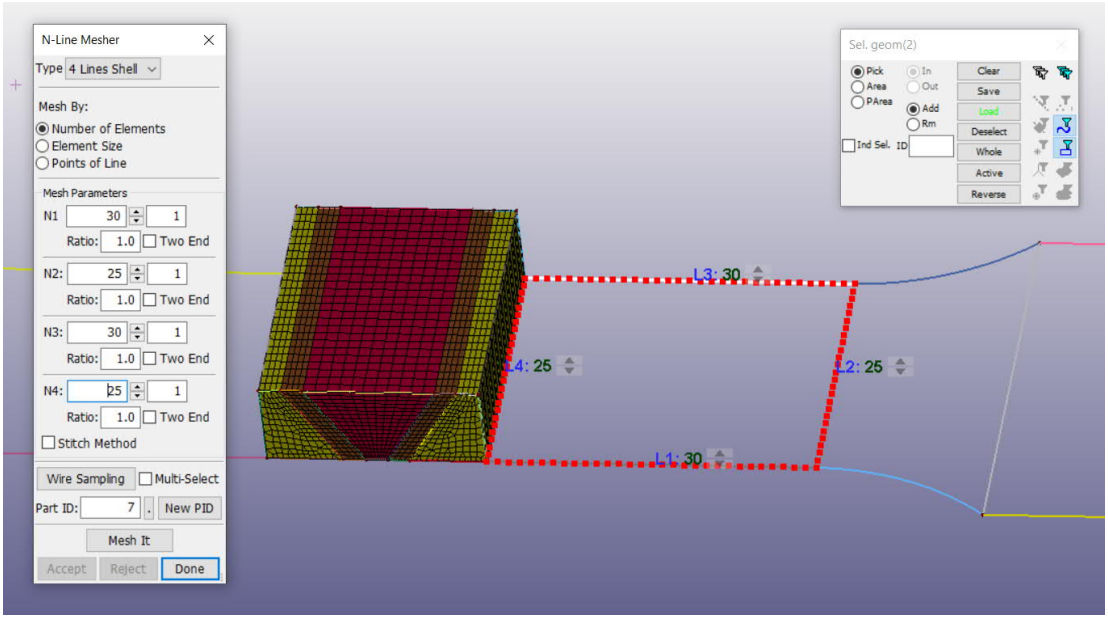

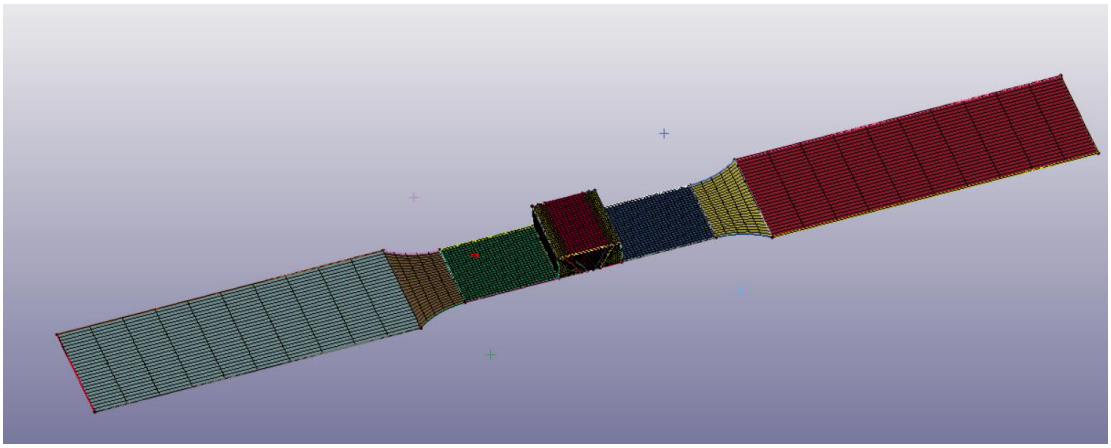

Step 7: Extrude as 1 part all the shell meshes to Z direction to create a solid part using Element Generation_ Solid

Using 8mm thickness and 8 segments for the element size

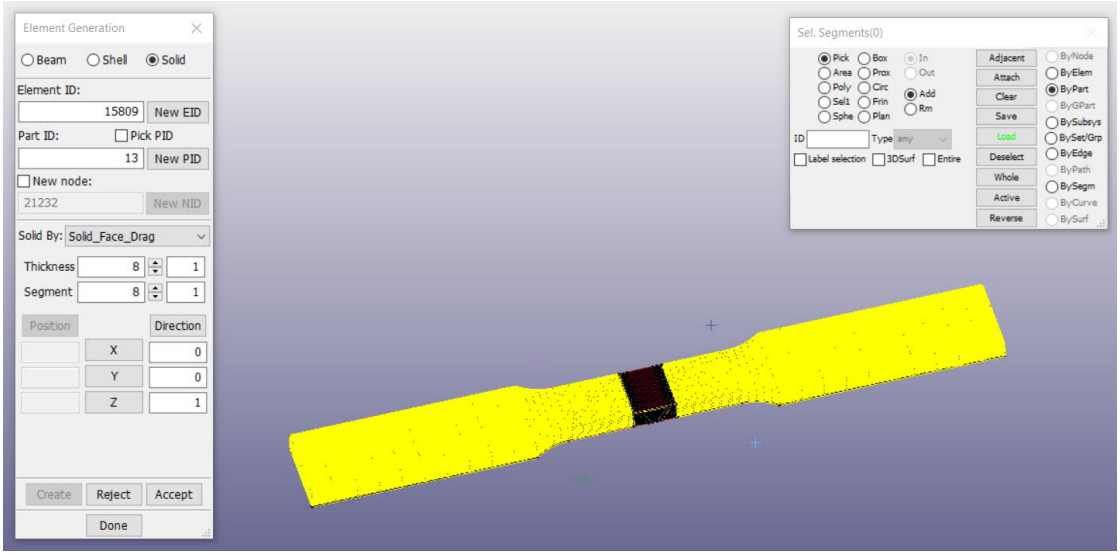

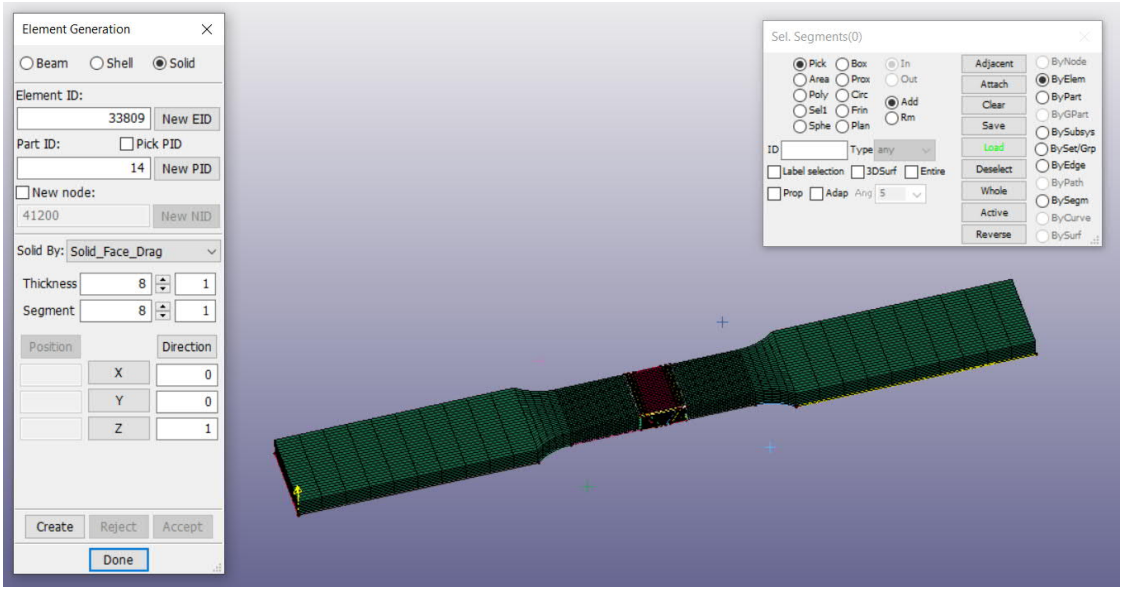

Step 9: Change the part ID of the solid meshes to the correct part ID for each material using Move or Copy tool:

Choose ByPart -> assign the part ID number -> Apply -> Accept

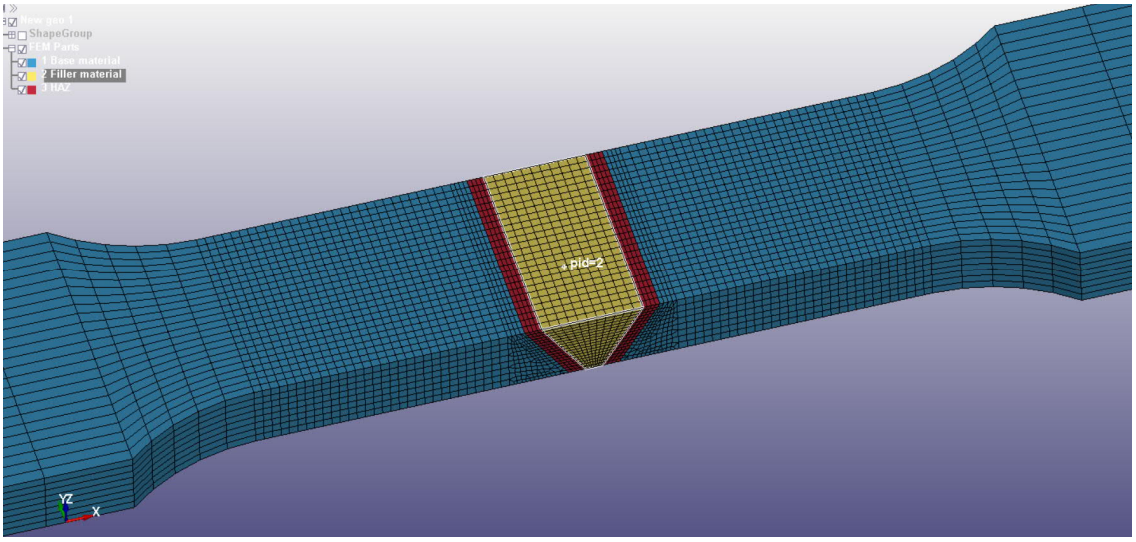

Step 10: After the solid meshes have been created, the duplicate nodes must be merged together between 2 different materials Show Dup Nodes -> Merge Dup Nodes:

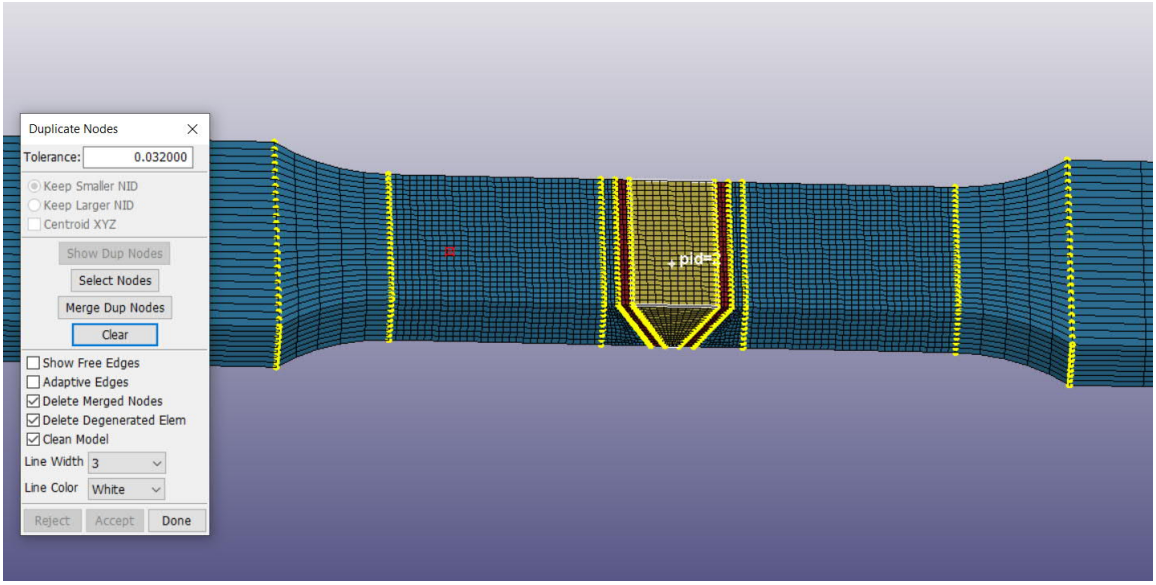

Click Accept, Done to finish the command.

Step 11: Define SECTION_SOLID keyword

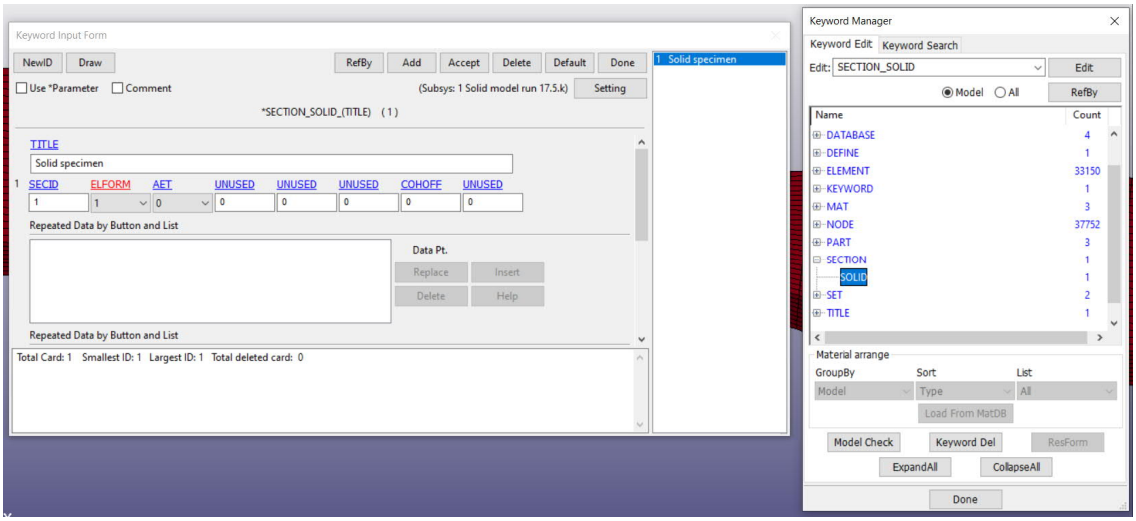

ELFORM 1: Explained in chapter 3.3

Step 12: Material properties must be defined in MAT024, specified in chapter 3.4

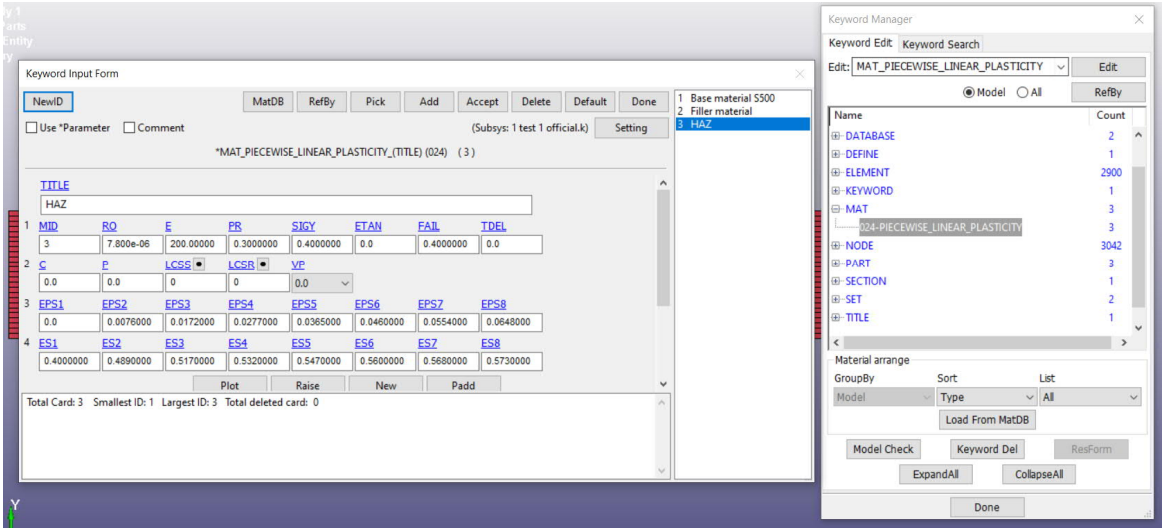

Step 13: Define PART keyword to assign the shell section and material to each part

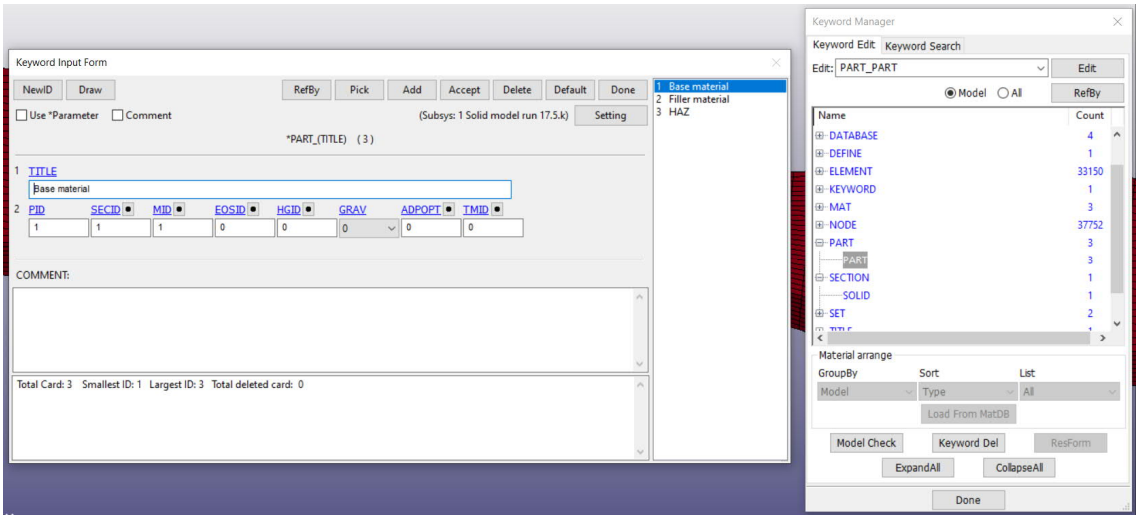

Step 14: Create node sets using Create Entity tool

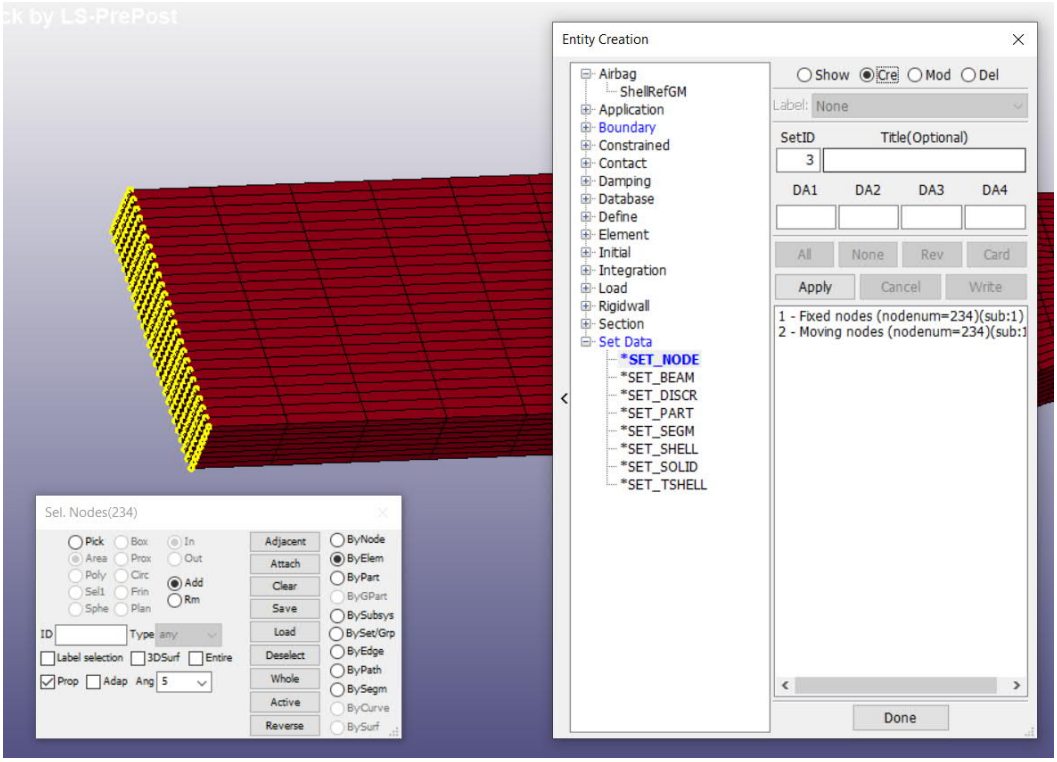

Choose ByElement, Area, Prop and click the end. After the end nodes have been highlighted, press Apply. 2 sets of nodes must be defined at 2 ends, 1 for fixed condition and 1 for pulling force.

Step 15: Define Load curve, details are mentioned in chapter 3.5.1

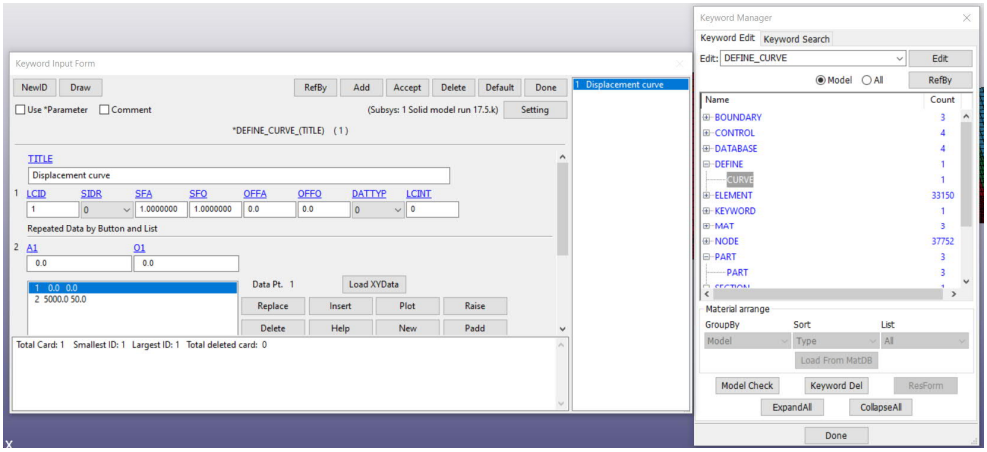

Step 16: Define Fixed condition at left side and X direction free at right side using BOUNDARY_SPC SET

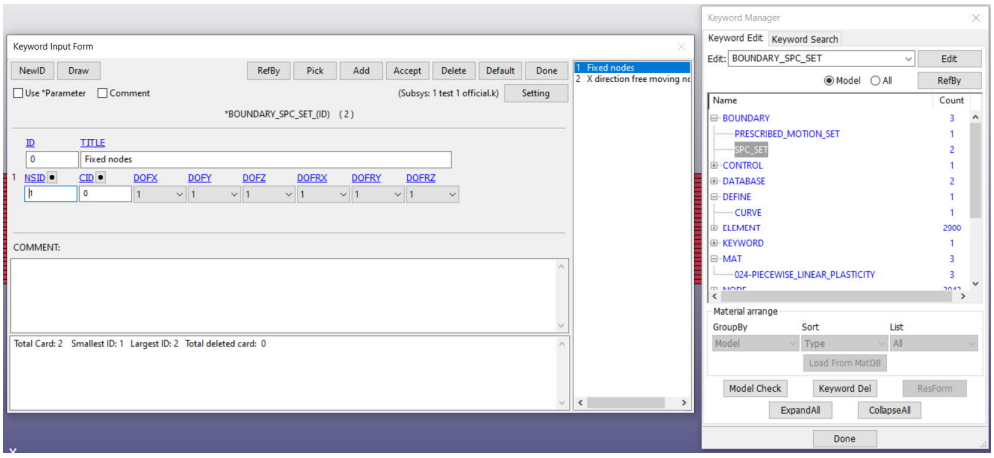

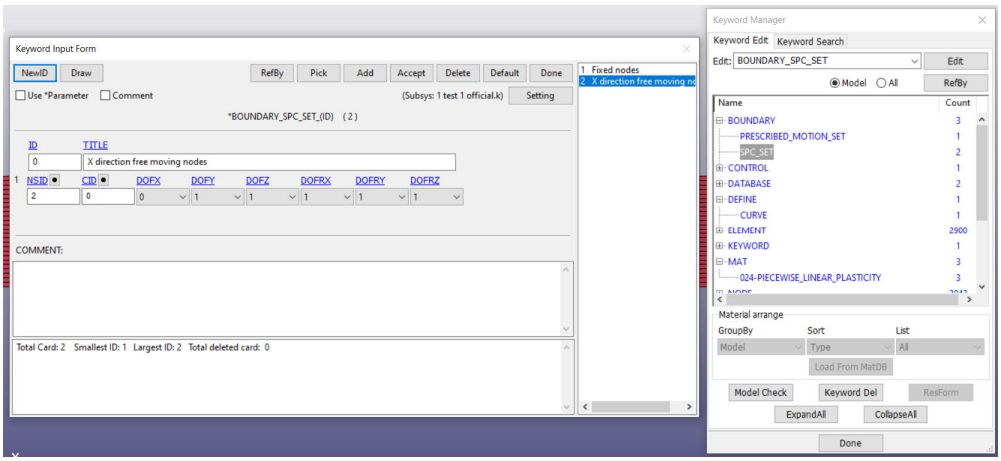

Step 17: Define Pulling force at right side by assigning load curve to the moving using BOUNDARY_PRESCRIBED MOTION SET

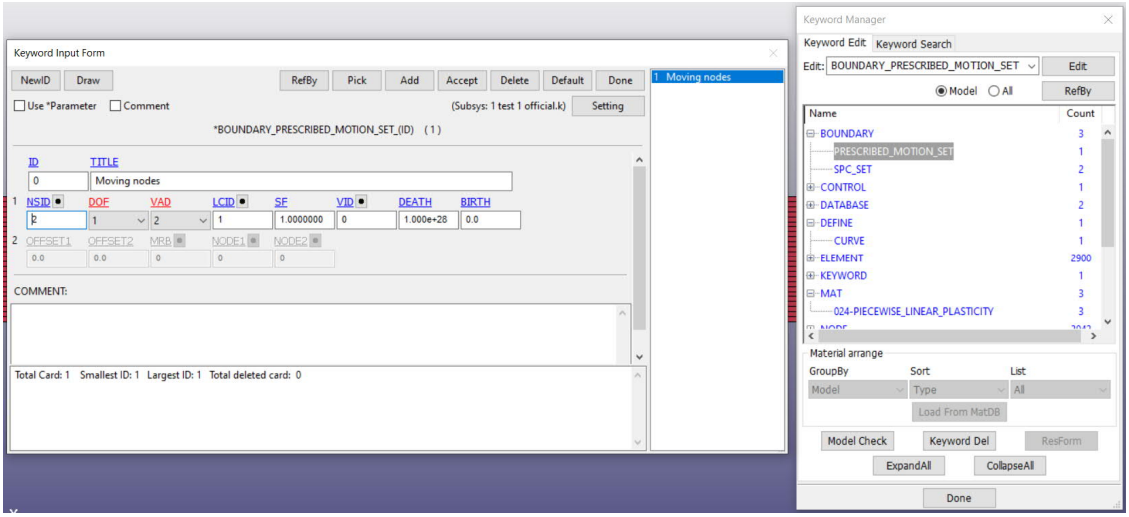

NSID: Node set ID, assign the moving node set

DOF: 1 for X translation movement

VAD: 2 for displacement equation

LCID: Load curve ID, assign displacement curve

Step 18: Define the simulation time for the model (the simulation time should be long enough for the specimen to fail). Keyword: CONTROL_TERMINATION

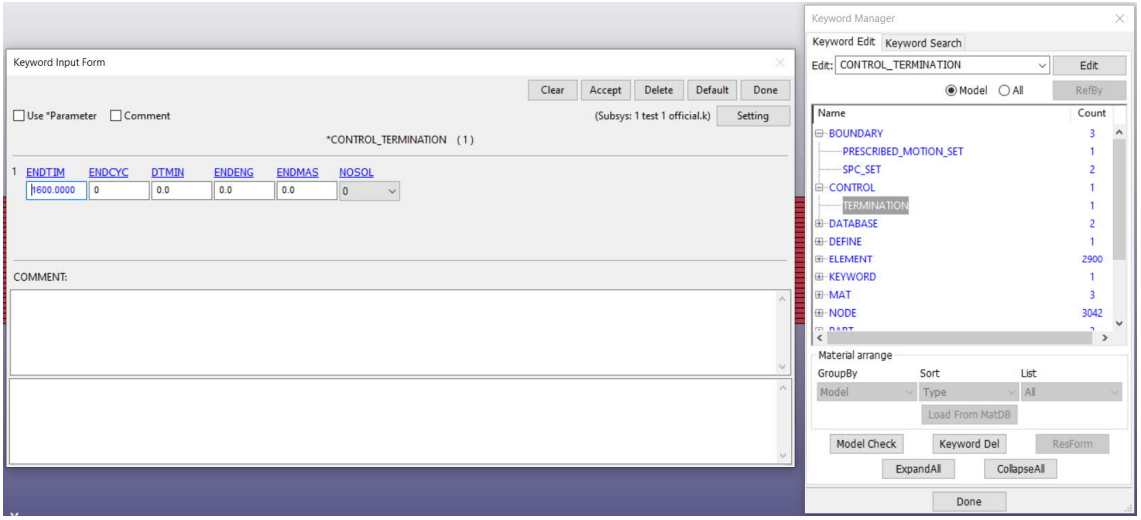

Step 19: Define the Hourglass control for the model, specified in chapter 4.4. Keyword: CONTROL_HOURGLASS

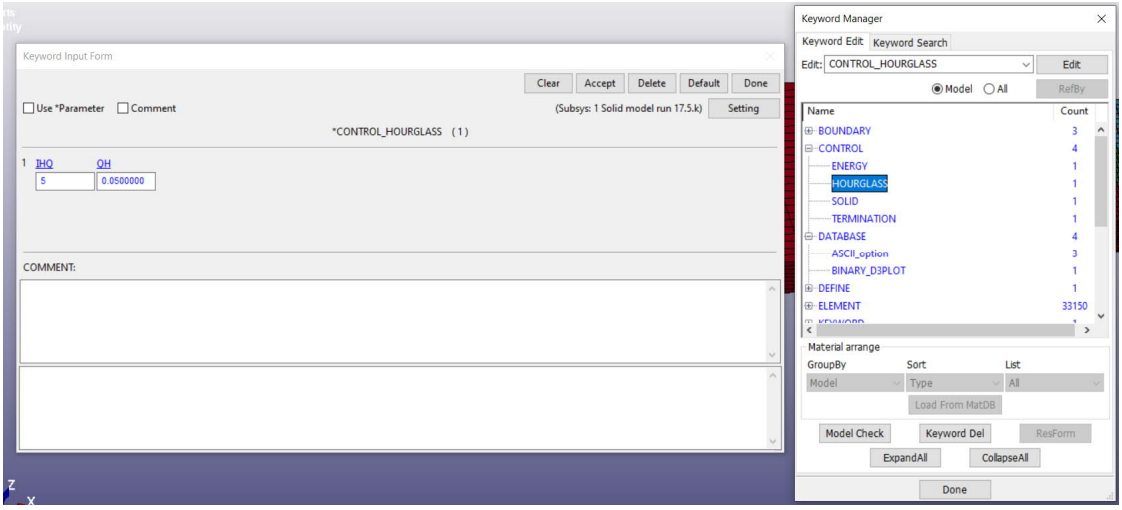

IHG: Hourglass formulation

QH: Hourglass coefficient

Step 20: Define the Element integration control for the model, specified in chapter 2.2 and chapter 3.3. Keyword: CONTROL_SOLID.

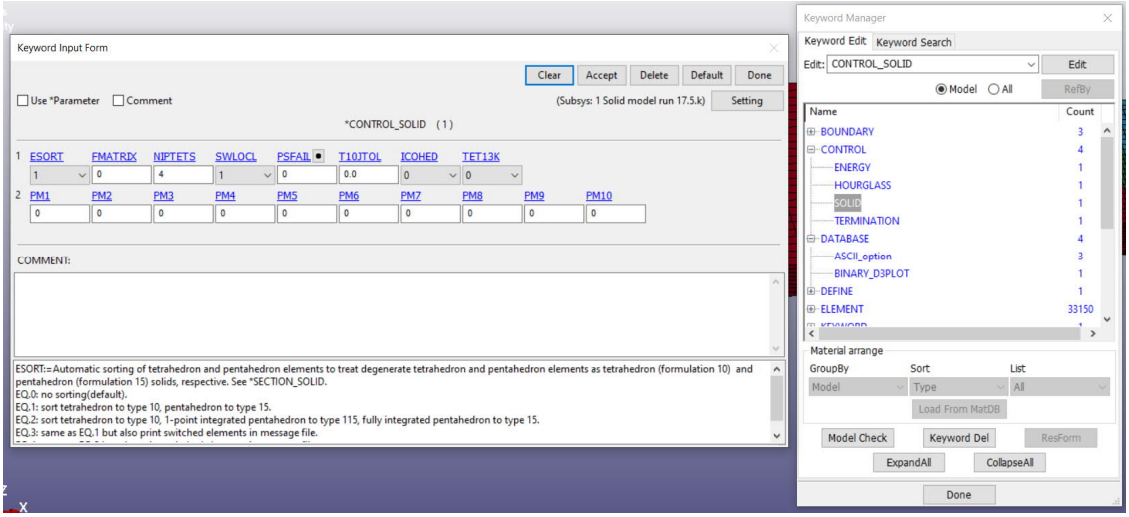

ESORT: Element sorting

Step 21: Define the Hourglass energy control for the model, specified in chapter 4.4.

Keyword: CONTROL_ENERGY.

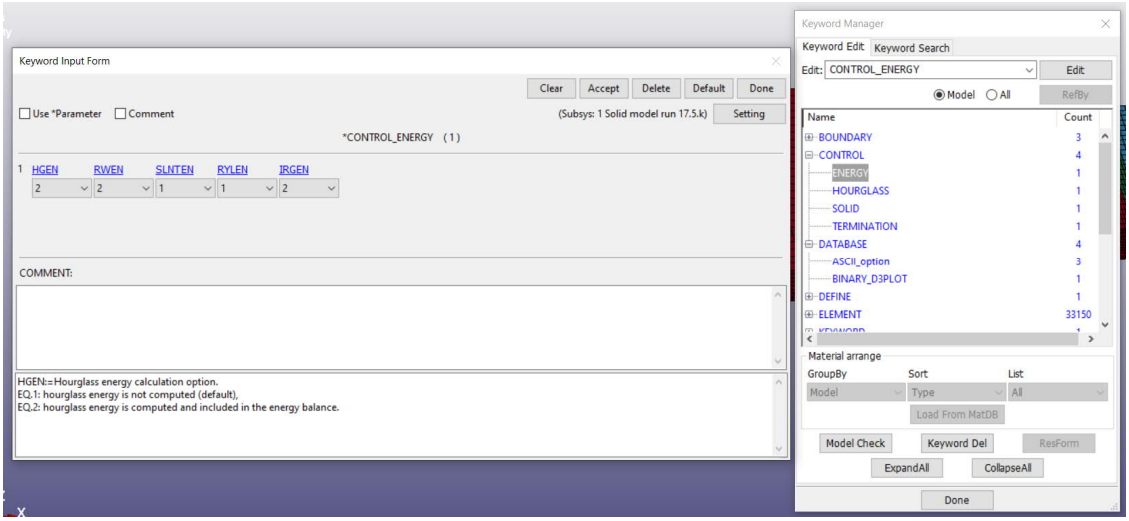

HGEN: Hourglass energy is set to 2

Step 22: Define output result which will be printed out through ASCII_option

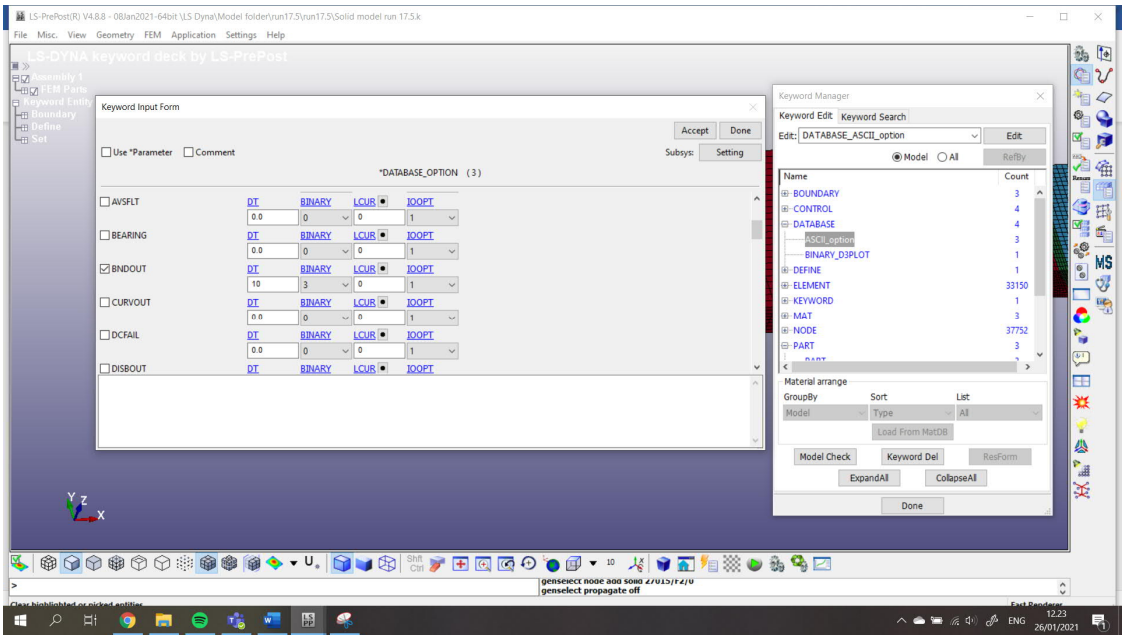

BNOUT: to output the load result of the simulation

GLSTAT: to output global energy

MATSUM: to output individual material energy

DT: the time intervals between each time your result is written out

BINARY: 3 so that your result is printed out to a BINOUT file, this is extremely important so that when the model is processed by an MPP solver, this is the only option to record your result data

Step 23: Define the time intervals between each time your result is written out for HISTORY output file (for displacement output)

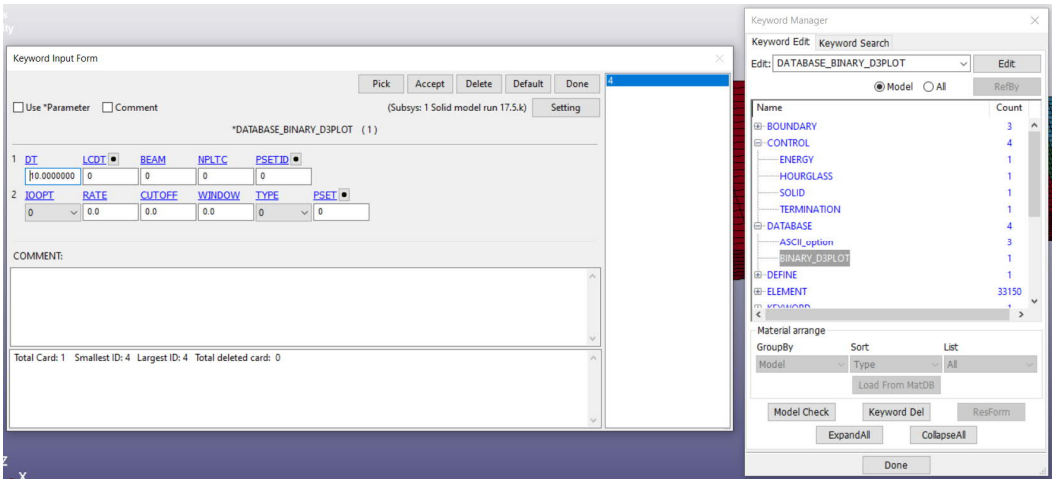

Step 24: For post-simulation process, to obtain load result:

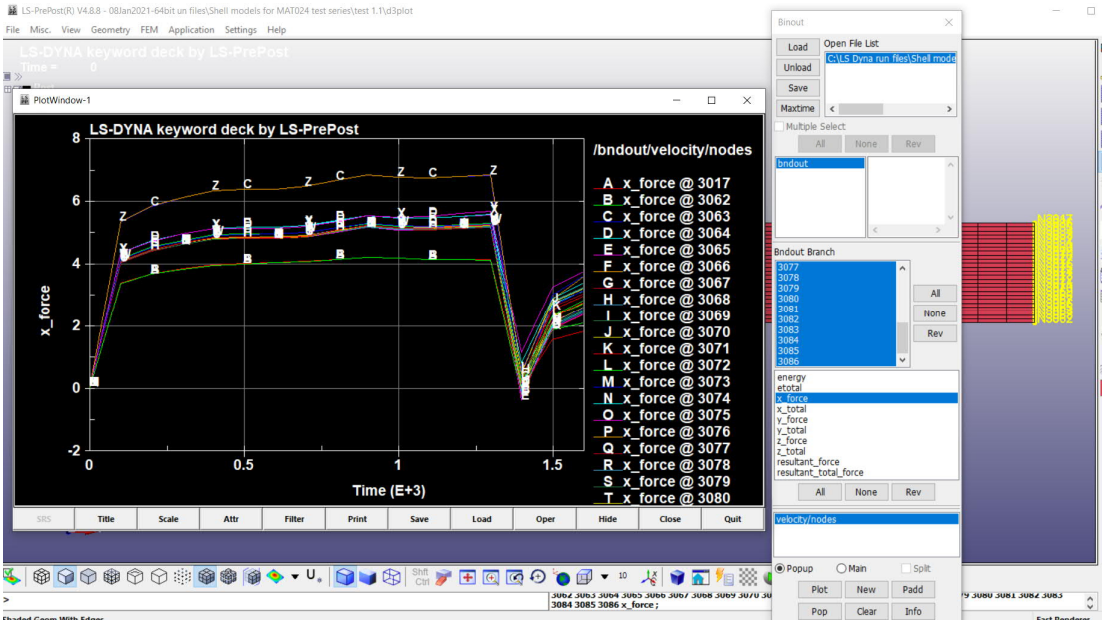

Open D3_Plot file, Binout -> Load printed binout file from the processed folder -> choose the file -> choose bnout -> choose All -> choose X force -> Plot

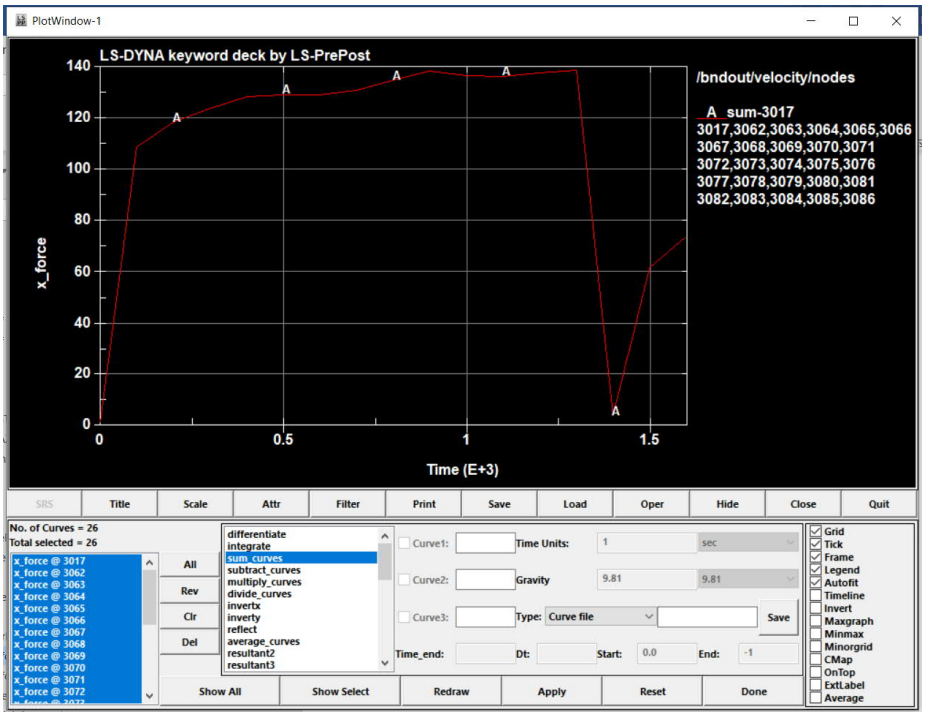

In plot window, Oper -> sum_curves -> choose All -> Apply -> Save -> Save csv file

Step 25: For post simulation process, to obtain displacement result:

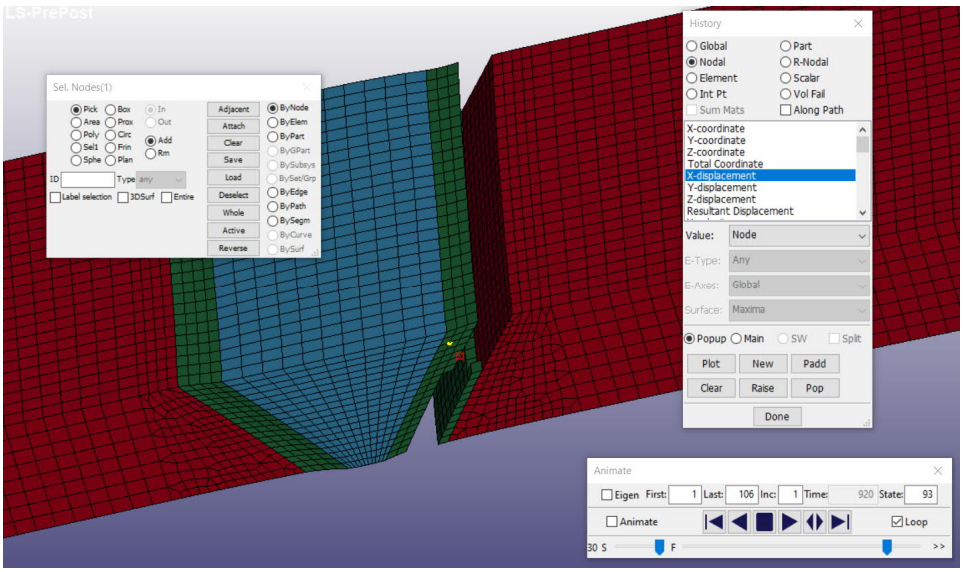

Open D3_Plot file, History -> Nodal -> choose the file -> X displacement -> choose a node at HAZ area -> choose X displacement -> Plot -> Save csv file

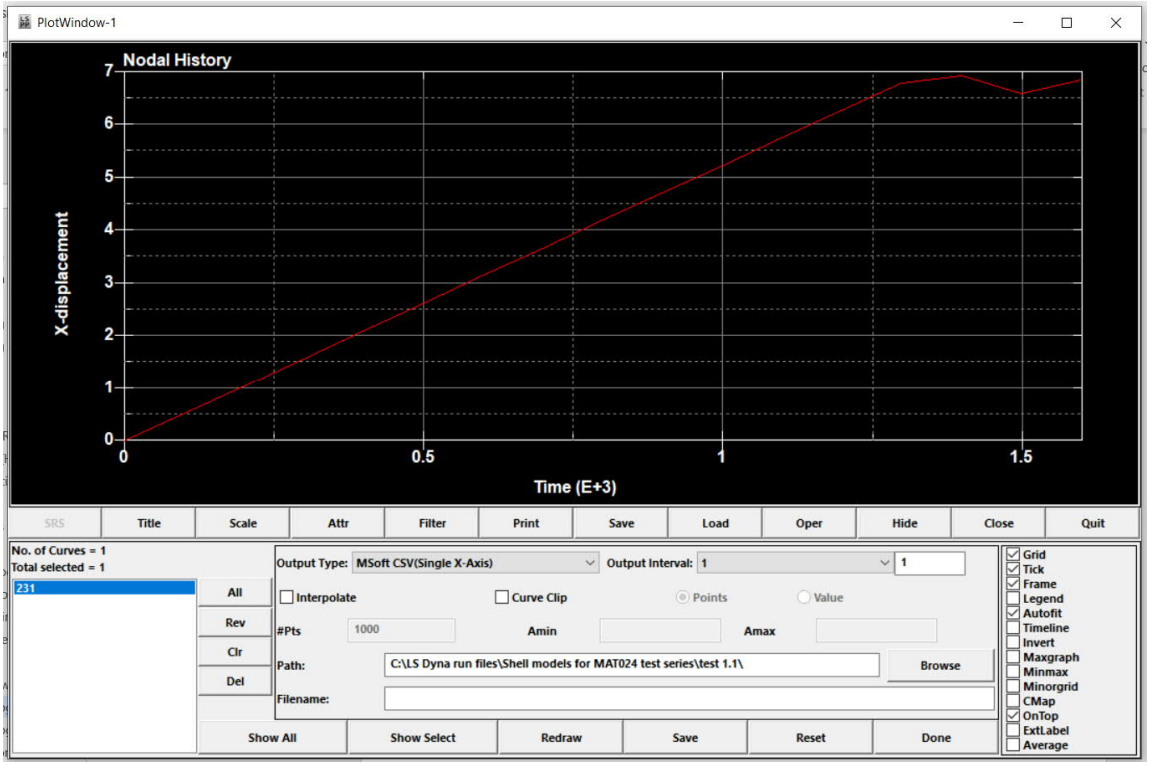

Appendix 3: Methodology of converting Engineering to True values

The conversion methodology follows the principles and formulations provided by:

https://www.dynasupport.com/howtos/material/from-engineering-to-true-strain-true-stress (accessed on 26th of January 2021)

True strain = ln(1 + engineering strain)

True stress = (engineering stress) * exp(true strain) = (engineering stress) * (1 + engineering strain)

Effective plastic strain (input value) = total true strain - true stress/E
Where E is modulus of elasticity.

Effective plastic stress (input value) = True stress at the point of effective plastic strain

Appendix 4: Approaches for material data input in MAT024

The approaches are referenced from LS-DYNA MORE NORDIC, 2017, Basic tutorials for tensile tests

MAT024 PIECEWISE_LINEAR_PLASTICITY, which is a keyword most used for elastoplastic material. This keyword allows the user to define the plastic behavior in several ways:

1. Define Yield stress SIGY and Tangent Modulus ETAN (see figure), which gives linear hardening.

2. Define effective plastic strain EPS and the corresponding yield stress value ES. At least two points need to be defined. This will give a piecewise linear plastic behavior. The failure of the material is defined at FAIL through the true failure strain value of the material.
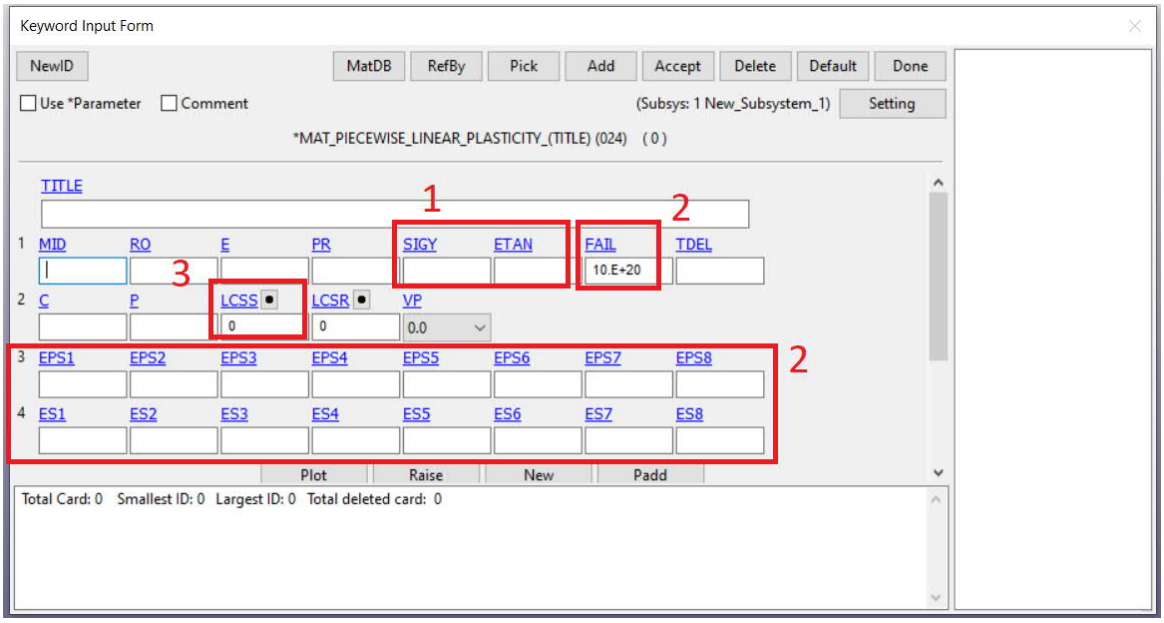
3. Define a curve of effective stress vs. effective plastic strain.